João Miguel Calmeiro Pereira

OPTOGENETICS AND BIOTECHNOLOGY: PRODUCTION AND IN VITRO CHARACTERIZATION OF AB-INITIO DESIGNED CHANNELRHODOPSIN-2 MUTANTS

Dissertação de Mestrado em Biotecnologia Farmacêutica, orientada pelo Doutor João Peça (Centro de Neurociências e Biologia Celular)
e pelo Professor Doutor Luís Pereira de Almeida (Universidade de Coimbra) e apresentada à Faculdade de Farmácia da Universidade de Coimbra

Setembro de 2015

· U C ·

UNIVERSIDADE DE COIMBRA

João Calmeiro

Optogenetics and Biotechnology: Production and *in vitro* characterization of *Ab-Initio* designed Channelrhodopsin-2 mutants

Dissertação apresentada à Faculdade de Farmácia da Universidade de Coimbra, para cumprimento dos requisitos necessários à obtenção do grau de Mestre em Biotecnologia Farmacêutica, realizada sob a orientação científica do Doutor João Peça (Center For Neuroscience and Cell Biology, University of Coimbra)

· U C ·

2015

This work was developed in the following institution:

Neuronal Circuits and Behavior Group, Center for Neuroscience and Cell Biology, University of Coimbra, Coimbra

"If you want something, go get it. Period."

Chris Gardner

Agradecimentos

À realização desta dissertação não era possível sem todo o apoio e colaboração de um grupo de pessoas pelo qual tenho um enorme apreço.

Ao Doutor João Peça, orientador desta dissertação, pelo privilégio diário de trabalhar e crescer profissionalmente consigo, pela oportunidade concedida, por toda a orientação, disponibilidade e confiança que depositou em mim, um grande obrigado.

Ao Professor Doutor Luís Almeida, orientador interno desta dissertação, pela total disponibilidade, ajuda e ensinamentos ao longo dos dois anos de Mestrado.

À Professora Doutora Ana Luísa Carvalho, pelo apoio, disponibilidade e conselhos dados na realização deste projeto.

Ao Centro de Física Computacional da Universidade de Coimbra pela disponibilização de dados fundamentais e base para este projeto.

À Professora Doutora Paula Veríssimo e Doutora Isaura Simões pela disponibilização de equipamento do seu laboratório e esclarecimentos, essenciais para o desenrolar deste trabalho.

À Doutora Joana Fernandes, pelo apoio e conselhos na elaboração desta tese.

Aos elementos do meu grupo, Mohamed, Joana, Lara e Gladys, por todo o constante apoio, disponibilidade, brainstorming científico e não científico, sorrisos, gargalhadas e pelo brilhante ambiente de trabalho que proporcionam.

A todos os membros de outros grupos de investigação no CNC com quem convivo diariamente, pela total disponibilidade ao longo deste trabalho.

A todos os meus amigos e, em especial aos residentes do peculiar 29 A, por todo o apoio, carinho e amizade que trazem diariamente.

À minha Patrícia, por ser a pessoa cativante que é, pelo amor, incentivo e muita paciência durante esta tese de Mestrado.

À minha família, em particular aos meus avós e mãe, por serem os melhores, por todo o amor, apoio e encorajamento incansável que me foi dado durante todo o meu percurso.

Por fim, um agradecimento póstumo ao Doutor Sukalyan Chatterjee, pelo apoio, conselhos e oportunidade concedida de iniciar uma carreira científica.

A todos, o meu muito sincero Obrigado !

Funding Acknowledgements

Index

Figure index

Table index

List of Abbreviations

7TM	Seven transmembrane helix
A.A.	Amino acid
AAV	Adeno-associated virus
Aox1	Alcohol oxidase 1 promoter
Asp	Aspartic acid
ATP	Adenosine-5'- triphosphate
BMGY	Buffered glycerol complex medium
BMMY	Buffered methanol complex medium
BR	Bacteriorhodopsin
BSA	Bovine serum albumin
Ca^{2+}	Calcium
C.C.F.U.C.	Center for Computational Physics at the University of Coimbra
cDNA	Complementary deoxyribonucleic acid
Chop-1	Channelopsin-1
Chop-2	Channelopsin-2
ChR1	Channelrhodopsin-1
ChR2	Channelrhodopsin-2
CIP	Calf-intestinal alkaline phosphatase
Cys	Cysteine
DDM	n-dodecyl-β-D-maltoside
DNA	Deoxyribonucleic acid
dNTP	Deoxyribonucleotide triphosphate

E	Glutamic acid
ECL	Extracellular lopp
EDTA	Ethylenediaminetetraacetic acid
GAP	Glyceraldehyde-3-phosphate dehydrogenase promoter
Glu	Glutamic acid
H^+	Hydrogen
hChR2	Humanized Channelrhodopsin-2
HEK 293	Human embryonic kidney 293
HR	Halorhodopsin
ICC	Immunocytochemistry
ICL	Intracellular loop
K	Lysine
kDa	Kilodaltons
LB	Luria-broth
LED	Light-emmiting diode
LV	Lentivirus
Lys	Lysine
MeOH	Methanol
MgCl2	Magnesium chloride
N	Aspargine
NEB	New England Biolab
O.D.	Optical density
PCR	Polymerase chain reaction
PDB	Protein data bank
Phe	Phenylalanine

PMSF	Phenylmethylsulphonyl fluoride
PVDF	Polyvinylidene difluoride
Q	Glutamin
S	Serine
Ser	Serine
SFO	Step –function opsin
RPM	Rotations per minute
RSB	Retinal Schiff base
SR	Sensory rhodopsin
T	Threonine
TAE	Tris-acetate-EDTA
TD-DFT	Time-dependent density functional theory
Thr	Threonine
TM	Transmembrane
Trp	Tryptophan
UV	Ultraviolet light
VChR1	*Volvox* channelrhodopsin-1
YFP	Yellow fluorescent protein
YNB	Yeast nitrogen base
YPD	Yeast peptone dextrose
WB	Western-blot
Wt	Wild-type

Resumo

Nos últimos anos têm sido desenvolvidas várias ferramentas para permitir o controlo de neurónios específicos, possibilitando o estudo da sua função. Estas novas ferramentas superam a falta de selectividade e o fraco controlo temporal proveniente do uso de estimulação eléctrica no controlo de actividade neuronal.

A optogenética refere-se á integração de óptica e genética para obter um ganho ou perda de função em eventos bem definidos dentro de células específicas em tecido vivo. A capacidade de "ligar" e "desligar" neurónios utilizando luz é de facto uma tecnologia inovadora que oferece uma solução para limitações passadas. A optogenética, considerada por vários especialistas como "método do ano" e "inovação da década", em 2010, é utilizada para hiperpolarizar ou despolarizar neurónios alvo, de uma forma menos invasiva, utilizando luz e usufruindo de uma alta resolução espacial e escala temporal na ordem dos milissegundos. Esta técnica tem permitido o mapeamento e estudo de redes neuronais com uma grande eficácia.

A "Channelrhodopsin-2" (ChR2) é um canal catiónico sensível à luz, derivado da microalga *Chlamydomonas reinhardtii*. Na última década, a ChR2 tornou-se o arquétipo central e a principal ferramenta da optogenética. Actualmente, a caixa de ferramentas optogenética está em contínua actualização, com contribuições de estratégias de engenharia protéica, tais como mutagénese dirigida e a construção de quimeras com troca de domínios de diferentes espécies de channelrhodopsin. No entanto, alguns aspectos da forma "wild-type" da ChR2 ainda requerem atenção e melhoramento. Estes incluem o seu espectro de acção, cinética, níveis de expressão, inactivação, condutância e exactidão de pico de absorção. Em termos de propriedades espectrais, poucas variantes desta proteína têm sido geradas e completamente caracterizadas com sucesso. No entanto, o aprimorar do espectro de activação da ChR2 e do formato do respectivo pico de absorção são algumas das propriedades mais desejadas.

A ChR2 é excitada preferencialmente com comprimentos de onda de luz azul (470nm), o que limita o seu uso em material biológico de alta taxa de difusão, tal como o cérebro. Luz de excitação com maiores comprimentos de onda diminui a difusão de luz produzida por tecidos biológicos, e não é absorvida pela hemoglobina, assim, formas da ChR2 "red-shifted", a absorver luz vermelha ou mesmo perto de infravermelha, são ferramentas desejáveis para a excitação de tecidos profundos.

Alem disto, variantes "blue-shifted" são também ferramentas atrativas para desenvolver,

dado que a combinação de várias ChR2 que apresentem sensibilidades a diversos comprimentos de onda permitiriam a estimulação de diferentes populações neuronais sem interferência entre si.

Neste projecto, realizámos um desenho *ab-initio* para produzir quatro novas variantes de ChR2, usando uma abordagem de mutagénese dirigida no ambiente do cromófero da ChR2 alterando de forma radical os resíduos alvo. As mutações foram selecionadas com a aplicação de *Time Dependent – Density Functional Theory* (TDDFT) para prever o espectro de absorção dos mutantes selecionados da ChR2. O "colour tuning" da ChR2 foi alcançado em quatro novas variantes criadas. Em particular, fomos capazes de gerar três variantes "red-shifted" e uma "blue-shifted". Após caracterização espectral, as variantes F217D e F269D apresentaram um "red-shift" significativo de 90nm, a variante L221D apresentou um "red-shift" de 180nm, a variante F269H apresentou um "blue-shift" de 20nm. Apesar dos nossos resultados, é necessária uma caracterização protéica adicional, tal como a avaliação do tráfego membranar em neurónios e as características electrofisiológicas destes novos mutantes para determinar as prioridades cinéticas do canal.

Neste trabalho, também conseguimos definir e descrever com sucesso a expressão e purificação da ChR2 "wild-type" e de todas as quatro novas variantes no sistema eucariótico de expressão heteróloga - *Pichia pastoris.* Por fim, o nosso estudo valida as previsões de Time-Dependent Density Functional Theory e revela que abordagens de simulação biofísica podem ser utilizadas com vista à criação de variantes de ChR2 inteligentemente desenhadas.

O desenho de novas variantes ChR2, seguindo a lógica racional aplicada, é uma abordagem poderosa e fiável para obter proteínas optimizadas para estratégias biotecnológicas. Os resultados originais obtidos com este trabalho demonstram potencial para aplicações futuras, já que novas e melhoradas variantes de ChR2 continuarão a desempenhar um papel central no desenvolvimento e implementação da optogenética.

Palavras-chave: Optogenética; channelrhodopsin-2; "red-shift"; "blue-shift"; TDDFT; *Pichia pastoris*

Abstract

Over the last few years, several tools have been developed to allow the control over specific types of neuron to enable the study of their function. These novel tools aim to overcome the lack of selectivity and the poor temporal control that derives from trying to control neuronal activity with electrical stimulation.

Optogenetics refers to the integration of optics and genetics to obtain gain or loss of function in well-defined events and within specific cells in living tissue. The capacity to turn neurons "on and off" using light is indeed a groundbreaking technology that has become a solution for past limitations. Considered by many, "method of the year" and "breakthrough of the decade", in 2010, optogenetics is used to hyperpolarize or depolarize specific targeted neurons using light in a less invasive manner, with high spatial resolution and a temporal resolution on the scale of milliseconds. This technique has allowed the mapping and study of neuronal networks with demonstrated efficacy.

Channelrhodopsin-2 (ChR2) is a light-gated cation channel, derived from the microalga *Chlamydomonas reinhardtii*. In the last decade, ChR2 has become the central archetype and the main tool of optogenetics. Presently, the optogenetic toolbox is under continuous update, with contributions from protein engineering strategies, such as site-directed mutagenesis and construction of chimeras with domain swaps between channelrhodopsins of different species. However, some aspects of the wild-type form of ChR2 still require attention and enhancement. These include its action spectra, kinetics, expression levels, inactivation, conductance and absorption peak sharpness. In terms of spectral properties, few variants of this protein have been successfully generated and fully characterized. Nevertheless, tuning of ChR2 activation spectra and absorption peak sharpness are one of the most sought after properties.

ChR2 is optimally excitable at a wavelength of blue light (470nm), which limits its use in high light-scattering biologic material, such as the brain. However, long-wavelength excitation light decreases the scattering of light produced by biological tissues and is not absorbed by haemoglobin. Thus, a red-shifted form of ChR2, absorbing red or even near infrared light would be a desirable tool for the excitation of relatively deep tissues.

Furthermore, blue-shifted variants would also be attractive tools to develop, since the combination of ChR2 proteins with well separate wavelength sensitivities, combined with multi-coloured optics, would permit the stimulation of different neuronal populations with no

interference between them.

In this project, we performed *ab-initio* design to produce four new ChR2 variants, using a radical site-directed mutagenesis approach on target residues in the environment of the ChR2 chromophore. The mutations were selected with the application of Time Dependent – Density Functional Theory (TDDFT) to predict the absorption spectra of ChR2 selected mutants. We achieved successful colour tuning of ChR2 with our four newly created variants. In particular, we were able to generate three red-shifted and one blue–shifted variant. After spectral characterization, the F217D and F269D variants presented a significant 90nm red shift, the L221D variant had a 180nm red shift and the F269H variant presented a 20nm blue shift. Despite our results, additional protein characterization is needed, such as the assessment of membrane trafficking in neurons and an electrophysiological characterization to determine channel kinetic proprieties for each of the variants.

In this work, we were also able to define and describe the successful expression and purification of wild type ChR2 and of all the new four variants using the eukaryotic *Pichia pastoris* heterologous expression system. Finally, our study validates Time-Dependent Density Functional Theory predictions and reveals that biophysical simulation approaches may be used towards the creation of intelligently designed ChR2 variants.

The design of new ChR2 variants, following our applied rationale, is a powerful and reliable approach to obtain enhanced proteins for biotechnological strategies. The original output obtained here shows potential for future optogenetic application, as new and improved ChR2 variants will continue to play a central role in the development and implementation of optogenetics.

Keywords: Optogenetics; channelrhodopsin-2; red-shift; blue-shift; TDDFT; *Pichia pastoris*

Chapter I – Introduction

1.1 – The history of Optogenetics

In 1979, Francis Crick claimed that to study the brain, it would be invaluable to have "…*a method by which all neurons of just one type could be inactivated, leaving the others more or less unaltered"* (Crick, 1979) . Since Galvani in the eighteenth century, electrical stimulation has been widely used by the scientific community to study tissue and brain activity in regards to behavioral outputs. However, it is not possible to do so selectively, since direct electrical stimulation unspecifically activates all cells near the insertion site of the device. Furthermore, these approaches have other restrictions, such as the inability to hyperpolarize neuron to induce silencing (Deisseroth, 2010). Therefore, precise and specific control over the activity of neurons submerged in the heterogeneous environment of the brain is a major goal in neuroscience.

It took more than three decades to "invent" Francis Crick's "method" and to solve the issue of selective stimulation of neurons. The technique itself became widespread after Karl Deisseroth and his group published seminal papers introducing 'optogenetics' (Boyden *et al.*, 2005; Deisseroth *et al.*, 2006). This new method allowed the manipulation of a specific cells using light ('opto') after the introduction of an exogenous protein in neurons, (e.g. Channelrhodopsin-2), while controlling its expression with the use of specific promoters ('genetic'). Although the term 'optogenetics' was created to describe the technique in a way that could be easily understood and readily used by the research community (Miesenböck, 2011), it should be considered carefully, as this technique itself does not generally involve the direct interaction between light and the actual genome (Miesenböck, 2009) – even though this is currently also a possibility. More strictly, optogenetics refers to the combination of optics and genetic approaches to obtain gain or loss of function for well-defined events within specific cells of living tissue, to allow a better understanding of biological systems (Deisseroth *et al.*, 2006; Miesenböck e Kevrekidis, 2005). Commonly, optogenetic proteins fall in the category of - sensors - such as the Green Fluorescent Protein (GFP) or - actuators - such as Channelrhodpsin-2 (ChR2)

The original aspects and theoretical backdrop for optogenetics started in the 1970s, when it was acknowledged that light could be a suitable tool to control neuronal activity - much

like what happens in the retina. Neverhteless, no specific knowledge on how to turn cells responsive to light was available at the time (Crick, 1979). The experimental implementation of optogenetics materialized with the prospect of introducing the relatively simple invertebrate photoreceptor siganlling cascade into non-photon sensitive neurons (Zemelman *et al.*, 2002). This technique – chARGe – involves the transduction of the Drosophila cascade of photoreceptor genes formed by <u>a</u>rrestin-2, <u>r</u>hodopsin and the alpha-subunit of <u>G</u> protein (Zemelman *et al.*, 2002). However, this approach has several limitations, such as the delay in activating target neurons and the variability and complexity involved in recrating a three-protein pathway. Therefore, an ideal technique would involve rapid photoactivation, precise temporal control, high spatial resolution and simple genetic targetability. A central aspect towards this was the the work performed by microbiologists focusing on understanding the phototaxic behavior of algae (Deisseroth, 2011). The studies performed to purify, identify and clone several members of the light-sensitive protein family of rhodopsins was a key aspect in the discovery of the tools best suited for optogenetic applications.

Rhodopsins are membrane proteins from the opsin protein family that are responsible for the transduction of light stimulation. One of the best characterized member of this family is the Bacteriorhodopsin protein, a single–component ion pump (Oesterhelt e Stoeckenius, 1971), and Halorhodopsin, a light-gated chloride pump (Bogomolni e Spudich, 1982; Crick, 1979; Kolbe *et al.*, 2000; Matsuno-Yagi e Mukohata, 1977; Schobert e Lanyi, 1982). These two proteins Bacteriorhodopsin and Halorhosopsin are the prototypical examples of the rhodopsins largely used in optogenetic applications.

Georg Nagel and collegues, using kidney cell lines first demonstrated that ChR2 was a light responsive ion channel (kidney cell lines (HEK293 and BHK)) capable of inducing photocurrents (Nagel *et al.*, 2003). Deisseroth and collegues followed up on this study and highlighted the possibility of using this tool to control complex neuronal circuits (Boyden *et al.*, 2005). Neurons are naturally excitable cells with the capacity to respond to changes in membrane potential and it was expected that the same molecular instruments that were used to change the membrane potential in kidney cell lines, could also be applied to mediate action potential activation in neurons or in other types of excitable cells (Palczewski, 2006).

Nowadays, in a more simple way, it is possible to state that optogenetics uses light sensitive proteins that are used to stimulate or to identify neuronal activity when exposed to specific wavelengths of light (Deisseroth, 2011). The genetic code of the optically sensitive protein is added to the genetic material of a specific type of neuron to make it responsive to

light (Lin *et al.*, 2009), thus allowing manipulation of neural activity (Pashaie *et al.*, 2014). Exposure to one color, or wavelength, activates the genetically modified cell (Figure 1). This procedure is non-invasive and has the advantage of having reduced fatigue and lower tissue damage when compared to microelectrode stimulation (Li *et al.*, 2011; Llewellyn *et al.*, 2010). It also provides both higher accuracy and precision along with the high speed and targeting capabilities that are achieved using molecular genetic techniques (Deisseroth, 2011). Another key feature is the ability to affect, with an unparalleled precision, specific neurons at a specific time. For these reasons, optogenetics technology has been considered 'Breakthrough of the Decade' by Science (The News Staff, 2010) and 'Method of the Year 2010' by Nature Methods (*Nat Meth*, 2010).

Nowadays, optogenetics is being used across several fields, such as in neurodegenerative brain disorders like Parkinson's disease (Vazey e Aston-Jones, 2013), in understanding the functional analysis of stem-cell derived grafts (Steinbeck *et al.*, 2015) and also as a promising future treatment for seizures (Wykes *et al.*, 2012) and blindness (Roska *et al.*, 2013).
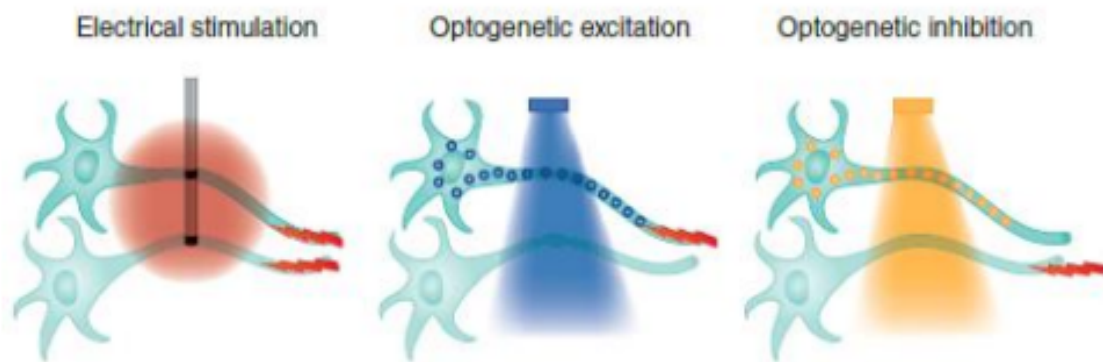
Figure 1 – Electric neural stimulation vs. Optogenetics. Electrical stimulation of neurons using electrodes, assuming that an electric field radiates outwardly in a uniform sphere any neuron or network within that sphere is unspecifically stimulated, including axonal fibers of passage. Optogenetic stimulation (e.g. for ChR2) or optogenetic inhibition (e.g. with Halorhodopsin), with specific wavelengths, presents specific and highly accurate mechanism for neuronal stimulation and inhibition. Adapted from (Deisseroth, 2011).

1.2   - The opsin family

Over time, evolution led organisms to develop the capability to perceive and respond to light. More than a century of scientific studies have focused on light sensitivity and how it regulate the behavior of organisms in reaction to light (Holmes, 1911). Light can affect single cell organisms (e.g. algae) as well as complex organisms like mammals. The perception of light allows entire range of organisms to react to environmental signals and to adapt their own behavioral responses. The cornestone of photodetection is normally supported throught the absorption of light by biomolecules such as chromophore.

Opsins belong to the retinylidene protein family and are one of the most studied, abundant and conserved protein families involved in this process. This family of light sensitive membrane receptors is characterized by its seven transmembrane helix structure (7TM) that features an internal pocket where a covalently linked retinal residue (vitamin-A aldehyde) works as a chromophore. The molecular complex of opsin bound to retinal is known as rhodopsin. Most known opsin genes come from bacterial or algal genomes, where they accomplish their roles as light-activated membrane ion channels.

Different members of opsins exist in prokaryotic and eukaryotic organisms. Therefore, the protein family can be divided into two large groups that share a certain degree of sequence homology. These two groups are type I opsins (microbial opsins) and type II opsins (animal opsins).

Type I opsins genes are expressed in prokaryotes, algae and funghi, and are responsible for distinctive functions such as energy storage, phototaxis and retinal biosynthesis (Spudich, 2006). Type I rhodopsins directly affect the cell or organelle membrane potential acting as direct light-gated channels. Type II opsins are primarily present in higher organisms; in humans, they are responsible for visual perception in a specialized subset of retina cells (Shichida e Yamashita, 2003). They also seem to be involved in processes like the circadian rhythm and pigment regulation (Hattar *et al.*, 2003; Terakita, 2005), detection of ambient light, season adaptation and phototaxis. Type II proteins indirectly influence transmembrane ion current throught coupling to G-protein based signal transduction pathways. This is a key difference between type I and II rhodopsins; type I proteins are not coupled to G-protein based signal transduction pathway but include in their structure direct-light-activated regulators of transmembrane ion conductance, such as the light-driven ion pumps or light-driven ion channels. The different types of microbial

rhodopsins will be analyzed later in this chapter. Retinal-binding proteins are the most effective light switches that have been used so far in optogenetics (Nogly e Standfuss, 2015).

The binding of retinal is one of the significant differences among type I and type II opsins. Type I opsin genes encode for proteins that use retinal in all-trans configuration, after photon absorption, retinal changes its conformation to a 13-*cis* configuration. Following activation, retinal returns to the all-*trans* state without dissociation from the protein.

On the other hand, type II opsin genes encode for G-protein coupled membrane receptors and retinal binding occurs in 11-*cis* state (Figure 2). With isomerization, retinal returns to the all-*trans* form resulting in changes to protein structure, allowing the initiation of a transducing cascade. This process results from conformation changes that allow protein-protein connections with their downstream protein, transducin.
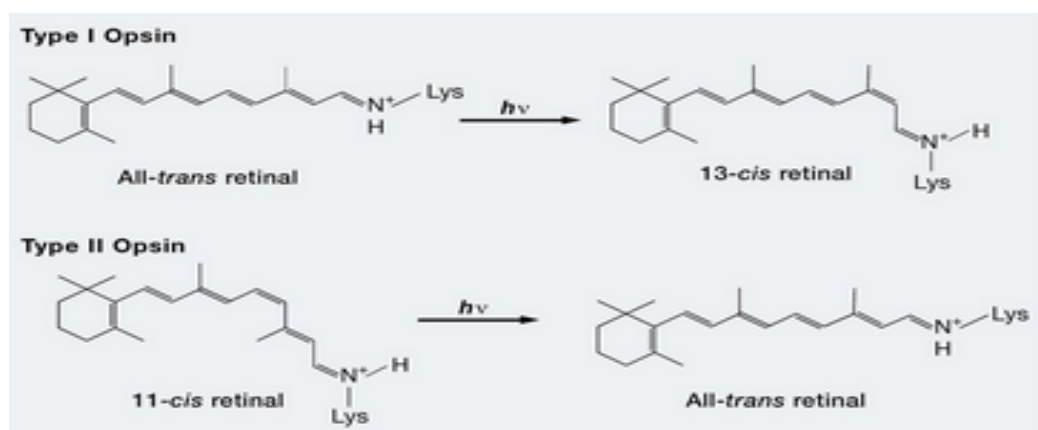
Figure 2 – Opsins structure. Chemical structure of different processes of isomerization between type I and type II opsin. In type I, light induction enables conformation of all-*trans* retinal to 13-*cis* retinal. In type II, protein chromophore conformation changes from 11-*cis* retinal to the general form all-*trans* retinal. Adapted from (Zhang *et al.*, 2011).

The light-driven proton pump bacteriorhodopsin is the best studied example of type I rhodopsins, and it provides a central reference for the study of other proteins in this class (Wickstrand *et al.*, 2015). In this case, light induces the isomerization of retinal from the all-*trans* to the 13-*cis* conformation, leading to the translocation of protons from the protonated Schiff base link to a hydrophilic pathway further across the proteins. In contrast, in a hyperpolarization protein like halorhodopsin, the inward transport of the negatively charged chloride is enabled by

stabilization of the positively charged protonated Schiff base, and retinal isomerization promotes its translocation along the hydrophilic path. This difference in the isomerization processes results in a difference in the mechanism through which the two types of rhodopsins induce downstream signaling (Figure 3).
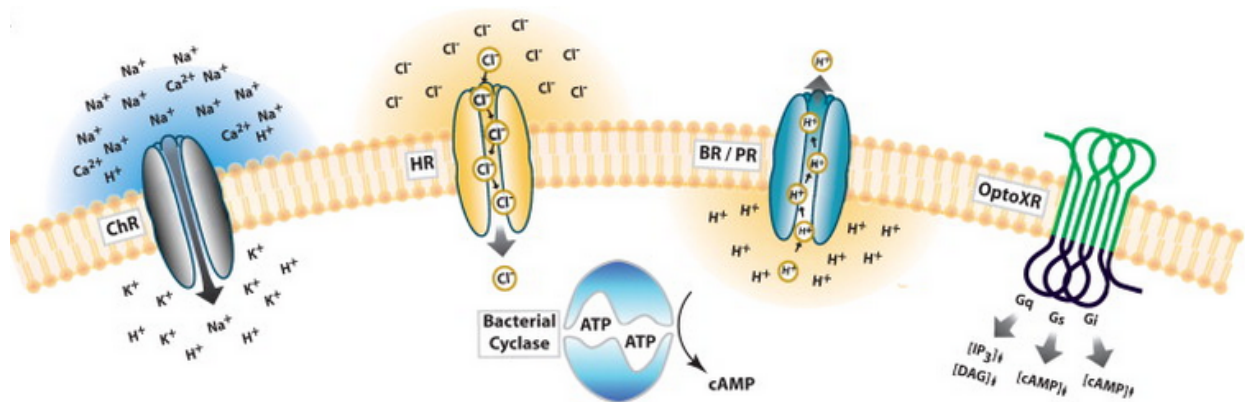
Figure 3 – Single-component optogenetics tool families. Illustrations of some members of type I and type II opsins with respective transported ions and signalling pathways indicated. Bacteriorhodopsin (BR), the haloarchaeal proton pump, was the first rhodopsin to be identified and the best studied type I protein. Its function is related to low-oxygen conditions, where BR is highly expressed in haloarchaeal membranes, and acts as part of an alternative energy production system, pumping protons from the cytoplasm to the extracellular medium to generate a proton-motive force to drive ATP synthesis. Halorhodopsin (HR) is a light-activated chloride pump. In contrast to BR, halorhodopsin (HR) direction of transport is done from the extracellular to the intercellular space. Channelrhodopsin (ChR) is a channel that conducts cations across the membrane along with the electrochemical gradient. The effective cation channel pore is opened, implying that an ion flux turns independently of retinal isomerization and rather depending on the kinetics of channel closure. OptoXR is a type II opsin, derived from protein chimera and used to hijack common signalling pathways, providing a precise control through light manipulation. G proteins, such as endocannabinoid and dopaminergic receptors, can be paired with optoXRs, simplifying the casual impact of intracellular signalling in the brain. Adapted from (Yizhar *et al.*, 2011).

1.3   Microbial rhodopsins

Bacteriorhodopsin (BR) was the first characterized microbial rhodopsin after being identified in the archeon *Halobacterium salinarum* (Oesterhelt e Stoeckenius, 1971). BR pumps one proton out of the cell per photocycle and the resulting electrochemical gradient is used to

drive the synthesis of ATP. This protein is a light-activated pump specialized in proton translocation from intercellular to extracellular cellular environment, and in maintaining a proton gradient across the membrane and, therefore, ATP synthesis and energy recovery in adverse conditions (e.g. low-oxygen) (Michel e Oesterhelt, 1976). For instance, using *Xenopus laevis* oocytes, it was possible to characterize the light induced photocurrent of this rhodopsin pump using a voltage-clamp technique (Nagel *et al.*, 1995). Bacteriorhodopsin transition states during retinal isomerization were also analyzed by real-time spectroscopy (Kobayashi, Saito e Ohtani, 2001). Bacteriorhodopsin research was crucial to the development of better tools for optogenetics and it remains a focus of interest.

Subsequent to bacteriorhodopsin, other rhodopsins were found and characterized in *Halobacterium salinarum*, these include halorhodopsin (HR) (Matsuno-Yagi e Mukohata, 1977) and sensory rhodopsin (Bogomolni e Spudich, 1982; Wolff *et al.*, 1986). Halorhodopsin is an inward-directed chloride pump with the ability to hyperpolarize the cell membrane first discovered in archaebacteria. This protein can be used to silence neuronal activity in response to yellow light. The operating principles of halorhodopsin are similar to those of bacteriorhodopsin (Essen, 2002); nonetheless, halorhodopsin pumps chloride ions and the direction of transport is from the extracellular to the intracellular space (Schobert e Lanyi, 1982). Consistently, specific amino acid residues have been shown to underlie the differences between halorhodopsin and bacterirhodopsin in directionality and preferred cargo ion (Sasaki *et al.*, 1995). Sensory rhodopsins are involved in phototaxis, the capability of the organism to sense changes in the intensity of light and are responsible for the response to different wavelengths, thus enabling movement towards or away from light (Ruiz-González e Marín, 2004; Spudich *et al.*, 2000; Spudich e Luecke, 2002).

Several studies focusing the rhodopsins have generated a substantial understanding on the mechanisms controlling the activity of these proteins. Bioinformatics, genome sequencing and continuous study of several other organisms also corroborate the new discoveries and the extensive presence of homologous rhodopsins in additional domains like Bacteria and Eukarya (Jung, Trivedi e Spudich, 2003; Sineshchekov, Jung e Spudich, 2002). Hence, analogues of BR with the ability to translocate protons using light have been found not only in *Archaea* but also in many other organisms, such as proteorhodopsin from the γ-Proteobacteria (Béjà *et al.*, 2000). Rhodopsin genes are strongly conserved, mainly the amino acid structure in the retinal-binding pocket. Their presence has been found in several environments and in a widespread phylogenetic array of microbial life, including cyanobacteria and green algae. Interestingly, it was

in the soil and fresh wild water that the most important rhodopsin used in optogenetics was discovered - the cation conducting channelrhodopsin from *Chlamydomonas reinhardtii* algae.

1.4 – Channelrhodopsins

Ideal light-gated actuators to be used in the "method" idealizd by Francis Crick would then be monolithic proteins, rather than multicomponent signalling cascades. The most useful of these tools were to be found in branches of biology far removed from neuroscience: the study of phototropism in unicellular algae and research on light-driven ion transport in halophilic archaebacteria.

Phototaxis in algae was first considered four centuries ago when several species were analysed for their behaviour when exposed to light (Hegemann e Nagel, 2013). Organisms can move towards or away from a light source, and this is defined as positive or negative phototaxis, respectively. Following this research topic, it was found that, after illumination, many algae changed their swimming direction and stood parallel to the direction of light. This led to the suggestion that this behaviour could be significant and pertinent (Schaller, David e Uhl, 1997) (Figure. 4).

The interference of cations, such as calcium, as essential components in this mechanism have been addressed (Foster e Smyth, 1980). Also, it was found that when recording photocurrents in *Chlamydomonas reinhardtii* algae there is negligeble delay between photostimulation and the observed currents, leading to the notion that light sensitive proteins in this process are probably connected and functioning as a protein complex or even a singular monolithic protein, with the photoreceptor and the channel forming a single structure, permeable to some kind of ions when illuminated (Harz e Hegemann, 1991). Additionally, in Schaller's experiment (Figure 4), a strain expressing a channelrhodopsin defective mutant presented no phototactic response at all. In fact, a key moment in optogenetics was when the structure of this microbial channel opsin was resolved, allowing further engineering methods and experimentation (Berndt *et al.*, 2014; Kato *et al.*, 2012; Wietek *et al.*, 2014).
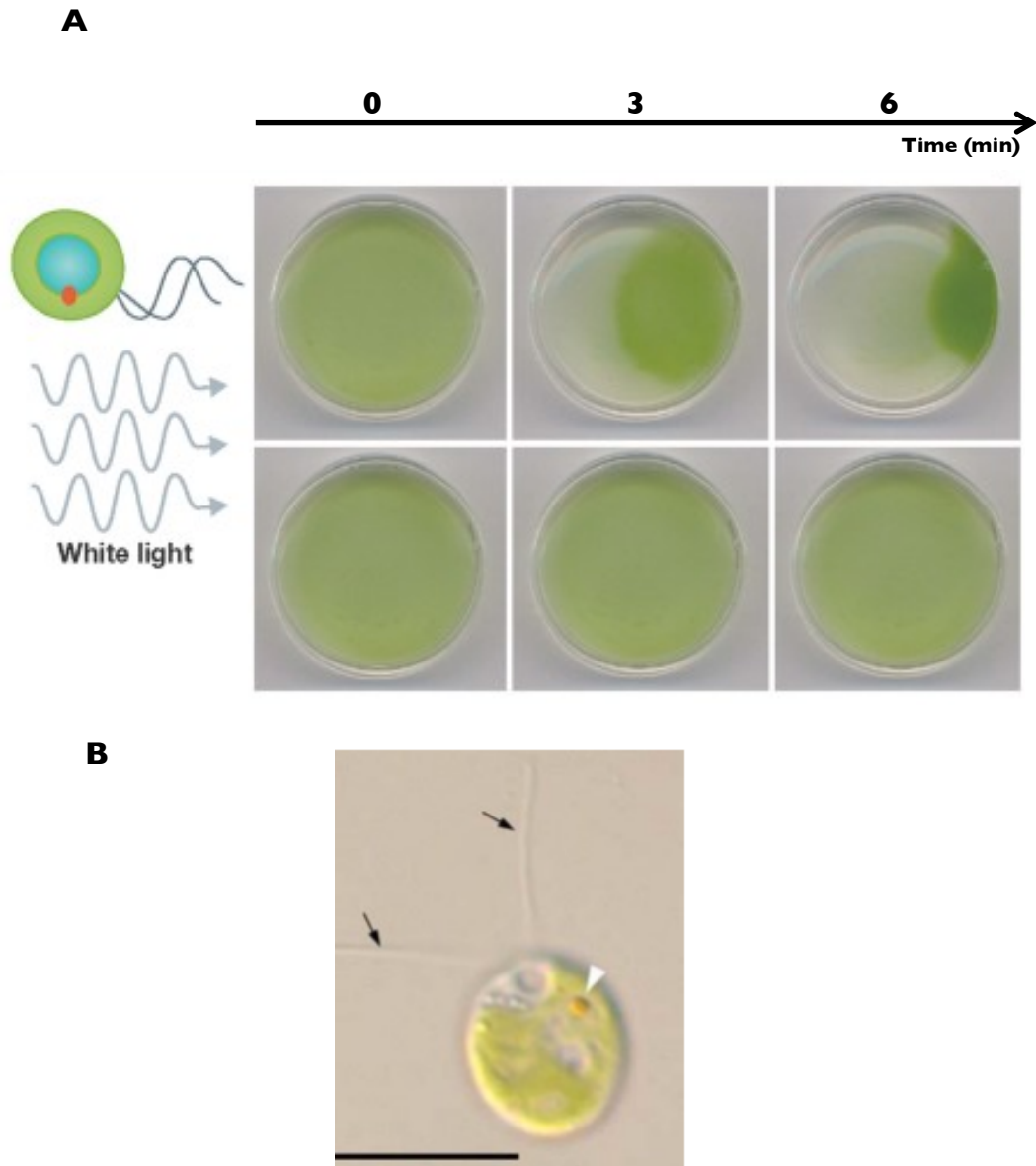
Figure 4 – Phototaxis in *Chlamydomonas reinhardtii* algae. (**a**) Phototactic behaviour of wild type strain *Chlamydomonas* in culture, when briefly exposed to high light intensity (first row). No phototactic behaviour is observed in algae expressing a defective mutant of channelrhodopsin (bottom row) (adapted from (Hegemann e Nagel, 2013)). (**b**) Image of microalgae *Chlamydomonas reinhardtii* in a scale bar of 10 μm. Rhodopsins are localized in the orange eyespot (white arrow). Under physiological conditions, Ca^{2+} ions are transported into the cell through light-gated cation channels, thus activating voltage sensitive channels in the flagella membrane (black arrow). The subsequent influx of Ca^{2+} into the flagella leads to a switch in movement (phototaxis) (Kateriya *et al.*, 2004) (adapted from (Kreimer, 2009)).

Chlamydomonas has long been a favourite organism for genetic and biochemical studies of flagellar motility and assembly, photosynthesis and organelle genomes. In particular, this specific strain, as well as other green algae species, show two main motility responses to light: phototaxis and photophobic response (Witman, 1993). Phototaxis is characteristic of algae and can be defined as the oriented swimming of cells along the direction of a light source, whereas the photophobic response is expressed as the reorientation of swimming cells, induced by an abrupt or strong increase of light intensity (Hegemann, 1997). This specific behaviour in these unicellular flagellated organisms is only achievable due to the presence of a system of photoreception inside the eyespot structure of algae (Hegemann, 1997).

Perception of light generated by this photoreceptive organelle helps the cells find an environment with optimal light context for photosynthesis. Eyespots can be considered the simplest, most common and primordial "eyes" established in nature, with its own structure composed by photoreceptors and areas of pigment granules (Kreimer, 2009). They are directly coupled to the algae flagella, and a phototactic response is generated by signals that, when transmitted from the eyespot photoreceptors, result in an alteration of the movement patterns of the flagella (Hegemann, 1997). In normal conditions, algae have a specific rotational movement around their own axis, however, when the eyespot perceive light, it disturbs flagella to adjust their swimming position from perpendicular to parallel to light (Schaller, David e Uhl, 1997). Initial studies had shown that calcium is involved in the regulation of the flagella characteristic beating (Schmidt e Eckert, 1976). Later, Hegemann's group elucidated this natural apparatus and proposed that there are two different photocurrents activated by calcium: one in the eyespot (photoreceptor current) and the other in the flagella (flagellar current). Hence, calcium and H^+ (Ehlenbeck *et al.*, 2002) mediate both photocurrents, whereas Ca^{2+} inhibitors supress the last ones. This suggest that the photoreceptor and flagellar currents are carried out by this component and that they mediate the single transduction chain regulated by rhodopsin, that is responsible for the cellular conduction under diverse light environments (Holland *et al.*, 1997; Nonnengässer *et al.*, 1996). Altogether, these different studies support the idea that photocurrents are mediated by rhodopsins with a photoreceptor role.

With a noticeable growing interest on this topic and following the use of cDNA libraries and DNA sequencing in more recent studies, new sequences encoding for microbial rhodopsins have been proposed using bioinformatics and information assembled from known opsins. Channelrhodopsin-1 (ChR1) (Nagel *et al.*, 2002) and Channelrhodopsin-2 (Nagel *et al.*, 2003) are two major examples of all the effort put together in this area. The nucleotidic sequences of

ChR1 and ChR2 were revealed in a large scale sequencing project in *C. reinhardtii* and were submitted to GenBank by the Hegemman's group, as well as by two other groups (Sineshchekov, Jung e Spudich, 2002; Suzuki *et al.*, 2003). Analysis of the *C. reinhardtii* genome database revealed two new cDNA sequences encoding apoproteins with a certain homology to microbial opsins and high conservation of amino acid residues forming the retinal-binding pocket: channelopsin-1 (Chop 1) and channelopsin-2 (Chop 2) (Nagel *et al.*, 2002). This study also showed that the expression of Chop 1 in oocytes of *X. laevis* produced a light-gated conductance that was highly selective for protons, implying that channelrhodopsin-1 (ChR1= Chop 1 + retinal) was the photoreceptor system that mediated the H^+ carried photoreceptor current (Nagel *et al.*, 2002). Moreover, it has been observed that both ChR1 and ChR2 (ChR2= Chop 2 + retinal) contribute to the photoreceptor currents, in an electrical cell population assay monitoring the differential response of cells facing light versus cells facing away from light (Sineshchekov, Jung e Spudich, 2002). ChR1-deprived cells photocurrents at high lash intensities were reduced, whereas ChR2-deprived cells photocurrents at low flash energies were reduced. Based on these findings, it was determined that ChR1 mediates the high-intensity response, whereas ChR2 is accountable for low-intensity photocurrents (Sineshchekov, Jung e Spudich, 2002). Later, antibodies against Chop1 and Chop were generated, boosting the creation of a model structure and enabling intracellular localization with specific membrane protein detection and recognition of its respective size in enriched eyespot membranes (Suzuki *et al.*, 2003).

Differently from the previously mentioned microbial opsins that work as light- driven ion pumps, channelrhodopsins act as light-driven channels. ChR1 is a light-gated proton channel, while ChR2 is a channel with particular ion selectivity, a single-protein membrane channel receptive to blue light. In 2005, the latter was recognized as a tool for genetically targeted optical remote control of neurons, neuronal circuits and behaviour. Karl Deisseroth's lab showed that ChR2 could be expressed to control mammalian neurons *in vitro*, achieving temporal precision on the order of milliseconds (Boyden *et al.*, 2005). This was a key finding, as all opsins demand retinal as the light-sensing co-factor and it was uncertain whether central mammalian nerve cells would contain enough retinal levels. Hence, it was demonstrated that ChR2 expressed in mammalian neurons could be used in the precise and reliable control of action potential firing in response to light pulses in vertebrate systems, without the necessity of exogenous retinal (Boyden *et al.*, 2005). Subsequent observations from the Nagel (Nagel *et al.*, 2005) and Hegemann groups (Li *et al.*, 2005) additionally established the ability of ChR2 to control the activity of vertebrate neurons.

Upon light stimulation, ChRs work as inward, nonspecific cation channels that can support neural depolarization (Nagel *et al.*, 2002), thus they were quickly adapted to neuroscience research, as expression of ChRs in neurons can support action potentials following millisecond pulses of blue light (Nagel *et al.*, 2003). Nagel's lab also expressed ChR2 in human kidney and other mammalian cells, showing large light-induced membrane depolarization and suggesting that, when expressed in cells of other organisms, ChRs could enable the use of light to control electrical excitability, intracellular acidity, calcium influx and other cellular processes.

Besides ChR2, other channelrhodopsins were discovered and successfully used in mammalian neurons, like VChR1 from *Volxox carteri* (Zhang *et al.*, 2008) and MChR1 from *Mesostigma viride* (Govorunova *et al.*, 2011). However, at the moment, ChRs are the only known protein channels directly gated by light, which renders them a very useful tool for optogenetic manipulation of the nervous system.

The key features of the structure of the ChR protein and its own specific mechanism of action, related to several engineered variants of ChRs, are going to be addressed and explored in the following section.

1.4.1 – Protein architectural design

Rhodopsins share similar structural features, composed by an opsin apoprotein and a retinal chromophore (Spudich *et al.*, 2000), and channelrhodopsin is no exception. Channelrhodopsins are protein channels expressed throughout the cell membrane, with a structure of seven-transmembrane α-helix topology.

The retinal chromophore molecule is covalently linked to an amino acid residue that works as a Schiff base connected to the protein backbone by a N=C bond. This vitamin A aldehyde is accountable for the absorption properties of the protein in the visible range of the electromagnetic radiation spectra. Modification of the opsin absorption spectra, by modulation of the electronic environment around the retinal molecule, represents an appealing target for protein engineering tactics.

Channelrhodopsin-2 is an 80 kDa protein, consisting of 737 amino acids, localized in the cell membrane. The protein has two domains: a membrane-spanning N-terminal portion

(nChR2$_{1-307}$) and a cytosolic C- terminal portion (cChR2$_{307-737}$) (Figure 5).
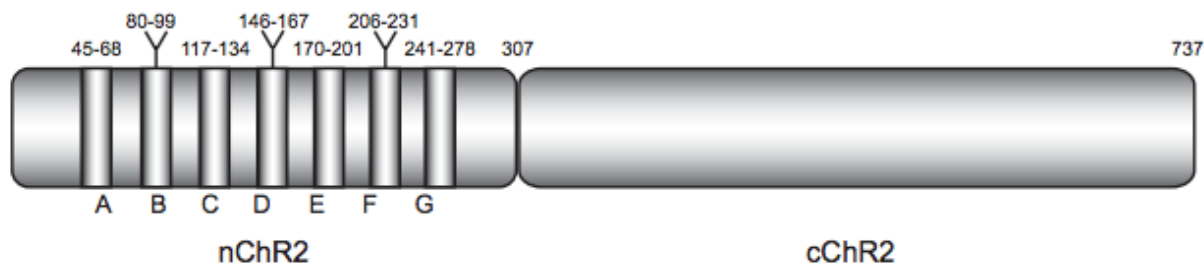
Figure 5 – Channelrhodopsin-2 end-terminals. Schematic view of the structure of the native ChR2 from *C.reinhardtii*. The left part represents the N-terminal (nChR2), with its 7TM helices at their respective site, in line to the X-ray structure of the ChR1-ChR2 chimera C1C2 by (Kato *et al.*, 2012). The right part of the figure represents the 430 amino acids that constitute the cytosolic cChR2 domain of the protein (from (*Introduction*, [s.d.])).

The nChR2 domain has similarities to certain regions of type I rhodopsin, both at the structural and sequence levels, such as the proton pump bacteriorhodopsin. It also has seven transmembrane helices, a feature that is characteristic of the ChR2 group of proteins. These seven transmembrane domain form an internal pore where the retinal molecule can bind, enabling the light-gated properties of the channel.

The cChR2 domain has shown no similarity with any known protein families so far, and it does not influence the channel function of the protein (Nagel *et al.*, 2005, 2003). For this reason, the amino acids of the cChR2 domain are usually removed in most ChR2 variants created and used for optogenetics.

Most research groups work with a humanized and truncated version of ChR2 (Figure 6). The light-absorbing chromophore is embedded within the hydrophobic center of the 7TM and the retinal molecule is connected to a conserved lysine via Schiff base linkage, which is protonated to shift the absorption into the visible range of the spectrum. The resulting color of this protonated retinal Schiff base (RSB) is fine-tuned by the distance of the negatively charged counter ion that together form the active site and also by the location of some polar residues nearby the retinal polyene chain (Figure 6).

When retinal absorbs light, isomerization of this molecule occurs, resulting in a specific

protein conformational change, opening the ion pore, as discussed in section 1.2. (Figure 2). These structural changes also include the closure of the conducting pore and the return to the dark state. The pathway for this opposite reaction differs from the initial opening path, and kinetics of dark state recovery are significantly slower (Hegemann e Nagel, 2013). Internal and external pH are known to influence the closure of the ChR2 channel, as well as the recovery after desensitization (Nagel *et al.*, 2003). Moreover, the OH-cluster and the residues C128 and D156 (DC-pair) have a central importance in both the opening and closing of the pore.

Bovine rhodopsin (Okada *et al.*, 2004) and BR (Nishikawa, Murakami e Kouyama, 2005) had their crystal structures identified first, allowing preliminary approaches to comprehend the structure of ChR2 based on sequence comparison, homology models and bio-computational techniques. Hence, it is considered that channelrhodopsin pioneering structural information was first obtained from homology modeling studies based on already known structures of other microbial rhodopsins (Plazzo *et al.*, 2012; Watanabe *et al.*, 2012). Regarding ChR2 engineering, mutation of any of these residues could result in a dramatic increase of the open state lifetime.

Remarkably, it was also found that isolating both retinal and the protein, each one absorbs primarily in the beginning of the UV range spectra (~380 nm) but, when bound together, forming the retinal binding pocket, they induce a red-shift in the retinal absorption spectrum. This outcome is known as "opsin shift" (Watanabe *et al.*, 2012) and is assumed to result from the conformational manipulation of the chromophore, the direct electrostatic interfaces settled between the adjacent protein residues and the retinal molecule (Wang *et al.*, 2012).
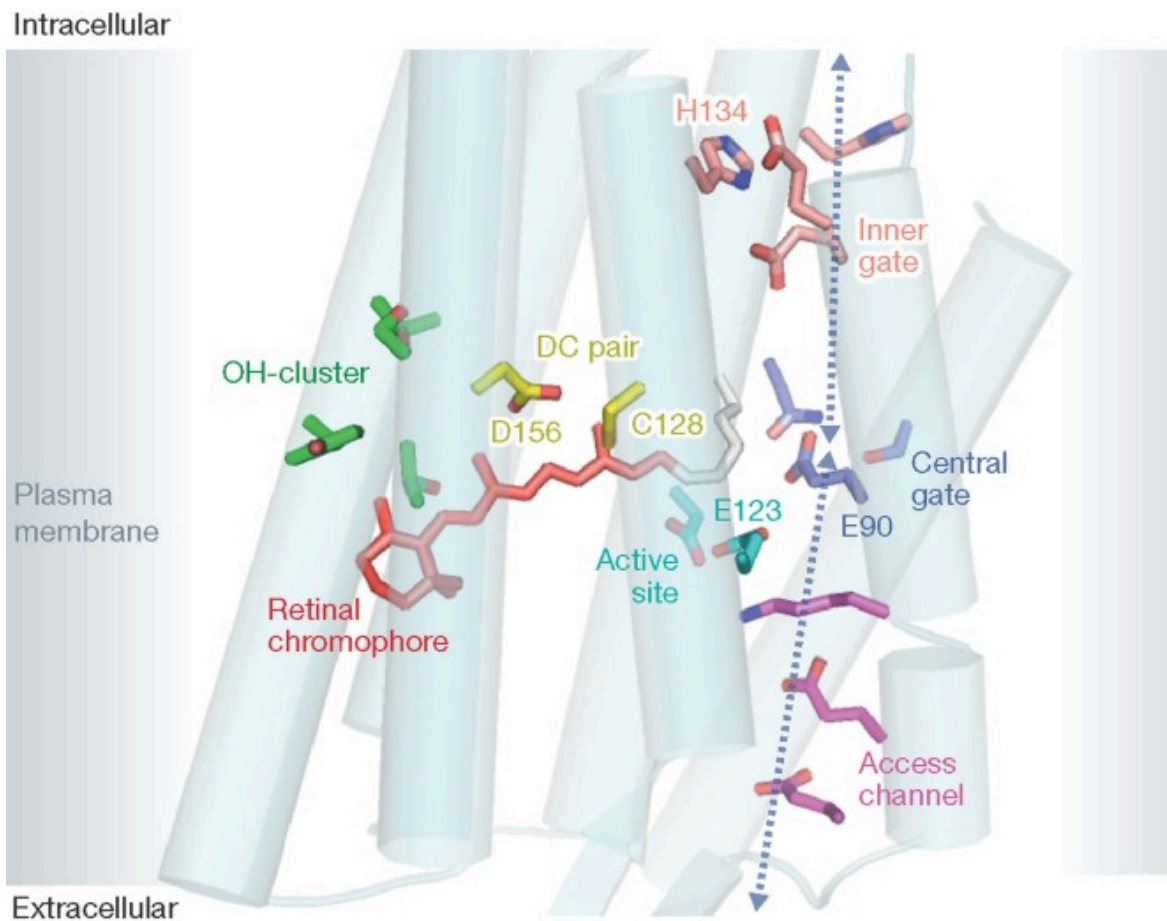
Figure 6 – Channelrhodopsin structure. Illustration of the seven transmembrane fragment of ChR highlighting the chromophore pocket. The c-terminal of ChR2 extends into the intracellular space and can be replaced by fluorescent proteins without affecting channel function. Hence, most used ChR2 forms are truncated in relation to the original protein recognized in *C. reinhardtii*, such that only the N-terminal part of protein is present. The structure and aminoacid numbering is represented according to the C1C2 chimera proposed by (Kato *et al.*, 2012). Key residues are shown in colour: voltage sensor E123 (cyan), residues of the access channel (magenta), central gate (blue) and inner gate (orange), OH-cluster (green), and finally the retinal Schiff base (RSB) is seen in red colour (adapted from (Hegemann e Nagel, 2013)).

Notwithstanding all collected knowledge on the structure of ChR2, more precise and accurate models are still needed. Elegant techniques such as the approach presented in this work, the *Ab initio* design using Time-dependent Density Functional Theory can be a conceivable methodology towards improved models.

In 2011, a projection of ChR2 structure was determined for the first time, using electron crystallography at 6Å resolution. This projection map, when compared to the one from BR confirmed that ChR2 was indeed formed by seven transmembrane helices, as all other known

17

microbial rhodopsins (Müller *et al.*, 2011). Next, the first crystal structure of a ChR2 was described (Kato *et al.*, 2012), based on a chimeric form of ChR1 and ChR2 (C1C2 chimera). This study reported the conformation of the ChR2 light-gated channel underlying the structural features of the C1C2 chimera. This primary ChR sequence can be considered similar to BR structure (Figure 7), with the end part of the 7TM being shifted to the central axis of the monomer (Kato *et al.*, 2012).

There are additional differences between BR and ChRs, such as the extracellular ends of TM1 and TM2 in C1C2 being tilted outwards. These tilts result in the enlargement of the cavity formed by the transmembrane domains, allowing water influx for the transport of cations (Kato *et al.*, 2012). The crystal structure of C1C2 revealed also the presence in the N-terminal domain of β-sheets that might contribute to dimer stabilization (Kato et al., 2012).
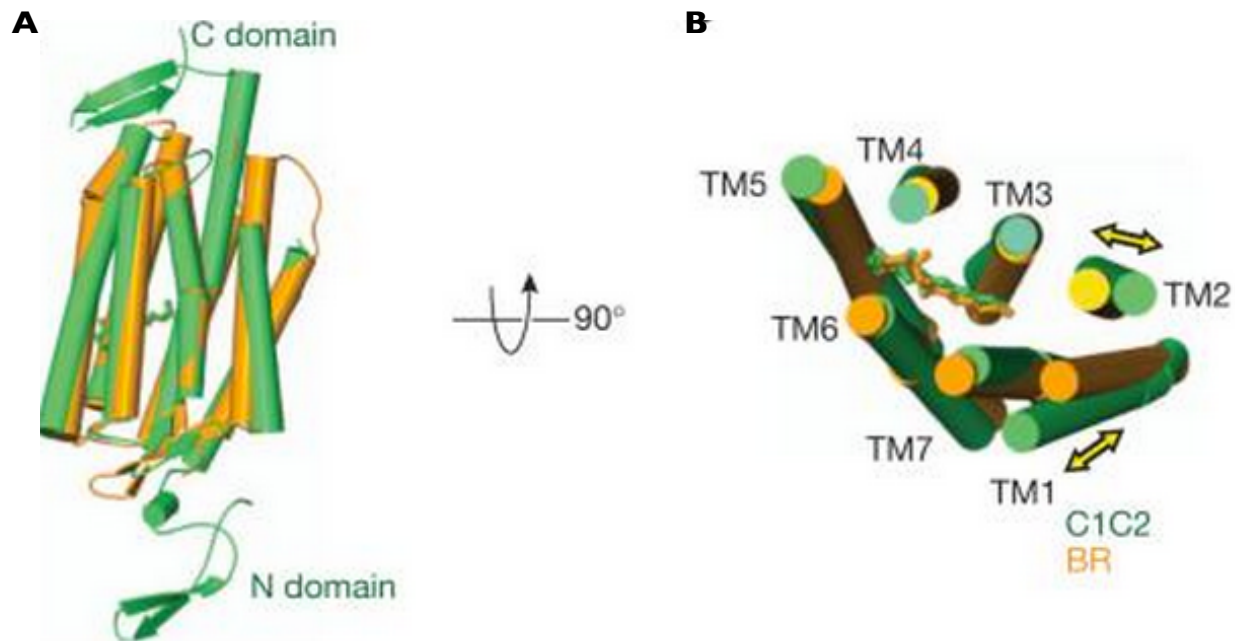
Figure 7 – C1C2 vs. BR structure. Side view (**a**) and extracellular view (**b**) of the superimposed TMs of C1C2 (green) and BR (orange). The yellow-paired arrows specify the shifts of the extracellular parts of TM1 and TM2 (adapted from (Kato *et al.*, 2012)).

1.4.2 Retinal binding pocket

The retinal molecule links covalently to the protein structure, working as its chromophore. This feature is shared by all rhodopsins, as all-*trans* retinal is covalently bound to Lys 296 (257) on TM7 (to refer to ChR2 numbering sequence it is subtracted 39 from the C1C2 residue number sequence), establishing the Schiff base connected to the protein through a N=C bond). Interestingly, the TM7 is highly conserved in type I rhodopsin.

Furthermore, five aromatic residues (Trp 163, Phe 217, Trp 262, Phe 265 and Phe 269) are positioned nearby the polyene chain and the β-ionone ring, forming a hydrophobic pocket for all-trans retinal (Figure 8 d). Moreover, the residues Cys 167 (128), Thr 198 (159) and Ser 295 (256) form a less-hydrophobic pocket (Figure 8 d), and could be responsible for the "opsin shift", and contribute some specific kinetic properties of the channel (Hegemann e Möglich, 2011; Kato *et al.*, 2012; Watanabe *et al.*, 2012).

As mentioned above, the C1C2 chimeric protein conserves the same arrangement as BR where a water molecule receives a proton from the protonated Schiff base and donates this same proton to an amino acid near the retinal binding pocket. Moreover, a specific residue was also identified, Asp 292, as the primary proton acceptor to the Schiff base, resulting from its proximity to Lys 296, and consistent with the abolished photocurrents derived from mutations in the C1C2 chimera (Kato *et al.*, 2012).

The retinal binding pocket structure is the light sensing foundation of the channel, and is responsible for the distinctive absorption properties of the protein. In the previous section, we discussed the "opsin shift", a process that enables a change in retinal absorption depending on the environment around the molecule. This effect is not yet completely understood, but it seems that the shift in the absorption spectra and the wavelength regulation is a result of the conformational manipulation of the chromophore and of the electrostatic interactions that occur in the retinal binding pocket (Welke *et al.*, 2011). Hence, changes in the protein properties targeting this same chromophore pocket will be discussed in the following sections.
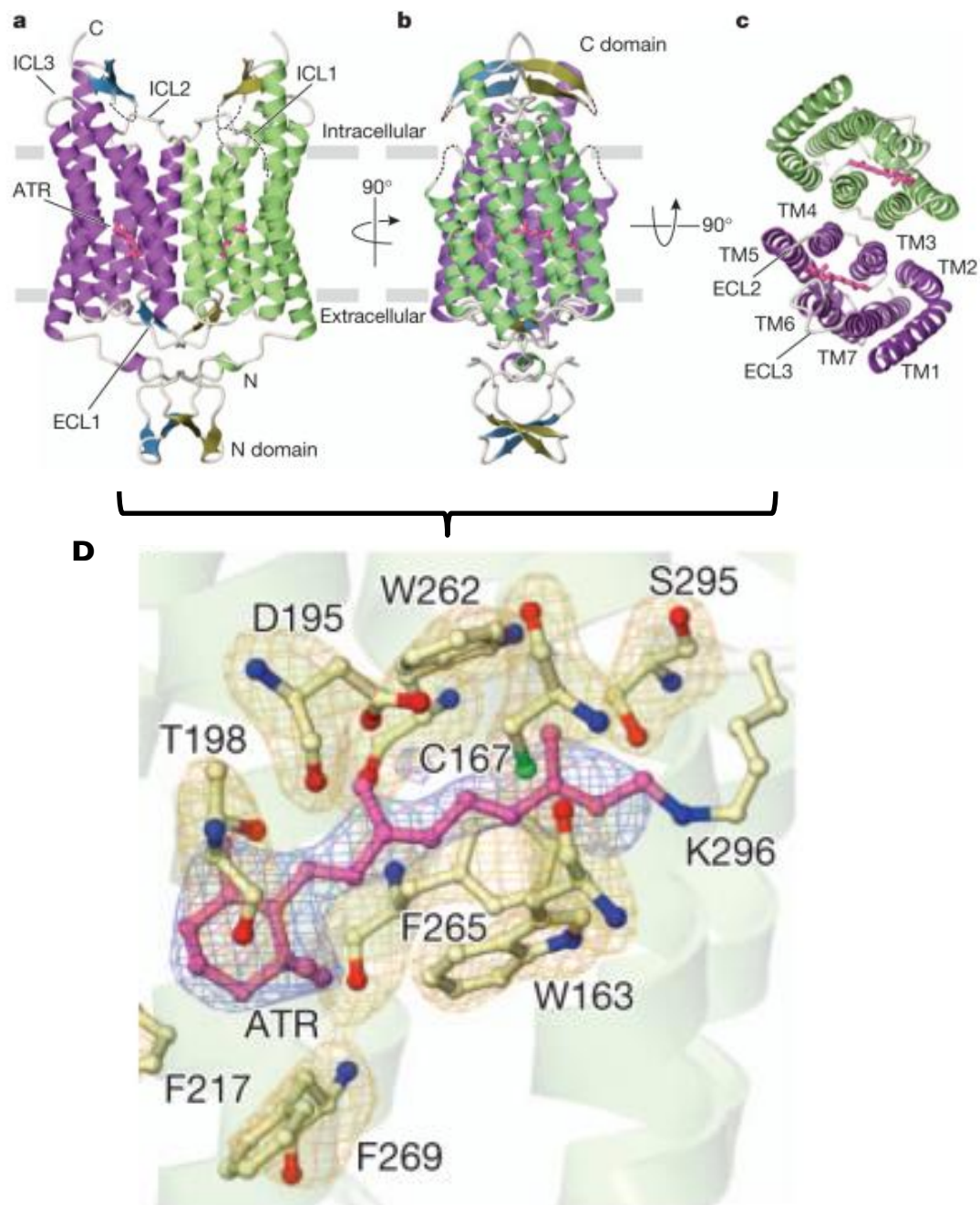
Figure 8 – The retinal-binding pocket. The structure of the C1C1 chimera consists on the five transmembrane domains of ChR1 and the last two of ChR2 (the ~400 a.a. C-terminal part was excluded). **a–c**, Crystal structure of the C1C2 dimer, viewed parallel to the membrane from two angles (**a, b**), and viewed from the extracellular side (**c**). The C1C2 truncated chimera consists of the N domain, the seven transmembrane helices (TM1–TM7) connected by extracellular loops (ECL1–ECL3) and intracellular loops (ICL1–ICL3), and the intracellular C domain. Disordered regions are represented as dotted lines. The all-*trans* retinal (ATR) is indicated in pink. **d**, Close-up on the structure of the retinal-binding pocket of C1C2, with an omit map of ATR at 3σ and of

the surrounding residues (subtract 39 from the C1C2 residue number to obtain ChR2 numbering) at 3.5σ (adapted from (Kato *et al.*, 2012)).

1.4.3   The Ion-Conducting pore

Channelrhodopsins allow a precise control of neuronal activity using light, but a complete and exhaustive understanding on how the protein channel is gated is lacking. Channelrhodopsins have seven transmembrane domains organized to form an inner pore, and that is stabilized by electrostatic interactions (Catterall, 1995). This pore is more permeable to cations than anions, which suggests that a highly electronegative region must form the pore structure.

Several studies have identified specific residues that may contribute to the formation of the ion pore (Watanabe *et al.*, 2012). These identified residues are Glu 90 (Eisenhauer *et al.*, 2012), Glu 97, Glu 101 (Watanabe *et al.*, 2012), Asp 156, Asp 253, His 134 and Glu 123 (Hegemann e Möglich, 2011), and are all considered vital for the kinetic proprieties of the protein, as part of the ion channel.

Based on the C1C2 structure model proposed by H. Kato, an electronegative region/pore was found to be constituted by TM1, TM2, TM3, and TM 7, rich in twelve charged and polar residues (Gln 56, Thr 59, Ser 63, Glu 83, Glu 90, Lys 93, Glu 97, Glu 101, Glu 123, Thr 246, Asp 253 and Asn 258), with the main contribute to the pore formation coming from five glutamic acid residues of the TM2 (Glu82, Glu83, Glu90, Glu97 and Glu101) (Watanabe *et al.*, 2012). These residues are positioned in the interior part of the protein and seem to connect, align and establish a tough hydrophilic and electronegative surface that might be included in the stabilization of cation species. This was supported by mutagenesis studies in which some of the identified residues were swapped, resulting in a loss of conductance and ion selectivity (Kato *et al.*, 2012; Ruffert *et al.*, 2011).

Besides the aforementioned electronegative side chains, other polar residues were found, located in the central part of the pore (Q56, T59, S63, E83, K93, T246, N258 and Y70). These residues form two constriction sites in the cytoplasmic side of the channel and are responsible for the gating of the channel, through their interactions (Kato *et al.*, 2012). Other studies combining bioinformatics, ChR2 and mutant forms of this protein suggested that, besides

the Gln 56 and Ser 63 residues, other residues, such as Asn 258 and Thr 250, could have a role in channel selectivity (Plazzo *et al.*, 2012).

The X-ray structural model in the closed state, proposed in 2012 (Kato *et al.*, 2012) marks an important step in understanding channelrhodopsin structure and mechanism, and has served as a basis for several studies in this area. More recently, the early formation of the ion-conducting pore of ChR2 was revealed. Indeed, the open state structure is presented and the early formation of the ion-conducting pore is clarified in atomic detail using time-resolved FTIR spectroscopy (Kuhne *et al.*, 2015). Photoisomerization of the retinal-chromophore causes a downward movement of the highly conserved E90, which opens the pore. Molecular dynamic simulations show that water molecules invade through this opened pore, Helix 2 tilts and the channel fully opens within milliseconds. As E90 is a highly conserved residue in the ChR2 structure, the proposed E90-Helix2-tilt model (Figure 9) could describe a general activation mechanism, providing a new path for additional mechanistic studies and protein engineering focusing on mutation of the amino acid E90 to control the properties of the protein in a targeted manner (Kuhne *et al.*, 2015).
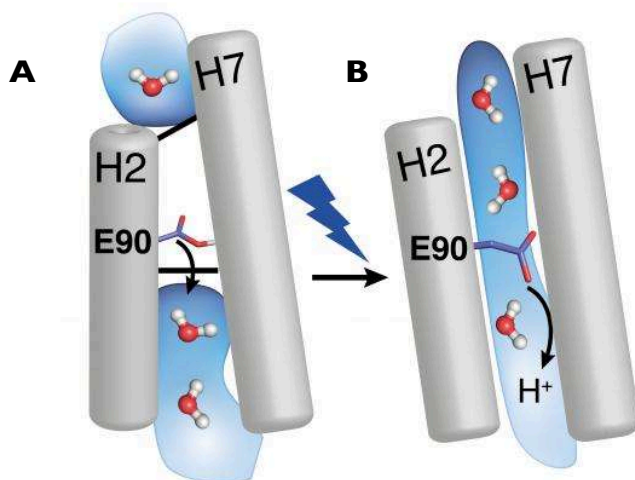
Figure 9 – The E90-helix 2-tilt model of action of ChR2. Water molecules are shown in colour, protein transmembrane helixes are shown in grey and protonated (**a**) and deprotonated (**b**) E90 residue is presented in purple in both centre of left and right image; The pore of the ion channel is opened by detaching the amino acid E90. Water molecules are transported and tilt Helix 2, therefore opening the continuous channel. The light-sensitive retinal is twisted under incidence of light. This twist then continues in the protein and opens rapidly a pore, which is closed by amino acid E90 in the dark. E90 marks the narrowest place in the pore and opens it through a downward move, similar to the motion of a "swing door", so that water can enter an empty vestibule above the narrowest place in the pore. The entering water then tilts the protein helix H2, which eventually triggers a protein-traversing open ion channel (adapted from (Kuhne *et al.*, 2015)).

1.4.4   Channelrhodopsin-2 photocycle

A few years before the discovery and publication of the crystal structure of ChR2, several studies had already focused on the specific mechanisms of the protein (Hegemann, Ehlenbeck e Gradmann, 2005; Nikolic *et al.*, 2009). Channelrhodopsin-2 has specific properties such as the ability to change its conformation to become permeable to a wide range of ionic species (Nagel *et al.*, 2003). Upon light stimulation, the mechanisms affecting the channel and all its structural modifications if called a "photocycle" (Watanabe *et al.*, 2013).

One of the most important questions about light-gated ion channels is related to the coupling between light activation, protein action, and the way the spectral properties can be associated with the opening and the closing of the channel (Bamann *et al.*, 2008). Recently, the photocycle of ChR2 has been widely studied using specific techniques as absorption and vibrational spectroscopy (Bamann *et al.*, 2008; Radu *et al.*, 2009; Ritter *et al.*, 2008; Verhoefen *et al.*, 2010). The known triggering event of this cycle is the absorption of a photon, which leads to light-induced isomerization of retinal from all-*trans* to 13-*cis* and its thermal isomerization to the initial all-*trans* state (Hegemann e Möglich, 2011). This cyclic reaction comprises several thermally unstable intermediates and the complete reaction is determined by light energy absorption and storage of a portion of this energy in the protein. Part of this energy is used to drive the photocycle, whereas the other part is transformed in energy that is essential for ion transport (Haupts *et al.*, 1997). Hence, this process is initiated by light absorption associated with electronic excitation and polarisation of the existing retinal chromophore.

In general, the chromophore relaxes by isomerising, most likely from all-trans to 13-cis resulting in the first intermediate P500 which is slightly red-shifted compared to the dark state D470 (the numbers represent the absorption maximum) (Nack *et al.*, 2009). As mentioned above, the retinal molecule is covalently linked to a lysine in helix VII via a Retinal Schiff Base (RSB) and embedded within the helices in the retinal binding pocket. Within microseconds, the RSB is deprotonated upon formation of the UV-absorbing P390 intermediate, which is also connected to structural changes of the protein backbone. P390 is in equilibrium with the conducting P520 state where the RSB is again reprotonated.

Alongside the passive transport of cations, that, under physiological conditions, is directed towards the intracellular side of the membrane, ChR2 has been proposed to act as a weak proton translocator where the proton on the RSB leaves on the extracellular side and

upon formation of P520 state, takes up on the intracellular side (Feldbauer *et al.*, 2009; Nack *et al.*, 2012). The closing of the channel (in milliseconds) involves the two intermediates P480a and P480b with absorptions similar to D470, and adaption of the structural rearrangements of the protein helixes, enabling the conduction of cations. The photocycle is complete after roughly a minute, which is considerably slower than proton-pumping rhodopsins like bacteriorhodopsin.

Several models for this mechanism have been suggested, one example is the two-cycle model based on ChR2 photocurrents, involving two open states of the channel with different ion selectiveness (Berndt *et al.*, 2010; Gradmann *et al.*, 2011; Stehfest e Hegemann, 2010). However, the model that gained more support in the scientific community is the six-state photocycle model (Ritter *et al.*, 2008) (Figure10, a). This model suggests that it is possible to identify three different states of ChR2: the non-conductive excitable state, the active or conductive state, and the non-conductive desensitized state. Specifically, this model proposes that ChR2, when in the dark, exists as a non-conductive and excitable form with a maximum absorption peak of 470nm (D470) (Ritter *et al.*, 2008). This state is then rapidly converted, in approximately 1ms (Bamann *et al.*, 2008), to a conducting state with peak absorption at 520nm (P520). Between these two states, two other quick intermediates, without measurable currents, are present: P500, consequence of the very fast photoisomerization of retinal, and P390, which is a product of the Schiff base deprotonation. After this deprotonation, the protein suffers severe conformation changes acquiring the P520 conducting state. P390 and P520 states are in a pH-dependent equilibrium. It is also known that the open state of ChR2 wild type protein lasts for around 10ms, after which the protein decays into a P480 state (under special circumstances the P520 can be directly converted to D470) (Ritter *et al.*, 2008). Since this is the slowest step of the cycle, under continuous light conditions these intermediates are accumulated and give rise to light-adapted forms of ChR2. The P480 state can be further divided into two sub-states that differ in their excitability to light. P480a is created from P520 and cannot be directly "reactivated" by light. On the other hand, the "a" state is in equilibrium with the "b" state, this last one activated by light of 480nm (P480→P500).

Though widely studied, the ChR2 photocycle is still not fully understood and some features remain undetermined. Certain steps can be skipped under defined light conditions with some shortcuts, such as the conversion of P480$_b$ directly in P500 without the reformation of the D470 or even the direct formation of the dark state from P520 (Bamann *et al.*, 2008; Ritter *et al.*, 2008). These shortcuts, loops and different kinetics (Figure 10, b) have been manipulated towards the modification of the cycle, enabling the prospect of developing ChR2 new variants

and mutants. ChETA variants are one example where there is a faster recovery from the P520 to P480 state, resulting in a considerable speedier reactivation that permits better temporal resolution and faster channel kinetics (Stehfest *et al.*, 2010). Another example are the SFO (step-function opsins) mutants that are able to remain in the P520 state for longer time periods, up to thirty minutes long in some variants. Consequently, this intermediate can maintain steady state currents and while engaging in this conformation for longer periods, the P520-D470 shortcut allows direct cutting of currents using precise and specific optical control (Zhang *et al.*, 2011).
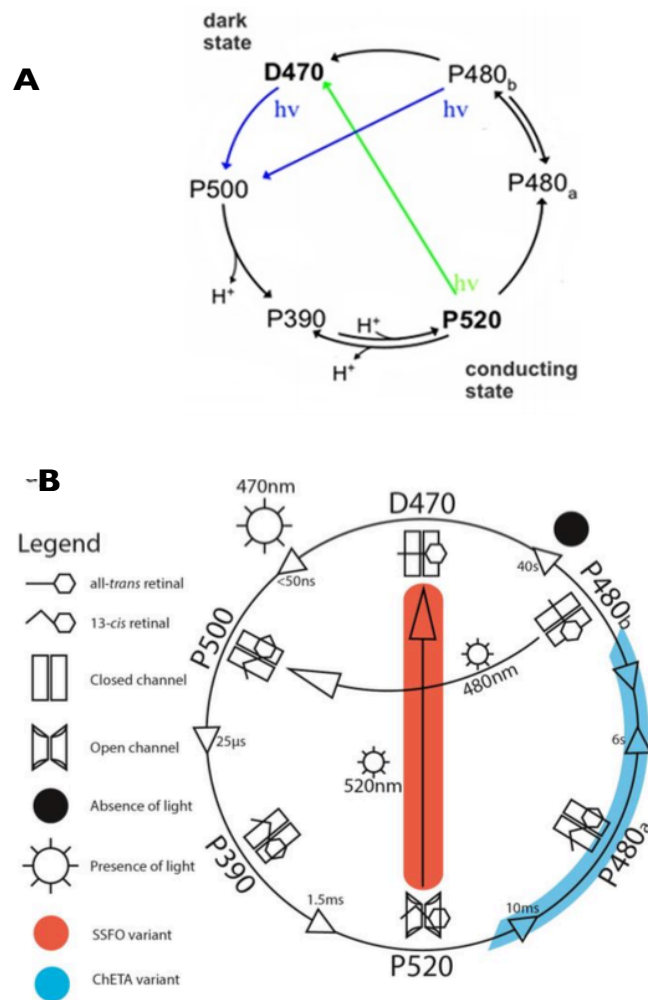
Figure 10 – Six-state ChR2 photocycle model. (**a**) Photocycle of ChR2 displaying the sequential order of the photocycle intermediates (P500, P390, P520 and P480a/b) after the retinal absorption of light in the dark-state (D470). Adapted from (Ritter *et al.*, 2008). (**b**) Alternative ChR2 photocycle diagram illustrating specific cycle changes with focus on relaxation time constants of protein states; shortcuts and state features of two ChR2 variants used in optogenetics are also presented in colour (adapted from (Nack *et al.*, 2010)).

1.5 – Optogenetic toolbox

A rich toolbox of genetically encoded molecules has been under active development. The variety of these tools has increased as they have been improved and combined together. Additionally, eventhough these molecules require vitamin A derivative all-*trans* retinal to properly work (its own chromophore), sufficient all-trans retinal existes in mammalian neurons in culture and *in vivo* to support the function of these molecules (Wang *et al.*, 2007) . Hence, microbial opsins offer high-speed neural activation and silencing, without the demand for chemicals in the mammalian brain. Even for non-mammalian species, like *Drosophila*, all-trans retinal is enough when supplemented in the food supply. There are four major classes of type I opsins with an emerging use in neuroscience and optogenetics (Figure 11), these are halorhodopsins, bacteriorhodopsin-like proton pumps, channelrhodopsins and other chimeric proteins.

First, halorhodopsins (HR) are light-driven inward chloride pumps from archaea that live in high-salinity environments. When expressed in neurons upon illumination, they pump chloride ions into the cells (Figure 11, a i). The first HR to be sucessfully used in neurons was from the archaeon *Natronomonas pharaonis* (known as Halo/NpHR) (Zhang *et al.*, 2007). Next, an enhanced HR was developed for optogenetic applications (eNpHR). This variant was engineered to achieve stronger expression without the cellular side effects, such as intracellular accumulations from expression at high levels (Gradinaru, Thompson e Deisseroth, 2008). Illuminating halorhodopsins with yellow light directly mediates hyperpolarization, allowing the silencing of neural activity (Figure 11, a ii). It is also known that HR is capable of supporting the perturbation of specific neurons to study their role in the brain functions in mouse behaviour, for example, acute optogenetic silencing of orexin/hypocretin neurons induces sleep in mice (Tsunematsu *et al.*, 2011). Halorhodopsins were also effectively expressed in other organisms such as the *Drosophila, to* mediate hyperpolarization in motor neurons (Inada *et al.*, 2011).

Overall, however, halorhodopsins have poorer neuronal expression than channelrhodopsins, and require the addition of trafficking sequences (e.g. from potassium channels) to express better at very high levels in mammalian cells (Gradinaru *et al.*, 2010; Zhao *et al.*, 2008). They also recover slowly after extended illumination, taking on average tens of minutes to achieve maximal photocurrent amplitude after initial activation (Bamberg, Tittor e Oesterhelt, 1993; Chow *et al.*, 2010; Hegemann, Oesterbelt e Steiner, 1985).

The second class of light-activated proteins are archaerhodopsin. These are light-driven outward proton pumps similar to bacteriorhodopsin, which have the feature of expressing well in heterologous cells and also to recover rapidly after activation. One subclass of these proton pumps is archaerhodopsin-3 (Arch) from *Halobacterium sodomense* (Chow *et al.*, 2010), which is also found in archaeal species. When these proteins are expressed in neurons and illuminated with yellow or green light, they pump positive charged ions outwards hyperpolarizing the cell (Figure 11, b i). As an example, Arch permits complete neuronal silencing in the cortex of awaked mice (Figure 11, b ii) (Chow *et al.*, 2010). New variants are also emerging, such as ArchT from the *Halorubrum genus,* which is 3.5 times more light-sensitive than Arch (Han *et al.*, 2011), enabling, for example, the silencing of large brain regions during experiments of optogenetic control of brains of nonhuman primates.

There are also variants of light-driven proton pumps with different absorption wavelengths, allowing the optogenetic control of two neuronal populations. This is the case of the light-driven outward proton pump Mac (from *Leptosphaeria maculans* fungus (Waschuk *et al.*, 2005), that reacts to blue-light to drive neural silencing. Combining the expression of Mac with Halo (which reacts to yellow and, to some extent red, light), it is possible to have a two-coloured neuronal silencing of two separate neural populations expressing Mac and Halo (Chow *et al.*, 2010).

A third class of light-activated proteins are the widely used channelrhodopsins, that, when expressed in neurons, are expressed on the cell membrane and, upon illumination, work as a channel that allows the entrance of positive charged ions (mainly sodium ions and protons, but also potassium and calcium), consequently depolarizing the cell (Figure 11, c i). Channelrhodopsin-2 was the first to be successfully expressed in neurons (Boyden *et al.*, 2005), quickly responding to brief pulses of blue light, with large enough depolarizing photocurrents to mediate action potentials at rates of tens of hertz (Figure 11, f ii). Due to the effectiveness of ChR2 to mediate the driving of specific cells or pathways *in vivo*, several variants of channelrhodopsins have been discovered, studied and engineered, with ChR2 as its predominantly model. This range of variants includes, for example, the calcium permeability-enhanced channelrhodopsin CatCh (Kleinlogel *et al.*, 2011), as well as channelrhodopsins that exhibit higher amplitude currents, or currents slower to run down than the original. This is the case of several channelrhodopsin mutants and chimeras, including ChR2(H134R) and ChIEF (Lin *et al.*, 2009), ChR2(T159C) (Berndt *et al.*, 2011), ChRGR (Wen *et al.*, 2010).

Furthermore, researchers have been developing channelrhodopsins that are faster or

slower to turn off after illumination, such as the channelrhodopsin mutants ChETA (Gunaydin *et al.*, 2010), SFO (Berndt *et al.*, 2009) and the ChR2 (D156A) mutant (Bamann *et al.*, 2010). Moreover, with specific interest to our own project, colour-shifted channelrhodopsins have also been designed. Examples of these new tools include VChR1 (Zhang *et al.*, 2008), MChR1 (Govorunova *et al.*, 2011) and C1V1 (Yizhar *et al.*, 2011), but strategies for new variants are under fast development (Chow *et al.*, 2011).

Finally, another set of optogenetic tools, based on type II opsins (animal opsins), have also been developed through the combination of naturally occurring light-driven G protein-coupled receptors (GPCRs) with other opsins. Based on the published work by Gobind Khorana lab (Kim *et al.*, 2005), Karl Deisseroth's team engineered chimeric receptors by replacing the intracellular loops of bovine rhodopsin with those of specific adrenergic receptors (Airan *et al.*, 2009), taking advantage of the common structure-function relationships between GPCRs. With these tools, it became possible to optically activate the intercellular pathways normally recruited by these receptors (the cAMP and IP3 pathways). As suggested by Deisseroth's team (Airan *et al.*, 2009), these tools were denominated as "opto-XRs", where X specifies the particular pathway that is being optically 'hijacked" (for example, opto-α1AR for α1 adrenergic receptors).

In the following sections, vital milestones about the specific manipulation of ChR2, and its engineering towards colour-tuning variants, are discussed.
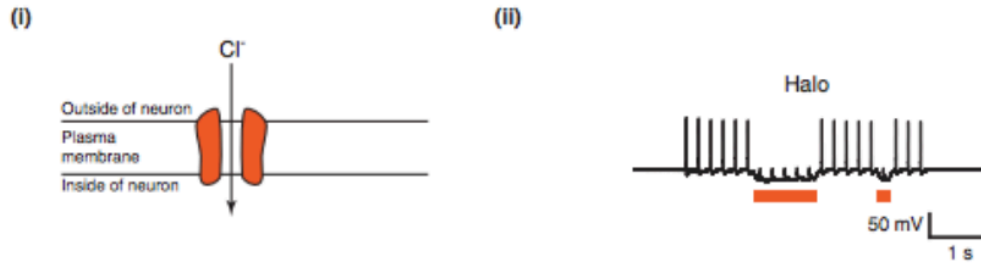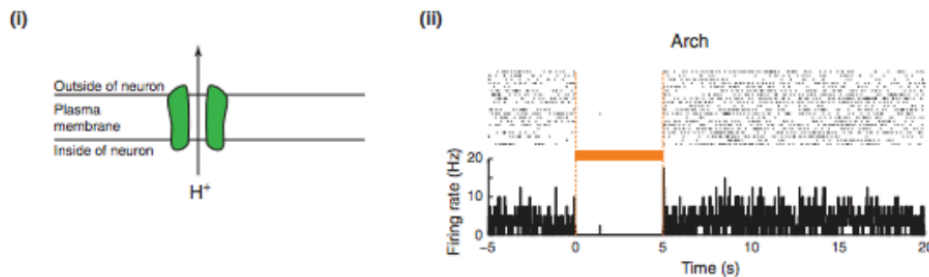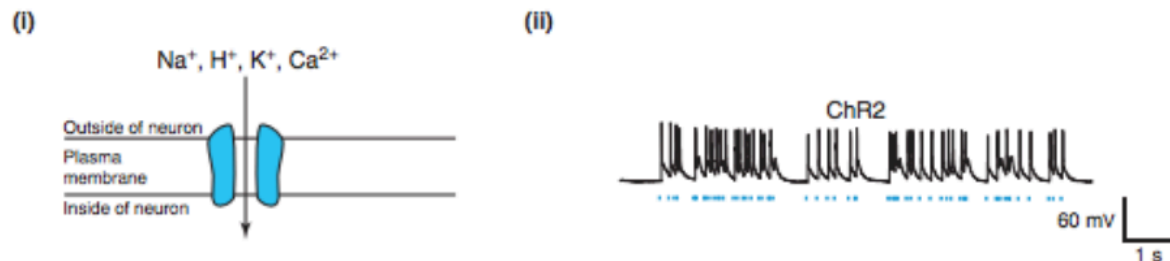
Figure 11 – Adaptation of microbial opsins from nature as optogenetic molecular tools for optical control of neural activity. (**a**) (**i**) Illustration displaying the physiological effect of expressing Halo/NpHR in neuronal cells after cell illumination and negatively charged chloride ions flow into the cell. (**ii**) Voltage trace (black trace) recorded, using whole-cell current clamp, from a cultured hippocampal neurons expressing Halo and illuminated by orange light (orange dashes under trace), showing light-driven action potential silencing. (**b**) (**i**) Physiological effect of expressing archaerhodopsin-3 protein (Arch) in neurons upon cell illumination. Positively charged protons flow out of cells. (**ii**) Neural activity in a representative neurons recorded using extracellular electrode recording in an awake mouse before, during and after 5 seconds of yellow light illumination, shown as a spike raster plot (top), and as a histogram of instantaneous firing rate averaged across trials (bottom). (**c**) (**i**) Physiological effect of ChR2 expression in a neuron upon cell illumination. Positively charged ions (mainly sodium and protons, but also potassium and calcium in a smaller amount) flow into the intracellular space, from the extracellular space. (**ii**) Raw voltage trace (black trace) recorded, using whole-cell current clamp, from cultured hippocampal neurons expressing ChR2, illuminated with brief pulses of blue light (blue dashes under trace), showing light-driven action potentials. Adapted from (Bernstein e Boyden, 2011).

1.5.1   – Channelrhodopsin-2 engineering

To date, six major channelrhodopsins variants have been discovered: ChR1 and ChR2 from *Chlamydomonas reinhardtii* (Nagel *et al.*, 2002, 2003; Sineshchekov, Jung e Spudich, 2002; Suzuki *et al.*, 2003), VChR1 and VChR2 from *Volvox carteri* (Kianianmomeni *et al.*, 2009; Zhang *et al.*, 2008) - these four have already been widely studied and characterized -, *Mesostigma viride* ChR (MChR1) (Govorunova *et al.*, 2011), and the most recently identified channelrhodopsin of the halophilic alga *Dunaliella salina*, DChR1 (Zhang *et al.*, 2011)*,* which was discovered less than five years ago.

'Optotools' have become indispensable in neuroscience to stimulate or inhibit excitable cells by light and channelrhodopsins have become of great interest, mainly because with optogenetics they can be used in numerous fields of biomedical research. To date, optogenetic application of microbial opsin genes benefited substantially from molecular modifications, such as mutating the opsin backbone (site-directed mutagenesis) or creating chimeras by mining related algal genomes (chimera approach by combining helices from different channelrhodopsins (Lin *et al.*, 2009; Tsunoda e Hegemann, ; Wang *et al.*, 2009)). Through a combination of molecular engineering and genomic discoveries of new light-sensitive proteins, the toolkit of neuronal modulators is rapidly improving in both specificity and versatility.

Overall, engineering of channelrhodopsins allows the modification of their spectral and kinetic properties and to improve the expression and membrane targeting in host cells. Up to now, a variety of channelrhodopsins emerged through codon optimization and site-specific mutagenesis. Related to this, a humanized form of the channelrhodopsin channel (hChR2) was created by substituting certain algae specific codons with mammalian codons (Adamantidis *et al.*, 2007). Since the initial description of ChR2 as an efficient tool to evoke neural activity in a light-dependent manner, an outbreak of studies have applied ChR2 in a variety of questions related with neuroscience.

There are several relevant parameters to evaluate a particular opsin, including the wavelengths of light to witch the opsin respond, the wavelength which generates the largest current, the magnitude of the current generated at the optimal wavelength, the rate to achieving maximal current, how fast the opsins channels close, and the degree to which cell membranes express the opsin. As such, with molecular mutagenesis studies, the function of ChR2 has been

engineered to have faster or extended open-state lifetimes, shifted absorption spectra, reduced desensitization and increased expression and photocurrent magnitude.

One important parameter is the rate of the channel closure (tau off) that corresponds to the minimum effective interpulse interval (a low tau off permits control of high spiking rates), as well as the length of time one light pulse alters membrane potential (a high tau off consents long-lasting effects, up to 30 min per light pulse). Furthermore, various opsins with fluctuating characteristics have been developed and particularly studied with multi-comparison.

A systematic comparison of microbial opsins under matched experimental conditions has been performed in order to understand the essential principles of each one, and identify key parameters for the design and interpretation of experiments involving optogenetic techniques (Mattis *et al.*, 2012). Moreover, a plot of peak wavelength versus rate of channel closure after a pulse (tau off) provides one way to organize the many available opsins, revealing the wide variety of possibilities for modulating neural function (Figure 12).
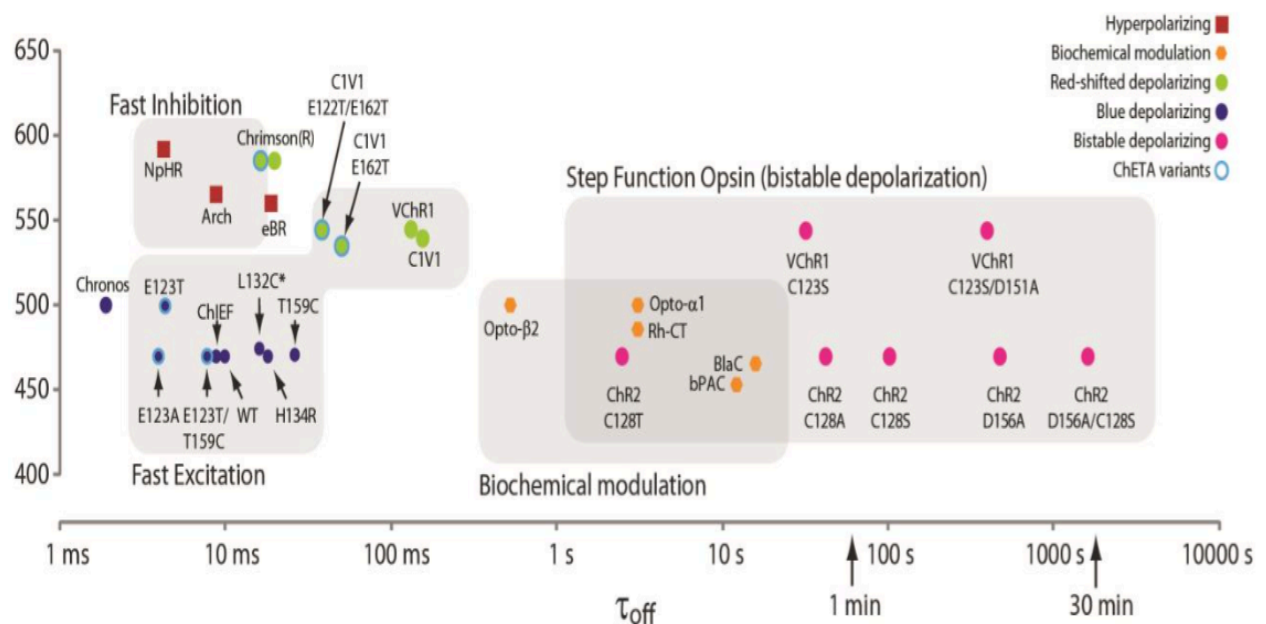
Figure 12 – Kinetic and spectral properties of optogenetic tools variants. Optogenetic tools span a large portion of the visible spectrum and a wide range of temporal kinetics. Decay kinetics are temperature dependent; all reported values are recorded at room temperature, with <50% decrease in tau off expected at 37ªC. Biochemical modulating opsins refer to G-protein-coupled opsins. Its *in vivo* properties may depend on the host cell responses to elevated intracellular calcium. > than 500 nm of peak activation predominantly lead to slow kinetic depolarizing variants (50 ms tau off). Red-shifted variants are regularly hyperpolarizing pumps. Adapted from (Yizhar *et al.*, 2011).

chARGe was considered an earlier tool for photo stimulation when it demonstrated proof of modulating neural fucntion in cultured neurons (Zemelman *et al.*, 2002), but its use was not extensive due to lack of precision (seconds), highly variation rates and the fact that it did not allow the control of individual action potentials. Hence, the first and pioneer opsin used in mammalian neurons was ChR2 (Boyden *et al.*, 2005; Nagel *et al.*, 2003), which has been established as the main prototype channelrhodopsin for optogenetic application.

It has been demonstrated that ChR2 can be used to control mammalian neurons *in vitro* with temporal precision in the order of the milliseconds (Boyden *et al.*, 2005). This was a meaningful finding that boosted ChR2 usage and toolbox expansion, since all opsins require retinal as its own light-sensing co-factor and it was unclear whether central mammalian nerve cells would contain sufficient retinal levels. Furthermore, it was shown that despite the small single-channel conductance, ChR2 has sufficient potency to drive mammalian neurons above the action potential threshold. ChR2 was, therefore, the first optogenetic tool with successful application. However, despite ChR2 being widely used to photo-stimulate neurons, its own full potential as a light-gated ion channel is still under development, with improvements developing occurring year by year.

The wild-type ChR2 presents a rapid on-rate and moderate channel closing rate (Ishizuka *et al.*, 2006; Lin *et al.*, 2009; Nagel *et al.*, 2003) but has some drawbacks, such as small currents and strong inactivation properties that are not adequate for certain biological applications. The wild-type form of ChR2 has a small single-channel conductance, and is optimally excitable at a wavelength of 470 nm, naturally not extended over 520 nm, thus limiting its use in a high-light scattering medium such as the brain (Hegemann e Möglich, 2011). Long-wavelength excitation light decreases the light scattering effect produced by biological tissues and it will avoid the absorption by haemoglobin. The more red-shifted a channelrhodopsin is the more desirable they become to use in relatively deep tissue penetration. In parallel, blue-shift protein would also be interesting to develop, given that the use of channelrhodopsins with various wavelength sensitivities combined with multi-coloured optics, would enable the stimulation of two different neural populations without overlap.

Channelrhodopsin-2 also has relatively long recovery time, limiting the maximal firing rate that can be induced in neurons to 20-40 Hz. However, the main deficiency of ChR2 is the high level of desensitisation that reduces the current by ~80 % at physiological pH (Ishizuka *et al.*, 2006; Lin *et al.*, 2009; Nagel *et al.*, 2003). The desensitised response fully recovers after 25s in the dark (Lin *et al.*, 2009). Furthermore, ChR2 traffics well to the membrane when expressed

at low levels, but forms intracellular aggregates when expressed at high levels (Lin *et al.*, 2009). Channelrhodopsin-2 can provide both temporal and spatial precision of stimulation in mammalian cells and living animals, and is therefore being extensively used for millisecond scale photo-control of cellular functions.

When ChR2 was expressed in mammalian neurons, a brief (1-2 ms) pulse of blue light (~470 nm) opens these channels, evoking an action potential in targeted cells. Cation conductance appears to depend primarily on the kinetics of channel closure (tau off) rather than other molecular events, such as retinal isomerization (Feldbauer *et al.*, 2009).

A variety of mutations have been introduced to alter these channel kinetics. While the kinetics of wild type ChR2 does not permit precise control over 40 Hz, mutations of the glutamate 123 residue to a threonine (T) or an alanine (A) created the known ChETA opsins with a tau off of approximately 4 ms against the 10 ms from ChR2. This allows evoking spikes over 150 Hz using 2 ms light pulses (Gunaydin *et al.*, 2010). Alteration of channel kinetics in the other direction, to very slow channel closure, allowed the creation of "step function" opsins (SFO), which cause prolonged depolarization using light at 470 nm, raising the excitability of targeted neurons. SFO is a version of ChR2 with the C128S and D156 mutations and has a tau off of almost 30 minutes. Yet, if shorter "on" states are experimentally desired, channel closure may be induced with light of approximately 600 nm (Yizhar *et al.*, 2011). This controllable long "on" state may be well suited for translation user. First, the stable state allows transduced cells to act as photon aggregators, allowing long pulses of light at lower powers to recruit larger volumes of tissue (Berndt *et al.*, 2009; Diester *et al.*, 2011). Second, by raising excitability rather than directly inducing spikes, the physiological activity patterns of an area may be preserved (Berndt *et al.*, 2009; Yizhar *et al.*, 2011). Raising excitability may allow targeted modulation in a more physiological manner, with the need of further studies to investigate the complete utility of these features.

Currently, the most prominent of these the red-shifted opsins is C1V1 (E122T/E162T), a hybrid of ChR1 and VChR1. Its peak activation occurs at approximately 560 nm, and its photocurrents exceed those of ChR2 (Yizhar *et al.*, 2011). A further red-shifted version, C1V1 (E162T), can consistently elicit action potentials at 630 nm with large photocurrents, however with slower off-kinetic (tau off >60 ms) (Mattis *et al.*, 2012; Yizhar *et al.*, 2011). While further red-shifts variants, including absorption into the infrared spectrum, may be desirable, C1V1 (E122T/E167T) has been mostly used in primate models.

1.5.2   – Channelrhodopsin-2 color tuning

After a significant amount of research on the unfolding structural features and photocycle of the protein, the first study concerning a red-shifted ChR was obtained. Firstly, VChR1, a channelrhodopsin presenting a 70 nm shift (Zhang *et al.*, 2008) with a subsequent yellow light excitation, was discovered and characterized. VChR1 structural sequence is similar to the previously identified ChR1 and ChR2, allowing the selection of residues thought to be accountable for the observed colour tuning on the absorption spectra. These specific residues are located in the TM5 domain of the protein, in close proximity to the retinal chromophore, and consist of a glycine 182 and a cysteine 184 that are substituted by serines, causing an increased polar electronic environment on and around the chromophore, which leads to a red-shifted absorption spectra. These discoveries suggested the possibility of colour tuning being based on the adjustment of the primary structure.

More target residues were identified in further studies, as is the case of C128 in a ChR2 versus bacteriorhodopsin sequence assessment (Berndt *et al.*, 2009). This residue was considered as a likely target for mutation that would result in slower channel kinetics. It was predicted that substituting this cysteine by a serine or alanine would create a bi-stable opsin capable of being turned on/off with different wavelengths (Berndt *et al.*, 2009). This mutant opsin was then upgraded with an additional mutation (D156A) to develop a closing constant of 30 minutes (Yizhar *et al.*, 2011). This allowed optical control of overall excitation state of a specific neuronal population across long periods of time.

The first high resolution model of a channelrhodopsin, the crystal structure of C1C2 (Kato *et al.*, 2012) (a chimera of ChR1 and ChR2)), allowed a deeper understanding of the architecture of the retinal binding pocket and ion pore of the protein. This achievement enhanced new designs methods focusing new variants, based on the protein 3D structure.

To understand the essential elements that contribute to spectral tuning of a chromophore inside the protein cavity, Wang et al. redesigned human cellular retinol binding protein II (hCRBPII) to fully encapsulate *all-trans-retinal* and form a covalent bond as a protonated Schiff base (Wang *et al.*, 2012). The hCRBPII is believed to be accountable for the transport of retinal in a way related to the mammalian rhodopsins. Hence, mutating several residues on the protein resulted in the achievement of peak absorption shifts on the retina molecule across a range of 440-644 nm (Figure 13).

Furthermore, by studying the structure of the protein relative to the retinal molecule they concluded that modifications that isolate the retinal molecule into a hydrophobic environment and even the electronic charges in the polyene chain, particularly near the protonated Schiff base, caused greater bathochromic shifts than modifications near the β-ionone ring, a result contradicting the findings regarding VChR1. However, given the differences concerning ChRs and hCRBPII, specifically in the protonated Schiff base motif, it is conceivable that these findings may not be completely comparable.
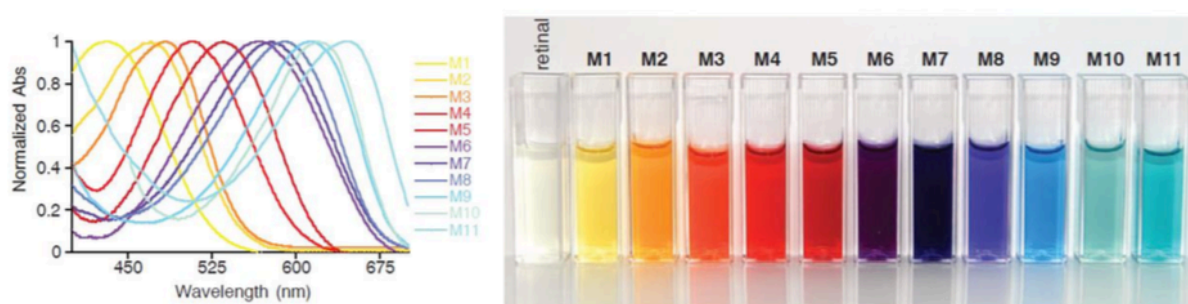
Figure 13 – Colour tuning of absorption spectra in a modified retinal binding protein. Normalized UV spectra of a selected group of hCRBPII mutants, obtained by directed site mutagenesis. Modified electrostatic environment surrounding the retinal molecule shown by pigments colour in cuvettes generated by incubation of *all-trans-retinal* with hCRBPII mutants. Adapted from (Wang *et al.*, 2012).

Additionally, the genomic search for new channelrhodopsins extended the palette of available variants, resulting in several screenings on algae species. With this search, two new opsins were revealed, Chronos (from *Stigeoclonium helveticum)* and Chrimson (from *Chlamydomonas noctigama)* (Klapoetke *et al.*, 2014).

Chrimson is the first known variant with yellow peak absorption (590 nm). It also presents low kinetics (low spike reliability over 10 Hz) but to overcome that fact, a Chrimson mutant was created (Chrimson R- K176R). This variant displays more appropriate kinetics, but due to its ChR2 similarity it shows blue light sensitivity overlapping when paired with ChR2. This fact also demands the need of blue-shift variants to achieve independent neuronal excitation of two different neuronal populations. Also, ChR-dependent photostimulation may be

used in combination with fluorescent probes of calcium, membrane potential or other cellular functions. For instance, the excitation spectrum of Fluo-3, one of the most popular fluorescent calcium indicators, overlaps with the absorption spectrum of ChR2. Therefore, it would be difficult to measure Fluo-3 fluorescence during ChR2-dependent photostimulation. This will only be achievable with blue-shifted variant of ChR2.

On the other hand, Chronos is a blue-light sensitive high frequency actuator comparable to ChETA variants. Regarding this blue-shift, a novel channelrhodopsin has been discovered and characterized, the PsChR from the algae *Platymonas (Tetraselmis) subcordiformis*. This variant has ~3-fold greater unitary conductance, faster recovery from excitation and higher sodium selectivity than ChR2 (Govorunova *et al.*, 2013). Its maximal spectral sensitivity at 445 nm which makes PsChR the most blue-shifted channelrhodopsin so far identified (Govorunova *et al.*, 2013).

Recently, a new approach based on the atomistic design of microbial opsin-based blue-shifted optogenetics tools has been published, in which the development of blue-shifts colour variants by rational design at atomic resolution, achieved through accurate hybrid molecular simulations, electrophysiology and X-ray crystallography, was obtained (Kato *et al.*, 2015). These molecular simulation models and crystal structure demonstrated the precisely designed conformation changes of the chromophore induced by combinatory mutations that shrink its π-conjugated system, alongside with electrostatic tuning, producing large blue shifts up to 100 nm (Kato *et al.*, 2015). Photosensitive ion transport activities were maintained, showing that this approach may be applicable to other microbial opsins, at least in the context of blue-shifted action spectra of recent proteins isolated from natural sources.

Another kind of ChR2 variants with great interest would be proteins with variable ion selectivity, which would enable broader applications. Although the membrane potential is shifted to the negative direction in a light dependent manner by the use of a chloride transporting tool such as NpHR, its efficiency is limited because only one ion is transported across the membrane with the absorption of a single photon rather than allowing many ions per photon to flow through a channel pore. Hence, if channelrhodopsins were designed to be selectively permeable to Cl^-, they would allow the bulk of ions to flow with the absorption of a single photon. Therefore, their hyperpolarizing effects would be expected to be much larger than those of Cl^-/H^+ transporters, such as NpHR or Arch. An example of a successful functional conversion regarding this topic is the conversion of ChR2 into a chloride channel by replacement of a single amino acid (Glu 90 to lysine, a positively charged residue) (Wietek *et al.*, 2014). This functional

conversion enables fast optical inhibition of action potentials, thus silencing neurons (Berndt *et al.*, 2014).

Concerning the most recent variants, the last published red-shifted variant is the red-activated ReaChR (Lin *et al.*, 2013). This variant if optimally excited with orange to red light in a range of 590 -630 nm and offers improved membrane trafficking, higher photocurrents and faster kinetics compared to the existing red-shifted ChRs(Lin *et al.*, 2013), such as C1V1(E122T) (Yizhar *et al.*, 2011) and VChR1 (Zhang *et al.*, 2008) .

ReaChR is a complete example of ChR engineering, since it was created by both several mutations already described in ChR2, combined with mining chimeras of other available variants. Succinctly, Lin and collegues used VChR1, which has minimal trafficking to the membrane, as well as poor expression in mammalian cells, as a template to engineer an efficient red-light-activated channelrhodopsin. To improve desired membrane trafficking, they examined the superior membrane trafficking of the available variant ChIEF (Lin *et al.*, 2009), known for an almost exclusive plasma membrane expression with minimal cytosolic aggregation in mammalian cells without the need for additional trafficking signals (unlike many other ChR variants) (Lin, 2011). Then, the N-terminus of VChR1 before the transmembrane domain was replaced with the equivalent ChiEF sequence. To increase the expression level, they followed a known and successful strategy previously used to increase the expression level of ChR in ChR1-ChR2 chimeras (Wang *et al.*, 2009). Such as, replacing one transmembrane domain of VChR1 with the corresponding VChR2 helix. They named this red-shifted intermediate variant VComet, displaying optimized membrane expression and trafficking and strong responses to light above 600 nm (Lin *et al.*, 2013). However, the responses at these longer wavelengths were desensitizing and did not recover completely in the dark without reconditioning with 410 nm light (Lin *et al.*, 2013). Hence, to reduce this desensitization of VComet to light above 600 nm, Lin and collegues decided to insert a known point mutation of ChRs. The ChETA mutation (Gunaydin *et al.*, 2010) was inserted but it did not red-shifted or reduces the desensitization of VComet. The next attempt was the H134 mutation of ChR2 (Nagel *et al.*, 2005) this howerver slowed channel kinetics and degraded the temporal fidelity of this variant. Finally, the mutation L171I, corresponding to the same position of the ChIEF mutation (Lin *et al.*, 2009), increased the amplitude of the photoresponse until 630 nm light through reduced desensitization while retaining the optimized membrane trafficking and expression of VComet. This created the ReaChR variant, with a spectral red-shifted peak defined at 630 nm (Lin *et al.*, 2013). This new variant describes perfectly the use of available engineering and biotechnological approaches

related to optogenetic tools and how all information can be helpful and used together to achieve higher development in optogenetics. In the same paper, this variant was also found to enable transcranial optical activation of neurons in mouse deep brain structures (Lin *et al.*, 2013).

Another new variant was presented last year, the ChR2-XXL (ChR2 mutant D156C) (Dawydow *et al.*, 2014). The XXL denomination comes from extra high expression and long open state, displaying also improved subcellular localization, elevated retinal affinity and photocurrent amplitudes greatly exceeding those of all previous ChR variants (Dawydow *et al.*, 2014). However, this variant was developed to be used in neuronal activity in adult *Drosophila melanogaster*, still lacking further characterization and applicability for example in mammalian neurons. Additionally, its maximum excitation wavelength is ~480 nm, which is similar to the 470 nm value of ChR2, with only a slight red shift.

A completely different and new approach to modify the spectral and kinetic characteristics of 'optotools' was conceived using synthetic retinal analogues (AzimiHashemi *et al.*, 2014). As an alternative strategy to mutating the opsin backbone or mining related algal genomes, synthetic retinal analogues were combined with microbial rhodopsins for functional and spectral properties. Dimethylamino-retinal (DMAR), compared with *all- trans-retinal,* shifted the action spectra maxima of some ChR2 known variants (H134R and H134R/T159C) in ~40 nm. DMAR also decelerates the photocycle of both ChR2 variants, thereby reducing the light intensity required for persistent channel activation (AzimiHashemi *et al.*, 2014). These results were also corroborated on assays in *C. elegans*, HEK cells and larval *Drosophila.* Yet, experiments using mammalian neurons are still to be performed. In parallel to more experiment tests and characterization, the use of retinal analogues can be a complementary strategy to obtain 'optotools' with modified characteristics as colour tuning, particularly in already existing cells or animal lines.

In summary, optogenetics are experiencing a fast evolution, much due to development of variants of existing optogenetics tools. Channelrhodopsin-2 kinetic variants as ChETA and SFO are one good example of successful new variants that resulted from protein engineering, and VCR1, Chronos, Crimson and ReaChR are examples of genome-mining approaches leading to ChR-like proteins.

However, there still is the necessity of selectively activating more than one neuronal population and to red-shift light activation to prevent tissue damage and increase the penetration or radiation. To achieve these goals, colour-tuned variants of ChR2 with activation

spectra are needed and the recently and growing knowledge about channelrhodopsin structure and variants will be on the base of fundamental importance. New variants should be developed, optimized and associated with the already existing range of channelrhodopsins to facilitate the diffusion and applicability of a groundbreaking technique like optogenetics.

1.6 – Optogenetic applications

In the last decade, optogenetics has been widely used as a method to study brain circuitry (Wang *et al.*, 2007), focused on a specific population of neurons, and even more than one population at the same time (Han e Boyden, 2007). It has also helped to elucidate pathways of many different diseases. For instance, optogenetics has been used in mice D1 and D2 cells (dopamine receptors) in the striatum (Kravitz *et al.*, 2010) and sub-thalamic nucleus (Gradinaru *et al.*, 2009), as a way to explore their role in Parkinson's disease. Regarding this neurodegenerative disease, halorhodopsin was also used to enable functional analysis and validation of human embryonic stem cell-derived grafts differentiating into dopaminergic neurons (Steinbeck *et al.*, 2015).

A substantial amount of data shows the use of optogenetics to find specific cells to be manipulated in order to alter fear memories, treat post-traumatic stress disorder (PTSD), as well as other illnesses that revolve around conditioned fear responses (Goshen *et al.*, 2011). It has also been used to gain insight into the neuronal networks involved in autism (Gunaydin *et al.*, 2014), to test the casual link between dopamine expression and positive reinforcement in mental health disorders such as addiction (Witten *et al.*, 2011) and depression (Tye *et al.*, 2013), to study social stimuli and social interaction (Yizhar *et al.*, 2011) - possibly providing a hint of how circuit-level manipulations might be used for the treatment of neuropsychiatric disorders (Peça and Feng, 2011) and to control of epilepsy (with acute potent neural silencers) (Tønnesen *et al.*, 2009). Also, optogenetics have been useful in the study of the role of specific neurons in behaviours such as breathing (using ChR2 to restore breathing in rodent models of spinal cord injury) (Alilain *et al.*, 2008; Arenkiel e Peca, 2009), awakening/sleep disorders such as narcolepsy (Adamantidis *et al.*, 2007) and appetitive or aversive learning (Schroll *et al.*, 2006).

However, there has been a scarcity of studies that demonstrate potential translational applications, with only a handful of experiments to have implemented optogenetics approaches

towards this goal and focusing on arguably less-tractable therapies than that being reviewed (Arenkiel and Peca, 2009).

Probably the best example with the strongest potential for translational applications to humans has been achieved by ophthalmology. In 2006, it was observed that it was possible to restore light-encoded signals to the visual cortex in mice lacking photoreceptor cells by expression and activation of ChR2 in subsets of inner retinal neurons (Bi *et al.*, 2006). This study established the groundwork for related manipulations in other cell types of the retina (Lagali *et al.*, 2008; Lin *et al.*, 2008).

More recently, viral delivery of ChR2 has shown to enable safe and effective restoration of the visual function in multiple mouse models of blindness (Doroudchi *et al.*, 2011; Macé *et al.*, 2015; Wyk, van *et al.*, 2015), thus starting the discussion of future perspectives to the use optogenetic approaches to retinal prosthesis, aiming for the first optogenetic human trials (Barrett, Berlinguer-Palmini e Degenaar, 2014). As such, GenSight Biologicals, a company founded by experts in the fields of ophthalmology and optogenetics, is aspiring to use this technique to treat blindness caused by diseases resulting from cell loss in the retina, including glaucoma and *retinitis pigmentosa*. The company is currently in pre-clinical development, based on a gene therapy product comprising a non-specified ChR2 and a delivery modified AAV2. However, it is important to take into consideration the importance of fully understanding the mechanism of how retinal maps translate to visual perception (Arenkiel *et al.*, 2007). In theory optogenetics could be used as a therapeutic intervention in conditions for which there is a clear benefit to be obtained from switching on or off specific cells types (Chow and Boyden, 2013). However, there are several problems that must be tackled before this becomes reality, such as the need to deliver genetic constructs into the body by means of viral vector, a technology that is far from being fully established in humans.

In summary, great progress has been made in a short period of time and optogenetics have made it conceivable to either increase or decrease the activity of specific neural populations in multiple brain regions. Mainly based in animal models of human disease, optogenetics have delivered new mechanistic insights into a significant range of human psychiatric and neurological diseases, with an expectable growing influence in the scientific community as new 'optotools' are being developed at a rapid pace.

1.7 – The *Pichia pastoris* protein expression platform

The methylotrophic yeast species *Pichia pastoris* is a widely used heterologous system for the expression of a large variety of recombinant proteins, and a remarkable example of a developed and settled biotechnologic approach used for biochemical, genetic, biotechnology research and industry.

The *P. pastoris* system was originally established as a supply for single cell protein used in animal feeding, due to its capacity to metabolize methanol as its sole carbon source. *Pichia pastoris* has also been used for the expression of heterologous proteins (Daly e Hearn, 2005; Macauley-Patrick *et al.*, 2005).

The popularity of this recombinant expression system can be attributed to various factors, but mainly to the simplicity of techniques that are necessary for the molecular genetic manipulation of this species. Also, *P. pastoris* can produce exogenous proteins intracellularly or towards secretion and perform post-translational modifications, such as glycosylation, disulfide bond formation and proteolytic processing (Cereghino, 2000).

The last few years this system has been improved in terms of expression of complex proteins, mainly by protein engineering or altering the *P. pastoris* protein expression host (Ahmad *et al.*, 2014). Comparing to other systems *Pichia* has advantages such as performing glycosylation process and presenting a more appropriate lipid membrane composition, thus allowing proper folding of proteins – these are not possible in prokaryotic systems (Higgins, 2001; Ramón e Marín, 2011). In fact, expression of membranar proteins (such as channelrhodopsin) is a specific advantage of this system, given that membrane proteins have a tendency to aggregate into inclusion bodies in *E. coli*. However, as a result of the existence of eukaryotic folding/targeting machinery, these proteins can be successfully produced in *Pichia pastoris* (Ramón e Marín, 2011).

The methylotrophic function in *Pichia* allows methanol or methane as sole carbon and energy source for growth. This feature is due to capability of the yeast cell to use its specialized organelle – the peroxisome. This organelle works by corralling reactive chemical metabolites, thus preventing cellular damage. The peroxisome contains a high concentration of the Alcohol Oxidase enzyme that mediats oxidation of alcohol into aldehyde. A specific promoter for this enzyme gene (*AOX* gene) is under tight regulation and behaves much like the *E.coli* lac promoter (Beckwith, 2013).

The *AOX* gene is very selective for methanol, and is activated only when methanol is present in the media, and is strongly repressed by alternative carbon sources (e.g. glucose, ethanol or glycerol). The *AOX* promoter is also capable of inducing the expression of very high levels of the enzyme, which may reach 5 to 30 % of *AOX* protein in the total soluble protein expressed under methanol induction. Consequently, the *AOX1* promoter has been inserted into several expression vectors for the tightly regulated methanol-induced expression of genes of interest (Ellis *et al.*, 1985; Koutz *et al.*, 1989; Tschopp *et al.*, 1987), and is one of the principal promoter used for the heterologous expression of recombinant proteins in *Pichia pastoris*.

However, alternative promoters can be selected to drive protein expression. The *GAP* promoter drives the expression the glyceraldehyde-3-phosphate dehydrogenase (GAPDH) enzyme in a constitutively manner and is expressed at high levels in many organisms, including *Pichia pastoris*. Therefore *GAP* promoter driven expression leads to a constitutive expression in *Pichia* (Qin *et al.*, 2011; Zhang *et al.*, 2009).

Budding yeasts such as *Saccharomyces cerevisiae* and *Pichia pastoris* are widely used as hosts to produce excreted proteins for research and therapeutic purposes (Gasser *et al.*, 2013; Hou *et al.*, 2012). Many of these excreted proteins cross the secretory pathway (Barlowe e Miller, 2013). Entry into the secretory pathway requires an N-terminal signal sequence that directs translocation into the endoplasmic reticulum (ER). A typical signal sequence includes a stretch of hydrophobic residues that are exposed following cleavage of the site that is recognized by signal peptidases in the ER lumen. After entry into the ER, proteins fold, and may undergo additional changes that include disulfide bond formation, glycosylation and oligomerization. Finally, the protein is delivered from the ER to the Golgi apparatus and then to the extracellular space. For different exogenous proteins expressed in yeasts, the level of secreted product varies widely, presumably because specific steps in the secretory pathway can be inefficient (Idiris *et al.*, 2010). Hence, in order to secrete proteins for easier purification from the extracellular medium, the coding sequence of recombinant proteins is initially fused to the *Saccharomyces cerevisiae* α-mating factor secretion signal leader (Lin-Cereghino *et al.*, 2013). Some proteins can be expressed fused to an N-terminal peptide encoding the *Saccharomyces cerevisiae* α-factor secretion signal encoded in a vector containing the *AOX* promoter sequence. A vector like this allows high-level, methanol inducible, secreted expression of the gene of interest in *Pichia pastoris*.

The *AOX* promoters are specifically used in the pPICZ vector series, the pPICZα vectors are used the secretion signal is included and the pGAPZ vectors display the *GAP* promoter use.

These vectors usually contain a 5' fragment containing the specific promoter for the selected expression type, a resistance gene for selection against Zeocin antibiotic in both *E. coli* and *Pichia* (Baron *et al.*, 1992; Drocourt *et al.*, 1990), a C-terminal peptide containing a polyhistidine (6xHis) tag for further detection and purification of a recombinant fusion protein, and three reading frames facilitating in-frame cloning with the C-terminal peptide. Thus, approaches for heterologous expression of recombinant proteins involve cloning the desired protein into an expression vector. For example, the pGAPZ series vector has a homologous arm to the *GAP* gene. It is thus important to consider that linear DNA can generate stable transforming of *Pichia pastoris* via homologous recombination between the transforming DNA and regions of homology within the genome (Cregg *et al.*, 1985, 1989). Hence, upon linearization of the vector and insertion into the cell, recombination events occur and the gene is inserted at the *GAP* locus (Figure 15a). Similarly, naturally and spontaneously multiple recombination events can occur and multicopy mutants can be found which usually tend to produce protein proportionally to the number of gene copies inserted into the genome (Daly e Hearn, 2005) (Figure 15b).

The low cost and high yield, combined with the advantages of a eukaryotic processing machinery makes Pichia *pastoris* an attractive system for small and large scale production of integral membrane proteins (Byrne, 2015).
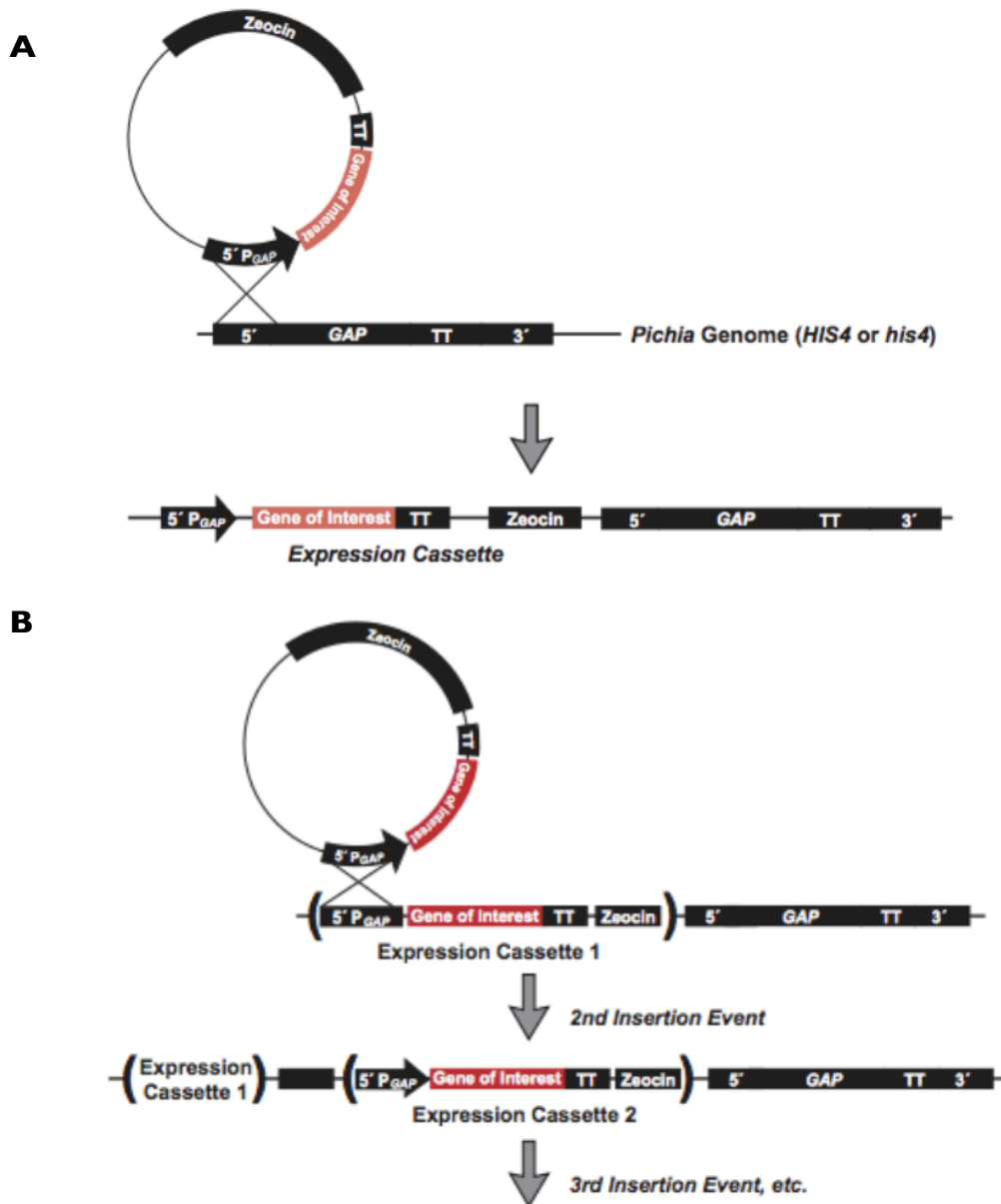
Figure 14 – Recombination and integration in *Pichia pastoris*. (**a**) Gene insertion at the GAP promoter and single copy integration. By homology recombination, the GAP *locus* promotes the insertion of the gene of interest into the *Pichia* genome normalized. (**b**) Multicopy gene insertion events and multicopy integration. Subsequent to the first integration, the homology sequence persists in the yeast genome and events of homologous recombination can occur. Although with a fewer incidence, this leads to generation of multicopy inserts of the gene of interest. Zeocin antibiotic resistance cassette is similarly inserted multiple times, creating Zeocin hyper-resistant colonies. (adapted from (Invitrogen, 2010)).

1.7.1 – Channelrhodopsin-2 and *Pichia pastoris*

The heterologous system mostly used to produce and purify ChR2 has also been the *Pichia pastoris* yeast (Bamann *et al.*, 2008, 2010). Many studies with channelrhodopsin use this expression system, including the first paper reporting the structural features and the photocycle of ChR2 (Bamann *et al.*, 2008). Moreover, protein engineering studies focusing on new variants and mutations also use this expression system, as demonstrated, using structural approaches, by the broadly characterization of the identified mutations C128S and D156A (SFO's), which operate with *Pichia pastoris* as the chosen model of expression (Nack *et al.*, 2010).

Interestingly, functional expression of channelrhodopsins, and specifically ChR2, in the standard system *E.coli* has proven to be difficult (Ernst *et al.*, 2008; Sineshchekov *et al.*, 2013). However, proton pump microbial rhodopsins can be successfully expressed in *E.coli,* particularly in the genetically modified strain BL21(DE3), which is more suitable for transformation and protein expression. This makes sense given that bacteriorhodopsin, the most studied proton pump, was originally isolated from prokaryotic *Archaea*. Insect cells (Sf9) have also been sucessefully used to produce active channelrhodospin (Kato *et al.*, 2012, 2015).

1.8 Time-Dependent Density Functional Theory

It is possible to describe quantum-mechanically the electronic dynamics of a particular system using the time-dependent Schrödinger's' equation (SEq). However, a system may be as "simple" as a single electron or it may refer to more complex molecules with many electrons, such as amino acids, retinal and proteins.

Despite this equation being well known and developed, its solution is only feasible for very small systems. Therefore, a reasonably sophisticated approach to solve this drawback of scalability is to use the Density Functional Theory (DFT) (Burke, Werschnik e Gross, 2005). Basic ideas of DFT are related to giving importance to density and non-interacting particles. That is, any observable of a quantum system can be obtained from the density of the system alone and secondly, the density of an interacting-particles system can be calculated as the density of an auxiliary system of non-interacting particles. This system is based in a formulation

like the Kohn-Sham one-particle equations (Kohn e Sham, 1965), that requires the use of a non-exact form to account for the electronic correlation and to correct the kinetic energy expression, and computational methods needed for appropriate process of high amount of data. Consequently, this theory stipulates a simple and exact reformulation of SEq for a multiple-particle system. For such complex molecules as proteins, DFT allows for the derivation of a set of equations that depend uniquely on the electron density, that is a function of the 3 space variables, instead of depending on many-body wave functions (in SEq), a function of 3 variables for each electron. Besides, these electrons with varying variables can be divided into different groups such as inert or dynamic ones, leading to simplifications that may drive the output of the equation to be somewhat different from what it is observed.

Furthermore, Time Dependent DFT is a large field of research concerned with many-electron systems in time-dependent fields, such as different phenomena like absorption spectra, energy loss spectra, photo-ionization and photo-emission..

In general, to achieve an absorption spectra simulation, TDFT role starts by firstly using the Kohn–Sham algorithm to have a value of the solution, then solved by a computational program that creates a 3D function of the electron density of the molecule as its base. Next, a stimulus is settled to the obtained simulation of the electronic cloud of the molecule and it is studied how it evolves during a specific time. In the case of ChR2, the interest is mainly on the effect of the visible spectra light on the molecule. Hence, the stimulus is a very fast flash of light, in the order of 10^{-17} seconds, and it is known as a "kick". It excites the molecule with electromagnetic radiation with a very wide spectrum of frequencies. This "kick" must be applied across the three different axis and later collected into a final effect. After each "kick" the system evolves and changes its dipole moment.

This system has the advantage of not accounting for energy transfers between adjacent molecules that may appear in nature, reinforcing the accuracy of the results and limiting the stimulus time propagation. After a certain and global amount of runs, it is created an output of several absorbance values as a function of wavelength which finally provides the simulated absorbance spectra of the studied channelrhodopsins. Hence, this system could be adapted to predict the effect of distinct mutations on a molecule, by changing the electron density cloud in the simulation and producing a novel hypothetical absorbance for the molecule.

In summary, the Time-Dependent Density Functional Theory (TDDFT) can be viewed as an exact reformulation of time-dependent quantum mechanics, where the fundamental variable is no longer the many-body wave function, but the density. This time-dependent density is

determined by solving an auxiliary set of non-interacting Schrodinger equations, the Kohn-Sham equations (Marques and Gross, 2004). Moreover, TDDFT has established extremely precise descriptions of biological chromophores such as fluorescent proteins like GFP (Marques *et al.*, 2003) and it was already used for the study of the excited state of DNA bases (Varsano *et al.*, 2006).

1.9 – Objectives

A major challenge facing neuroscience is the need to control one type of cell in the brain while leaving others unaltered. Francis Crick's goal has become a reality in the last decade. Optogenetics has emerged as a technique that allows the precise control over genetically altered neuronal populations, with a high degree of spatial and temporal resolution. A key component in optogenetic strategies is the protein ChR2, a light-gated channel that can be controlled with blue light, and that is currently the central paradigm of several improved tools driving the evolution of optogenetics.

Taking advantage of the recently published crystal structure of a model channelrhodopsin we applied Time Dependent–Density Functional Theory (TDDFT) to calculate specific point mutations predicted to induced red- and blue-shifts in the absorption spectra of ChR2. These mutations, if successful, may then be subsequently inserted in other rhodopsins for greater effect.

The relatively short supply of a red-shift alternative handicaps the use of ChR2 for deeper tissue stimulation, but also disqualifies its use for the distinct excitation in spatially overlapping neuronal population. For this last case, we also aimed to create a a blue-shift variant, leading to a separation of the maxima peaks of red and blue shifted mutants, but also further validating TDDFT predictions.

The main goal of the present project is to test the *in silico* prediction from TDDFT, provided by the Center for Computational Physics of University of Coimbra, and to create several mutant forms of ChR2 that display compounded red-shifted absorption and other characteristics desirable for future biotechnological, neuroscience, pharmaceutical and biomedical applications. As such, our goals included the use of site-directed mutagenesis to

generate new ChR2 mutants, and then the optimization of their expression and purification from two different heterologous systems (*E. coli* and *Pichia pastoris*), as well the characterization of the absorption spectra of the modified channels.

Validation of TDDFT will create an original method to produce a platform to requested colour-tuned ChR2 mutants towards the development of the optogenetic toolbox, with also a contribution to a wide range of previously mentioned scientific applications. We believe the same rationale can be applied in the future to create additional colour-tuned molecules.

Chapter II – Materials and Methods

II.1 – Materials

II.1.1 – Organisms

In this work, cultures of bacteria (*Escherichia coli*), yeast (*Pichia pastoris*) and primary rat cortex neurons were used. Their experimental use and source (table 1) are described in the following table.

Organisms	Use	Source
Escherichia coli DH5α	Molecular cloning	Invitrogen
Pichia pastoris X-33	Protein expression/purification	Invitrogen
Pichia pastoris SMD 1168H	Protein expression/purification	Invitrogen

Table 1 – List of organisms used in the present work.

II.1.2 – Vectors

Different vectors were used in this study, for different purposes, such as cloning and protein expression. After each molecular cloning experiment, each vector was analyzed by restriction enzyme digestion and sequencing, to confirm and validate the cloning process.

Vector name	Features	Source
pcDNA3.1-hChR2	CMV promoter; hChR2-eYFP; AmpR	addgene.org (from Karl Deisseroth)
pPICZ A	AOX1 promoter; c-myc tag; 6x His tag; ZeoR	Invitrogen
pPICZ(alpha) A	AOX1 promoter; α-factor signal sequence; c-myc tag; 6x His tag; ZeoR	Invitrogen
pGAPZ A	GAP promotor ; c-myc tag; 6x His tag; ZeoR	Invitrogen

Table 2 – List of vectors used in the present work.
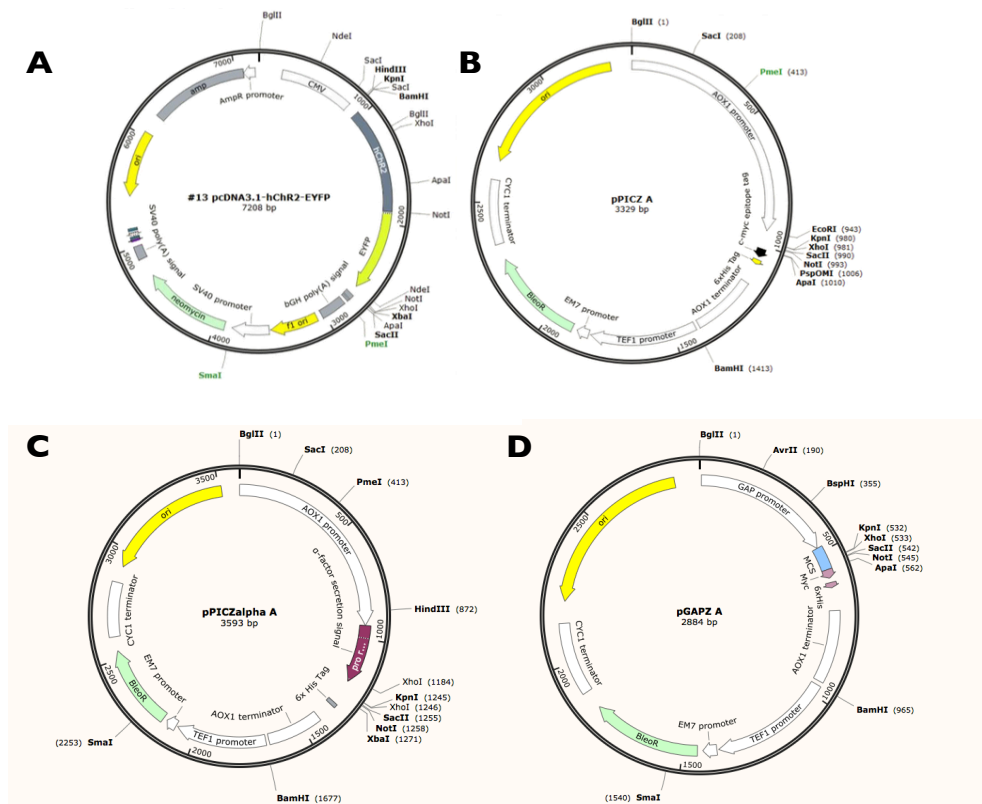
Figure 15 – Maps of vectors used in the present work. (**a**) The pcDNA3.1 vector includes a fusion protein of ChR2 and eYFP, regulated by the CMV promoter, an ubiquitous mammalian promoter. This vector was kindly provided by Karl Deisseroth (Stanford University, USA). (**b**) The pPICZ A vector includes AOX1, a specific inducible promoter for expression in *P. pastoris* and a Zeocin cassette used for positive clones selection. (**c**) The pPICZ(alpha) A vector shares the same features as the pPICZ A vector, but includes an α-factor signal sequence that enables the protein of interest to be secreted to the extracellular medium. (**d**) The pGAPZ A vector has a constitutive promoter, GAP, also suitable to be used in *P. pastoris*. All the vectors underwent restriction enzyme digestion and sequencing to confirm the presence of all the described features in each vector.

II.1.3 – Primers

All primers used in this work were synthesized in Stabvida (Lisbon, Portugal) and its name, sequence and purpose of use are described in Table 3, at the end of this chapter.

III.1.4 – Antibodies

Primary antibodies	Application (dilution)	Source
His-Tag	WB (1:1000)	Cell signaling technologies (MA,USA)

Table 4 – Primary antibody used in this study.

Secondary antibodies	Application (dilution)	Source
Anti- rabbit	WB(1:10000)	Jackson Immunoresearch Inc.(PA,USA)

Table 5 – Secondary antibody used in this study.

II.2 – Methods

II.2.1 – Channelrhodopsin-2 absorption spectra predictions and mutations rationale

Fernando Nogueira at the Center for Computational Physics at the University of Coimbra (C.C.F.U.C), provided the theoretical predictions of wild-type and mutants of channelrhodopsin-2 (ChR2) absorption spectra using created based on the Time dependent-Density Functional Theory (TD-DFT).

To create the ChR2 new variants, numerous aspects related to the choice of the residues to be mutated were considered. For instance, to maintain the channel activity of ChR2, no mutations were designed for the residues of the ion pore transmembrane sequence. Additionally, it was defined that the change of polarization/charge in mutated residues should result into larger effects than mutating a residue for a similar amino acid. Final residues choice was also complemented with additional information concerning the polarization of the retinal molecule, also provided by our collaborators at the C.C.F.U.C.

II.2.2 – Molecular Biology experiments

Site-directed mutagenesis

To generate the new variants of ChR2, site-directed mutagenesis was performed. Before the mutation procedure, the original DNA containing ChR2 (plasmid 20939: pcDNA3.1-hChR2-eYFP from addgene.org) was analyzed by enzymatic restriction digestion. This analysis was performed using enzymes such as XbaI and BamHi (NEB, MA, USA). The digestion product was

then loaded with DNA loading buffer (0,25% Bromophenol blue; 40% sucrose) into a 1% agarose gel and separated by electrophoresis in TAE buffer (40mM Tris Acetate; 1mM EDTA), until the correspondent bands were observable under UV light.

The site-directed mutagenesis strategy includes the use of specific synthesized primers (Table 3) (Stabvida, Lisbon, Portugal), designed using the PrimerX algorithm (http://www.bioinformatics.org/primerx/). These primers were designed to hybridize with part of the original ChR2 except for the nucleotides targeted for mutation. Polymerase chain reaction was performed to obtain mutated, linear DNA fragments (PCR) (Table 6). The temperatures and number of cycles used in this reaction are indicated in Table 7.

Mutagenesis PCR products were then incubated with DpnI enzyme for 2 hours and 30 minutes to remove parental methylated DNA, in a 1% agarose gel. A DNA recovery kit (Zymoclean Research, CA, USA) was used to recover and purify the digested DNA from the agarose gel. Of the total purified DNA, 20 uL were used for bacterial transformation.

Reagents	Concentration	Volume
5X PrimeSTAR buffer	5x	10 μl
dNTP mix	200 nM	4 μl
FW primer	200 nM	1 μl
REV primer	200 nM	1 μl
Template DNA (pcDNA3.1-hChR2)	500 ng	1 μl
DNA polymerase (PrimeSTAR HS DNA Polymerase)	2,5U/ μl	1 ul
dH2O		32 ul

Table 6 –PCR reaction mix for ChR2 directed mutagenesis.

Temperature(°C)	Cycles	Time(sec)	ChR2 variants
92		30	
95		30	
55	18	30	F217D and L221D
68		510	
98		30	
98		30	
65	18	30	F269D and F269H
72		510	

Table 7 – PCR programs for specific ChR2 mutations.

Bacteria transformation

The *E.coli* DH5α competent bacteria used for bacteria transformation was prepared with standard protocols. Briefly, after inoculation of 150 ml of LB media, cells were allowed to grow at 37°C until $O.D._{600}=0,4$ was reached. Cells were then pelleted at 3000 xg for 10 minutes at 4°C and the media removed. The pellet was ressuspended in 20 mL of cold 0.1 M CaCl2 and incubated for 30 minutes at 4°C. The suspension was then centrifuged at 3000 xg for 10 minutes and ressuspended in 3 mL of 0.1 M CaCl2 supplemented with 15% glycerol. The competent cells were then aliquoted and frozen in dry ice/ethanol slurry and stored at -80°C until further use.

Bacteria transformation was performed by adding plasmid DNA (~ 100ng-1ug) to an aliquot of competent cells previously thawed on ice. The suspension was then incubated on ice for 30 minutes. Subsequently, a heat shock treatment of 45 seconds at 42°C was done to the suspension, which were then allowed to recover on ice for 5 minutes. Afterwards, 9 volumes of LB (Fisher scientific, PA, USA) were added and the suspension was incubated at 37°C for 1

hour. Finally, cells were plated in LB/Agar plates previously prepared with the appropriate antibiotic, to allow the growth of only the bacteria expressing the antibiotic resistance cassette, present in the vector.

DNA isolation

Sixteen hours after bacteria transformation, colonies were picked and allowed to grow overnight in LB solution supplemented with the appropriate antibiotic. Plasmid DNA was then extracted and purified using a NZYMiniprep kit (NZYtech, Lisbon, Portugal), according to the manufacturer's instructions. Purified DNA was eluted with 15 µl of dH_2O.

DNA sequencing

To confirm the success of the site-directed mutagenesis and all cloning procedures in this project, a sample of the obtained DNA was sent to Stabvida (Lisbon, Portugal) for sequencing. The primers used for the sequencing procedures are indicated in Table 3.

ChR2 cloning into the pPICZ A vector

The sequences encoding the wild type and mutant forms of ChR2 were cloned into the pPICZ A vector (Invitrogen, PA, USA) in frame with 6x His TAG sequence. A set of specific primers (Table 3) were designed to add a 5' EcoRI and 3' KpnI restriction sites to the desired ChR2 fragment. Furthermore, a yeast Kozac sequence (AAAAATGTCTG) was added to the 5' end to further increase the expression efficacy (Kozak, 1987, 1990, 1991). The final fragment

was amplified by PCR reaction (Table 8), performed with the same protocol in Table 6, previously established and optimized. After DNA amplification was complete and confirmed in an agarose gel, the sample was treated with 1 μl of Proteinase K (NEB) for 30 minutes at 55°C to remove Taq polymerase and possible contaminants and finally digested with KpnI and EcoRI (NEB, MA, USA) restriction enzymes for 3 hours. The digestion product was then loaded into a 1% agarose gel and, after excision of the correspondent band the DNA was purified using the Gel DNA Recovery Kit (Zymoclean Research, CA, USA). The vector was also digested with the same enzymes, followed by incubation with calf-intestinal alkaline phosphatase (CIP) (NEB) to prevent vector re-circularization. The vector was purified using the same kit, and ligation with the ChR2 PCR insert was performed in a total volume of 10 uL using T4 Ligase (NEB) according to manufacturer's instructions. Once ligation was completed, the total reaction volume was transformed into *E.coli* DH5α and colonies were grown in LB/Agar plates supplemented with the appropriate antibiotic (25 ug/ml Zeocin (Invitrogen). Colonies were then screened by PCR reaction (table 9 and 10), using AOX primers (Table 3) and the DNA the from positive ones isolated and sent to sequencing to confirm the correct insertion and frame of the different variants of ChR2 (wild-type and mutants).

Temperature(°C)	Cycles	Time(sec)	ChR2 variants
98		30	
98		10	
55	35	10	F217D; L221D; F269D; F269H and
72		120	Wild-type
72		300	

Table 8 – PCR program for ChR2 insert into pPICZ A vector.

Reagents	Concentration	Volume
FW primer	200 nM	1 µl
REV primer	200 nM	1 µl
Template DNA	0.01-0.5 µg	Pick colony
NZYTaq 2x Green Master Mix (NZYtech)	0.2 U/ µl	12,5
dH2O		10.5

Table 9 –PCR screening reaction mix for ChR2.

Temperature(°C)	Cycles	Time(sec)	ChR2 variants
95		120	
95		60	
52	30	30	F217D; L221D; F269D; F269H and
72		60	Wild-type
72		300	

Table 10 – PCR screening program for ChR2.

ChR2 cloning into pPICZ(alpha) A and pGAPZ A vectors

Channelrhodopsin-2 was cloned into two suitable vectors for recombinant expression in *Pichia pastoris*, the pPICZ(alpha) A and pGAPZ A vectors (Invitrogen, PA, USA), using a cloning strategy similar to the one used for the pPICZA vector.

In pPICZ(alpha) A vector (Fig. 17) cloning, to amplify the ChR2 insert (from pcDNA3.1-hChR2- eYFP), a different designed set of primers (Table 3 and 11) was used containing the same restriction site sequences used for pPICZ A vector cloning. After digestion of the vector and the ChR2 inserts of the wild type and mutant forms of the protein with the same restriction enzymes, the screening was performed by PCR with the same primers and reaction mix used in the cloning of the pPicZ A vector. In this cloning the ChR2 sequence was fused with the α-factor signal sequence and in frame with the referred one, with the AOX1 promoter and with the 6x His Tag sequence.

Cloning the ChR2 forms into the pGAPZ A vector was done with the same protocol used for the cloning of the pPICZ A vector, including the primers (Table 3, 6 and 8). However, a different forward primer (Gap_Scr_FW) (Table 3, 9 and 12) was designed specifically for the screening step. This specific primer makes pair with the AOX REV (Table 3), since this vector, despite including a GAP constitutive promoter, still presents the AOX1 promoter terminator. Importantly, the sequences for ChR2 were in frame with the GAP promoter, with the added 5' end Kozac sequence and with the Histidine tag.

Temperature(°C)	Cycles	Time(sec)	ChR2 variants
98		30	
98		10	
60	30	15	Wild-type
68		120	
68		600	

Table 11 –PCR program for ChR2 insert into pPICZ(alpha) A vector.

Temperature(°C)	Cycles	Time(sec)	ChR2 variants
95		120	
95		60	
60	29	30	Wild-type
72		60	
72		300	

Table 12 –PCR screening program for ChR2 cloning into pGAPZ A vector.

Vector linearization

The efficiency of yeast electroporation is higher when the plasmid DNA is linearized, facilitating homologous recombination in the *Pichia pastoris* genome. As such, all vectors cloned with the different ChR2 forms were digested to generate a linear fragment. Briefly, 10 ug of each ChR2 DNA (wild-type and mutants) were digested with 5 ul of CutSmart buffer (NEB, MA, USA), 2 ul of PmeI enzyme (NEB) in a final volume of 50 ul, for 3 hours. After that, an additional 1 ul of enzyme was added and the digestion continued for more 2 hours. After digestion, linearization was confirmed in a 1% agarose gel. Finally, the digestion product was purified using the DNA Clean & Concentrator kit (ZymoClean Research, CA, USA). For the linearization of the vectors pPICZ A and pPICZ(alpha) A, specific restrictions enzymes that cleave the promoter region once but do not cleave within the ChR2 sequence were chosen. The PmeI enzyme was used with the pPICZ A and pPICZ(alpha) A vectors , whereas the Bsp HI enzyme was used with the pGAPZ A vector.

Pichia pastoris electroporation

The heterologous system chosen for the expression of wild type and mutant forms of the ChR2 protein was *Pichia pastoris*. The integration of the ChR2 protein sequences in the yeast genome was obtained with electroporation. Before the procedure, the selected *P.pastoris* strain (X-33 and SMD 1168H) was grown for 48 hours on YPD plates (1% yeast extract, 2 % peptone, 2% dextrose and 2% agar; from Fisher scientific, PA, USA). Then, a pre-inoculum of 10 mL of YPD media (1% yeast extract, 2 % peptone and 2% dextrose) was inoculated from a single *P.pastoris* colony and grew allowed to grow overnight in a 50 mL conical tube (Falcon™; Fisher scientific) at 30°C. On the following day, the culture was used to inoculate a 500 mL YPD culture in a 2.8 L Fernbach culture flask to a starting OD600 of 0.01. The culture was allowed to grow to an OD600 of 1.0 for 12 hours. Then, cells were harvested by centrifugation at 2000g at 4ªC, the supernatant was discarded, and the cells ressuspended in 100 mL of fresh YPD medium with HEPES (pH 8.0, 200 mM, Fisher scientific) in a sterile 250 mL centrifuge tube. Next, 2.5 mL of 1 M DTT (Fisher scientific) was added to the cells, gently mixed and incubated at 30°C for 15 minutes. After incubation, 150 mL of cold water was added to the culture and washed by centrifugation at 4°C with an additional 250 mL of cold water. At this stage, and from here on, the cells were kept on ice and in each step cells were ressuspended with slow pipetting, avoiding vortex. A final wash step was done with 20 mL of cold 1 M sorbitol (Sigma, NJ, USA) and then ressuspended in 0.5 mL of cold 1 M sorbitol, resulting in a final volume of 1.0-1.5 mL, including cells. These cells were used directly and freshly in the electroporation.

For the electroporation procedure, up to 1 ug of linearized plasmid DNA sample (in no more than 5 ul of water) was added to a tube containing 40 ul of fresh competent cells. The entire mixture was transferred to a 2 mm gap electroporation cuvette, on ice. The cell suspension was pulsed using MicroPulserTM Electroporator's "Pic" protocol (BioRad, CA, USA). Then, 0.5 mL of cold 1M sorbitol and 0.5 mL of cold YPD were added immediately to the cuvette and its entire content was transferred to a sterile 2.0 mL mini-centrifuge tube. Cells were incubated for 3.5-4 hours at 30°C with slow shaking (100 rpm). Finally, cells were spread onto YPD plates with 0, 100, 1000 and 2000 ug/ml Zeocin plates, to ensure the growth of recombinant colonies only. Agar plates were incubated for 2-4 days at 30°C before screening.

II.2.3 – ChR2 expression and purification from *P.pastoris*

Protein expression and extraction

Protein expression was first done in small scale, with the objective of screening the best colonies expressing ChR2. After choosing the colonies, ChR2 expression was done in a larger scale, to obtain higher amounts of protein.

For the expression of ChR2 in small scale, several single colonies were picked from higher resistance plates, 2000 ug/ml Zeocin plates (hyper resistant clones). These colonies were re-streaked onto 1000 ug/ml Zeocin plates to obtain isolated colonies and at the same time, to evaluate the expression of clones. Each colony was grown in 5 mL of BMGY (1% yeast extract, 2% peptone, 100 mM potassium phosphate pH 6, 1.45& YNB, $4x10^{-5}$ biotin, 1% glycerol) and allowed to grow overnight. Then, 100 uL of the culture was added to 10 mL of buffered glycerol complex medium (BMGY) and grown overnight again, until a 4-6 OD600 was achieved. The cells were harvested by centrifugation at 3000xg for 10 minutes and then ressuspended in buffered methanol complex medium (BMMY) (1% yeast extract, 2% peptone, 100mM potassium phosphate, pH 6, 1.45% YNB, $4x10^{-5}$ % biotin; 2.5% MeOH and 10uM *all-trans-retinal*) in a final volume of 50 mL to achieve a final OD600 of 1, with further incubation for 24 hours at 30°C. After induction, cells were harvested again at 3000xg for 10 minutes. Using the cell pellets obtained, 15 mL of homogenization buffer (11,3mM NaH2PO4 (Acros, NJ, USA); 100mM NaCl (Acros); 5% glycerol (Fisher, PA, USA); 1mM PMSF; 0.1 mg/ml pepstatin; 0.03 mM leupeptin; 145 mM benzamidine; 0,37 mg/ml aprotinin (Sigma, NJ, USA)) was added to the 50 mL culture pellet. To induce cell lysis, a cell pressure French press system was used (Thermo, MA, USA). Each cell suspension was run through the French press three times at ~7000 psi. After this step, intact cells and unwanted cell debris were removed by centrifugation at 8000 xg for 20 minutes and the pellet was discarded. To achieve the enriched membrane fraction, the supernatant was then ultra centrifuged at 180000 xg for 1 hour, ressuspended in solubilization buffer A (20 mM potassium phosphate pH 7,4 (Acros); 200 mM NaCl; 5% glycerol; 1% (m/v) n-Dodecyl β-D-maltoside (Calbiochem/Merch, Nottingham, UK); 250 mM l-arginine (Sigma, Buchs, Switzerland); 3uM *all-trans*-retinal (Sigma); 10mM imidazole (Sigma); 0,1mM PMSF (Acros)) in a ratio of 500 ul

per 50 mL of the initial culture. Ressuspended membrane fraction was then solubilized overnight and a new ultra centrifugation at 180000 xg for 1 hour was performed to remove insolubilized membrane fraction.

After the small-scale expression protocol, glycerol stocks were made from the screened positive colonies with high expression of ChR2, by diluting 800uL of culture into 500uL of 50% glycerol. These stocks were then used to obtain higher amounts of the different forms of ChR2cprotein for purification, using the same protocol previously described but now using increased volumes of the different solutions, to a final volume of 3 L of BMMY. As such, for the larger expression of the ChR2 proteins, a homogenization buffer ratio of 25 mL per 500 mL of initial culture was used and the ratio of solubilization buffer was increased to 5 mL per 500 mL of starting culture. Importantly, in this case, the EmulsiFlex-C5 system (Avestin, ON, Canada) was used to lyse cells, since the higher volume, viscosity and thickness of the cell suspensions after large-scale expression renders samples unable to flow properly through the French Press.

Protein purification with nickel affinity chromatography

Solubilized membrane fractions obtained for the clones expressing wild type and mutant forms of ChR2 were diluted 1:10 in solubilization buffer B (20mM potassium phosphate pH 7,4; 200mM NaCl; 5% glycerol; 0,03%(m/v) n-dodecyl β-D-maltoside; 0,1 mM PMSF; 10mM imidazole). This dilution was made to decrease the concentration of protein and DDM to values compatible with the columns used during the purification step (1 or 5 mL HisTrap FF Crude; GE Healthcare, NJ, USA). By means of peristaltic pump (~0.5 ml/min), 10-15 volumes of solubilization buffer B were used to equilibrate the column. Protein extracts were then loaded using the same system and samples were collected as flowthroughs. After all the ChR2 protein extracts had passed through the column, 10 more volumes of solubilization buffer B were loaded to make a re-equilibration and the columns were inserted into an AKT FPLC system (GE Healthcare) where OD_{260} was supervised. This system was set to a flow rate of 0.7 mL/min and equilibrated with solubilization buffer B until a stable baseline of OD_{260} was reached. Next, the column was washed with the solubilization buffer B containing 25 mM imidazole and eluted with an increased gradient of imidazole concentration, namely 100mM, 250 mM and 500 mM. At the

end of this process, fraction samples of 1.7 mL were collected and stored.

Protein dialysis and concentration

After successful purification, samples containing the wild-type and mutant forms of ChR2 were mixed, dialyzed and concentrated using Amicon® Ultra-15 Centrifugal Filter Units 10kDa (Millipore, MA, USA), following the manufacturer's protocol. The total volume of the dialysis unit was replaced at least 5 times. A second and final concentration was done using Vivasping 500 tubes (Sartorius Stedim Biotech, Aubagne, France), also according to the manufacturer's instructions.

Protein quantification

Protein quantification was achieved using Pierce™ BCA Protein Assay Kit (Thermo, MA, USA), following manufacturer's protocols and using the kit supplied 2 mg/ml BSA standard.

Gel electrophoresis (SDS-PAGE)

Protein samples were run on SDS-PAGE, providing separation of denatured proteins, in 12% polyacrylamide resolving gel (1.5 M TriS pH 8.8 (Fisher, PA, USA), 40% acrylamide (Fisher), 20% SDS (Fisher), 10% APS (Acros, NJ, USA) and TEMED (NZYtech, Lisbon, Portugal)) and 4% acrylamide stacking gel(0.625 M Tris pH 6.5 , 40% acrylamide, 20% SDS. 10% APS and TEMED). Samples were ran in 1x Running buffer (5x running buffer- 15 g of Tris base (Fisher); 72 g of glycine (Fisher) and 5 g of SDS (Fisher)) at 50-90 V. Previously, proteins were also diluted into 4x Laemmli buffer (Biorad, CA, USA) with β-mercaptoethanol and were incubated overnight at

4ªC in the denaturing buffer.

Western-blot

In western blot analysis, proteins were transferred to a PVDF membrane (GE Healthcare, NJ, USA) by electroblotting in a Mini-trans blot system (Biorad, CA, USA) with a 1x transfer buffer (transfer buffer 5x - 0.025 M Tris base; 0,192 M glycine) plus 5% methanol. The transfer ran at 100 V for 2 hours at 4°C. First, membranes were activated in methanol, and after transfer were washed in Tris-buffered saline (137 mM NaCl, 20 mM Tris-HCl pH 7.6) containing 0,1% (v/v) Tween-20 (TBS-T). After that, membranes were blocked in TBS-T with 5% (w/v) low-fat milk and probed with His-Tag antibody (Cell signaling technologies, MA, USA) diluted (1:1000) overnight in TBS-T with 5% BSA, at 4ªC. Then, it was done another thorough wash in TBS-T followed by la 2 hour incubation at room temperature with the secondary anti-rabbit antibody (Jackson ImmunoResearch Inc., PA, USA) diluted (1:10000). Another wash was done and membranes were finally revealed using Pierce ECL Western Blotting Substrate (Thermo scientific, MA, USA) according to manufacturer's instructions. Membranes were scanned with Storm 860 scanner (Amersham Biosciences, NJ, USA).

Comassie protein staining

Gels were incubated for 10 minutes in Comassie staining solution (0.05% Comassie Brilliant blue R-250 (Fisher, PA, USA), 25% methanol (Fisher) and 5 % acetic acid (Fisher)). Then, the gel was washed in a distaining solution (25% methanol; 5% acetic acid) once for 1 hour and then overnight. The gel was imaged with a standard computer scanner.

Silver protein staining

Silver staining of gels containing different fractions and the different forms of ChR2 were treated with a solution of 25% Methanol (Fisher) and 5 % acetic acid (Fisher, PA, USA) for 30 minutes, washed twice, first with 50% ethanol and then with 30% ethanol. Afterwards, gels were incubated and sensibilized in Sodium Thiosulfate 0.2 g/L (Acros, NJ, USA) for 1 minute, accelerating and enhancing further reaction with silver and reducing background staining. After washing twice with water for 20 minutes, gels were incubated in Silver Nitrate 2 g/L (Acros) for another 20 minutes. Finally, after another quick wash with water, gels were developed in a solution made of 30 g/L Sodium Carbonate (Acros), 10 mg/L Sodium Thiosulfate and 0.02 % formalin (Sigma, NJ, USA). The developing reaction was stopped by removing the gels from previous solution and incubating them in a solution of Tris 50 g/L and 2,5% acetic acid for 1 minute. The gels were then washed with water several times, imaged with a standard computer scanner and stored at 4°C.

II.2.4 – ChR2 absorption spectra determination

The concentrated and dialyzed forms of the ChR2 protein were inserted in a quartz cuvette (Quartz Suprasil; Hellma, Mullheim, Germany) in a final volume of 500 uL and the absorbance measured in a spectrophotometer (SpectraMax PLUS 384; Molecular devices, CA, USA), using a wide range of UV 200-800 nm. The absorbance of the buffer used to purify the different forms of ChR2 was also measured. The absorption spectra curves for ChR2 were then achieved by subtracting the absorbance of the buffer to the absorbance values obtained for the different ChR2 forms

Primers

Primer name	Sequence (5' to 3')	Goal
MutScr_1_F	GAGAACCATGGGACTCCTTGTC	L221D/L217D mutation screening
MutScr_1_R	CATACCCCAGCTCACGAAAAAC	L221D/L217D mutation screening
L221D_F	GTCATCTTCTTTTGTCTTGGAGATTGCTATGGCGCGAACACATTTTTTC	Directed site mutagenesis
L221D_R	GAAAAAATGTGTTCGCGCCATAGCAATCTCCAAGACAAAAGAAGATGAC	Directed site mutagenesis
F217D_F	CGGCTATGTTAAAGTCATCTTCGACTGTCTTGGATTGTGCTATGGC	Directed site mutagenesis
F217D_R	GCCATAGCACAATCCAAGACAGTCGAAGATGACTTTAACATAGCCG	Directed site mutagenesis
yChR2_F	GCCGAATTCAAAAATGTCTGACTATGGCGGCGCTTTGTC	ChR2 fragment to pPICZ A and pGAPZ A
yChR2_R	GCCGGTACCGGCGGCCGCTGGCACG	ChR2 fragment to pPICZ A and pGAPZ A
AOX1_F	GACTGGTTCCAATTGACAAGC	pPICZ A, and pPICZ(alpha) A Screening
AOX1_R	GCAAATGGCATTCTGACATCC	pPICZ A, pPICZ(alpha) A and pGAPZ A Screening
F269D_mut_FW	GTTCCCAATTCTCGACATTTTGGGGC	F269D directed site mutagenesis
F269D_mut_REV	GCCCCAAAATGTCGAGAATTGGGAAC	F269D directed

		site mutagenesis
F269H_mut_FW	GTTCCCAATTCTCCACATTTTGGGGC	F269H directed site mutagenesis
F269H_mut_REV	GCCCCAAAATGTGGAGAATTGGGAAC	F269H directed site mutagenesis
Seq_FW	CATTTTTTCACGCCGCCAAAGC	F269H/F mutation screening
Seq_REV	GGCTTCGTCTTCGACGAGAGTC	F269H/F mutation screening
pPicZ(alpha)_FW	GCCGAATTCGACTATGGCGGCGCTTTGTC	ChR2 fragment to pPICZ(alpha) A
pPicZ(alpha)_REV	GCCGGTACCGTGGCGGCCGCTGGCACG	ChR2 fragment to pPICZ(alpha) A
Gap_Scr_FW	GGTTTCTCCTGACCCAAAGAC	pGAPZ A screening

Table 3 – List of primers used in the present work.

Chapter III – Results and Discussion

III.1 – Molecular simulations of ChR2

Novel mutations for channelrhodopsin-2 (ChR2) were designed in order to obtain new useful variants of the protein, in particular to obtain forms of ChR2 that have a blue or red shift in the protein absorption spectra maximal peak. The theoretical prediction of the target residues to be substituted in the wild type form of ChR2 was performed in collaboration between our lab and the group of Fernando Nogueira at the Center for Computational Physics from the University of Coimbra.

Four mutations were proposed and selected, namely F269D, F269H, F221D and L221D. The protein structure used as reference for Time-Dependent Density Function Theory (TDDFT) computational calculations was the light-gated cation channelrhodopsin crystal structure (Kato *et al.*, 2012). Hence, designated residues were numbered in line with this structure (3UG9) that can be found at http://www.rcsb.org/pdb.

The F269D, F217D and L221D mutations were predicted to induce a red shift in the absorption spectra of ChR2, whereas the F269H mutation was expected to result in a blue-shift variant of the protein. These absorption spectra predictions were presented as putative shifts (Figure 16) and were based on TDDFT calculations for the four chosen mutants.

With the availability of the crystal structure of ChR2 (Kato *et al.*, 2012), other aspects of the fundamental molecular architecture of the channel were analyzed, including the retinal binding pocket, the inner pore and the cationic conductance, which enhances protein engineering pointed at the design of novel ChR2 variants with improved features. As such, all selected residues for mutation are located near the retinal molecule and are involved in the formation of the retinal-binding pocket (Kato *et al.*, 2012), but they are also positioned away from the hydrophobic ion pore (Figure 17), which further preserves and retains the gating properties of the rhodopsin channel. The proximity to the site where retinal binds renders these mutations suitable candidates to develop novel ChR2 variants, as corroborated by a study using site-direct mutagenesis to alter of the electrostatic environment in the retinal binding pocket, inducing several shifts and color tuning in the absorption profile of a protein-embedded *all-trans* retinal (Wang *et al.*, 2012).
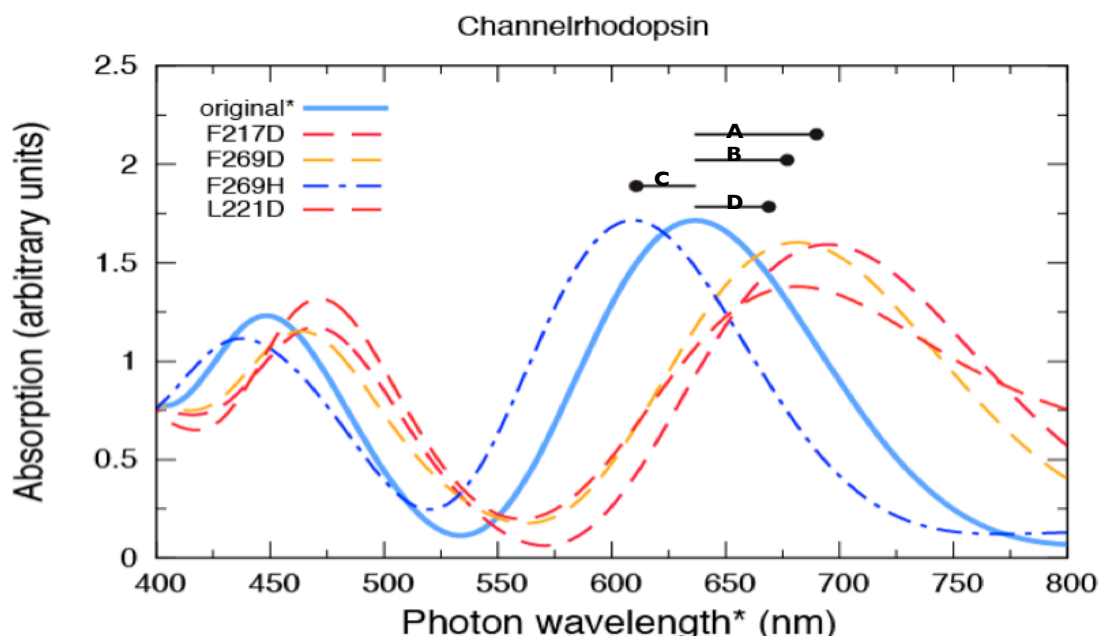
Figure 16 – Theoretical putative shift in ChR2 mutants achieved from TDDFT. Predicted spectral features of ChR2 wild type and four new mutants. ChR2 wild type absorption spectra is represented by full light-blue line. F269H (**c**) mutation induces a blue shift of ~30nm while F269D (**b**) is expected to induce a ~50 nm red shift in the abortion of the retina chromophore. F217D (**a**) mutation induces a red shift of ~60nm. L221D (**d**) mutation also produces a red shift of ~45. Note (*): wavelength output form TDDFT analysis is systematically right-shifted, e.g. the experimental absorption peak at pH 6.0 of dark adapted WT-ChR2 is centered at 480nm. These results are from Micael J.T. Oliveira, Bruce F. Milne and Fernando M.S. Nogueira (unpublished data).

With the aim of generating the biggest conceivable effect on the absorption spectra, the charge of each selected residues was changed. Specifically, phenylalanine (F) and leucine (L) have no charge in their side chains in physiological conditions, and are highly hydrophobic as a result of their non-polar nature. In consequence, both amino acids where mutated to aspartate (D), a residue exhibiting a negative charge at physiological pH. Indeed, the key amino acids chosen to be mutated in the variants of ChR2 were two phenylalanine residues in positions 269 and 217, and a leucine residue in position 221. All these residues were substituted by aspartate. According to the predictions, these changes would give rise to differences in the electrostatic environment surrounding the protein chromophore, the retinal molecule, and give rise to red-shifted ChR2 variants.

Besides the generation of original ChR2 red-shifted variants, the creation of a blue-shifted variant of ChR2 was necessary to further validate the TDDFT theory and all the

rationale behind these mutations with an opposite logic than the one used for red shift of absorption spectra. Furthermore, it would allow the use of a pair of ChR2 variants with non-overlapping absorption spectra, such as F269F (red) and F269H (blue). Therefore, the identical target F269 residue was replaced by a positively charged amino acid, histidine (H), to obtain a protein exhibiting a blue shift on the opsin absorption spectra.

This theoretical approach based on molecular simulation models using TDDFT can be considered original, as it has never been done before concerning rhodopsins and optogenetics tools such as ChR2. A similar approach done to generate new optogenetics tools consisted in an atomistic design of blue shifted "optotools". However, this method aims to mutate residues far from the retinal molecule environment, a less radical approach than the one we have performed in the present work. Furthermore, it uses different theoretical and mathematical calculation methods and it still bases its molecular simulations on classic molecular dynamics with several varying variables that may be divided into different groups and calculation phase steps, leading to simplifications that may drive the output of the simulation to be somewhat different from what it is observed. More importantly, our approach created wider predictive results, for both red and blue shift new variants, while the appeoach by Kato and collegues focused mainly on discovering blue shifted opsins.
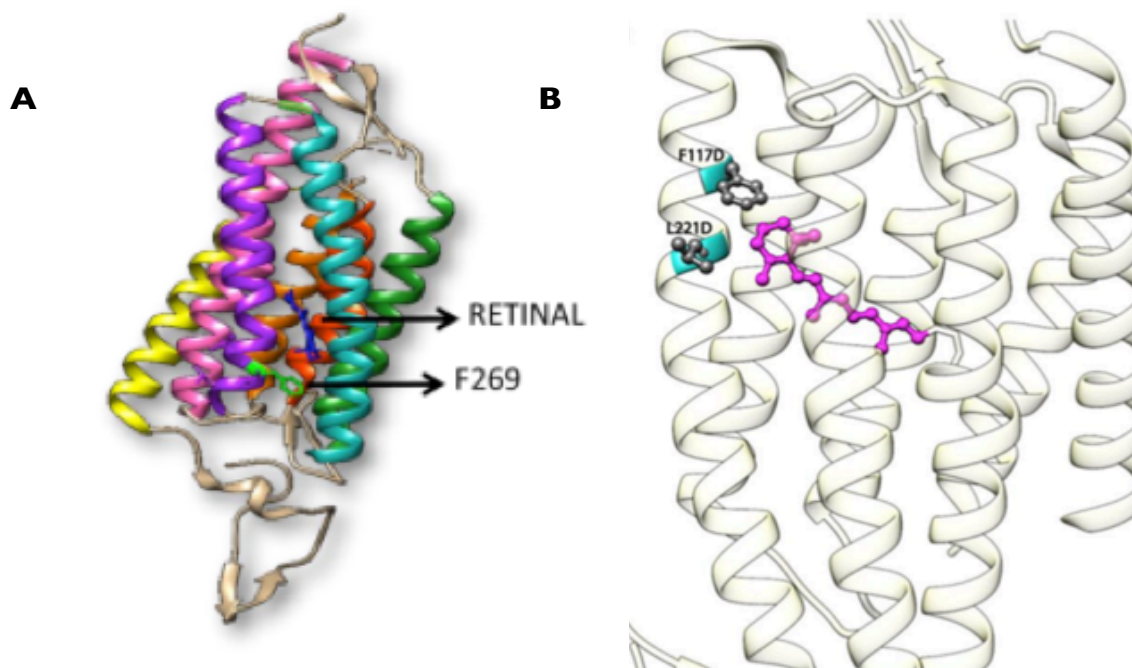
Figure 17 – Location of selected residues to mutate in ChR2 structure. (**a**) 3D structure of ChR2 light-induced cation channel. The structural seven transmembrane domains (7TM) are represented in seven different colours. Retinal molecule is emphasized in blue and F269 residue in green. (**b**) Alternative illustration of ChR2 structure comprising selected residues to mutate. F217 and L221D are represented in blue and black. Retinal is represented in pink. Selected residues and protein structures are based on ChR2 crystal structure by (Kato *et al.*, 2012).

III.2 – Site-directed mutagenesis of four novel ChR2 mutants

To test the feasibility of the proposed alterations to the ChR2 primary structure, we performed directed site mutagenesis on the original pcDNA3.1-hChR2 vector (plasmid with ChR2 wild type sequence), using phenylalanine 269 (F269), phenylalanine 217 (F217) and leucine 221 (L221) as targets. For one variant, the purpose was to substitute the TTC codon from F269 with a GAC codon that codified an aspartate, whereas for the second one, to substitute the same TTC for a CAC codon encoding a histidine. For the third mutation, the aim was to replace the TTT codon from F217 with a GAC codon codifying an aspartate. Finally, for the fourth mutation, the TTG codon from L221 was replaced by GAT, an aspartate codon. Hence, as theoretically suggested, all the non-polar targeted residues were substituted by polar amino acids.

PCR amplification was done using specific sets of primers to insert two mismatched based for each mutation. Once the mutants were obtained, sequencing was performed to confirm the modified bases (Figure 18).

The four novel mutations, predicted by TDDFT studies, were sucessfully generated by site-directed mutagenesis on the humanized ChR2 sequence (Lin *et al.*, 2009; Yizhar *et al.*, 2011), similarly to other channelrhodopsin structural and new variants studies (Berndt *et al.*, 2011; Govorunova *et al.*, 2011; Ritter *et al.*, 2008). We aimed to achieve color-tuning of ChR2 with single point-mutations, contrarily to the commonly adapted strategy of inducing several consecutive mutations, such as the development of new ChR2 variants like ReaChR (Lin *et al.*, 2013) or the nine point-mutations necessary to fully tuned the absortpion spectrum of a protein embedded all-*trans* retinal (Wang *et al.*, 2012).

A

ChR2 wt	504	AACCGGCTATGTTAAAGTCATCTTCTTTTGTCTTGGATTGTGCTATG
F217D Fw primer	576	AACCGGCTATGTTAAAGTCATCTTCGACTGTCTTGGATTGTGCTATG
F217D Rev primer	601	AACCGGCTATGTTAAAGTCATCTTCGACTGTCTTGGATTGTGCTATG
L221D Fw primer	570	AACCGGCTATGTTAAAGTCATCTTCTTTTGTCTTGGAGATTGCTATG
L221D Rev primer	598	AACCGGCTATGTTAAAGTCATCTTCTTTTGTCTTGGAGATTGCTATG

B

ChR2 wt	662	GCTGGGGTATGTTCCCAATTCTCTTCATTTTGGGGCCCGAAGGTTT
F269D Fw primer	728	GCTGGGGTATGTTCCCAATTCTCGACATTTTGGGGCCCGAAGGTTT
F269D Rev primer	757	GCTGGGGTATGTTCCCAATTCTCGACATTTTGGGGCCCGAAGGTTT
F269H Fw primer	733	GCTGGGGTATGTTCCCAATTCTCCACATTTTGGGGCCCGAAGGTTT
F269H Rev primer	758	GCTGGGGTATGTTCCCAATTCTCCACATTTTGGGGCCCGAAGGTTT

Figure 18 – Sequence results of ChR2 new variants induced mutagenesis. Alignment of the sequencing products of mutagenesis and respective analysis. (**a**) F217D and L221D mutations sequenced with specific forward and revers primers, MutScr_1_F and MutScr_1_R (Table 3). (**b**) F269D and F269H mutations sequenced with specific set of primers, Seq_FW and Seq_REV (Table 3).

III.3 – Molecular cloning into the pPICZ A vector

The heterologous system mostly used to produce and purify ChR2 is *Pichia pastoris* yeast (Bamann *et al.*, 2008, 2010; Nack *et al.*, 2010). Besides the low cost and high yield, the eukaryotic processing machinery renders *P. pastoris* a viable system for the small and large scale production of many integral membrane proteins for structural studies (Byrne, 2015).

Expressing functional proteins in E.coli system may be standard for some recombinant proteins, but it seems to be difficult for channelrhodopsins (Ernst *et al.*, 2008; Sineshchekov *et al.*, 2013). We excluded this possible approach predominantly due to the importance of similarity to the host, enabling the functioning of the needed post-translation modifications, protein targeting and folding. These particular features are not achieved in the prokaryote *E.coli* not capable to adapt to the eukaryotic ChR2. Other options have also been used, such as the Sf9 insect cells used in the ChR2 crystal structure experiments (Kato *et al.*, 2012) and in the atomistic design of new blue shifted variants based on molecular simulation models (Kato *et al.*, 2015).

However, we decided to use the *Pichia pastoris* model, for the reasons aforementioned. Furthermore, *Pichia* cells have an easier manipulation grow in high-density cultures that can possibly enhance higher levels of protein expression. Concordantly, other groups with comparable goals to this project already described expression of ChR2 in *P.pastoris* (Bamann *et al.*, 2008, 2010).

After the validation of the obtained mutations, encoded in mammalian vector pcDNA3.1 vector, each ChR2 sequence was cloned into a pPICZ series expression vector. This specific vector, contrarily to the mammalian vector, is a suitable heterologous expression vector to express recombinant protein in the selected *Pichia pastoris* system. All four mutants were cloned into the pPICZ A vector, including the wild type protein to be used as a control.

Specific primers (Table 3) were designed to shuttle each ChR2 sequence into the pPICZ A vector and, to improve expression in yeast, a Kozak sequence (Kozak, 1987, 1990, 1991) was included with two new restriction sites. Inserting a Kozak sequence in the *Pichia* genome along with our gene of interest would increase the level of protein expression by improving the translation process and facilitating the recognition of the initiator codon by ribosome (Mark Cigan e Donahue, 1987). Equally to our approach, other ChR2 variants studies also added Kozak sequence to enhance protein expression in Pichia pastoris(Lin *et al.*, 2013).

All ChR2 DNA sequences to be inserted into the pPICZ A vector were amplified by PCR, using as a template the mammalian pcDNA3.1 vector and the described set of primers (Table 3), respective for each protein variant. Using these primers, the amplified fragments were flanked with *EcoR*I and *Kpn*I restriction sites, previously added in the primers. The amplified fragments and the original pPICZ A vector were digested both with the same set of enzymes and purified. The cut with these restriction enzymes creates "sticky ends" at the extremities of both constructs (vector and amplified DNA), ideal for the ligation step. The ligation mix was used in transformation of *E.coli DH5α* competent cells on Zeocin plates. Since the resistance for this antibiotic is carried on the pPICZ A vector, only positives clones which incorporate the product of the ligation grow on Zeocin plates. The colonies were picked and used directly for PCR amplification as screening for positive ligation result. In this PCR screen, AOX_FW and AOX_REV primers were used (Table 3). These primers amplify the region in which the mutated sequence is inserted. The positive colonies were selected based on the expected weight of the bands in an agarose gel and a single colony was sequenced to confirm the presence of the formerly created mutation and the insertion of the fragment in frame with the histidine tag present in pPICZ A vector (Figure 19).

The same rationale was used for all ChR2 protein forms, that is, the four mutations and the wild-type control.

Similarly to other reports of ChR2 mutant structures (Bruun *et al.*, 2011), this approach led us to have the possibility of having channelrhodopsin-2 sequences successfully cloned in the pPICZ A vector, allowing to proceed with a methanol inducible expression of ChR2 in *Pichia pastoris*.

A

B

Figure 19 – Cloning strategy and sequence results of ChR2 mutants in pPICZ A vector. (**a**) Illustration of final expected fragment from cloning strategy used to transfer ChR2 protein forms from pcDNA 3.1 vector to pPICZ A. Aox1 promoter is presented in black, Kozak sequence (K) is shown in dark grey, ChR2 inserted sequence is presented on regular grey and 6x histidine Tag is presented in light grey. (**b**) Alignment of sequencing results from screened ligation products of all ChR2 protein forms cloned into pPICZ A vector. AOX forward and reverse primers were used for all these sequencing purposes.

III.3.1 – Linearization of the pPICZ A vector containing ChR2

Before *Pichia* pastoris wild type strain (X-33) cells were transformed by electroporation, the cloned vector pPICZ A encoding the inserted ChR2 protein forms was linearized. This protocol was done due to the fact that integration events occur with a higher probability with a linearized vector than with a circular one (Cregg *et al.*, 2009).

To achieve DNA linearization, the final vector containing ChR2 was digested with *PmeI* enzyme. This enzyme cuts in the AOX1 promoter region. To corroborate the successful vector linearization, samples were digested for five hours and ran on an agarose gel in parallel to the same, uncut, vector (Figure 20).

This achieved linearization, before electroporation, proved to be essential to strong integration of the plasmid into the Pichia pastoris genome and further effective expression of our protein of interest, as reported in several structural studies of ChR2 (Ernst *et al.*, 2008; Govorunova *et al.*, 2013; Müller *et al.*, 2015).

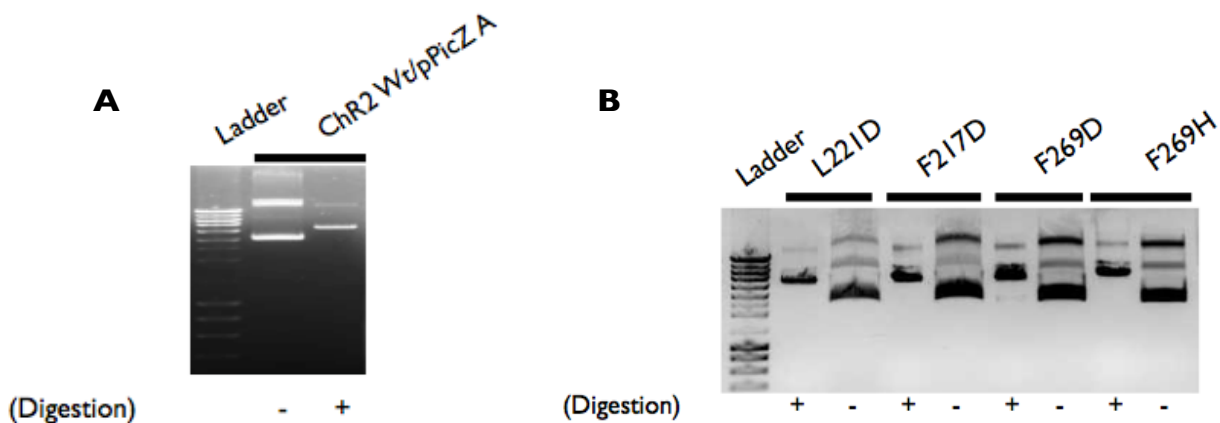**Figure 20 – Linearization of pPICZ A vector containing ChR2 protein forms.** Linearized vectors against non-linearized vector in 1% agarose gel. (**a**) ChR2 wild type in pPICZ A vector, linearized and non-linearized. (**b**) ChR2 mutants, L221D, F217D, F269D and D269H in pPICZ A vector, linearized and non-linearized. Non-digested vector runs at multiple different sizes due coiling of double stranded DNA,

III.4 – Heterologous ChR2 expression in *Pichia pastoris*

The first results are related to the wild type ChR2, from protein induction, small and large-scale expression and purification until the expected absorption spectra was achieved. This strategy was performed as a control, a first and crucial step to validate TDDFT predictions and to further optimize the protocol of induction, expression and purification of wild type ChR2. Only after completing this successful optimization, experiments were applied to the ChR2 mutants.

We established our experiments on successful preceding approaches to isolate ChR2 from *P. pastoris* (Bamann *et al.*, 2010; Ernst *et al.*, 2014; Lórenz-Fonfría *et al.*, 2013; Yizhar *et al.*, 2011). Nonetheless, we also established and optimized our own protocols directed to ChR2.

Several studies showed the competence of yeast to integrate multiple copies of the expression vector providing fast and improved means to obtain multi-copy expression colonies through colony selection on plates with higher concentration of antibiotic. Based on this findings, we defined our ChR2 selection method to maximally enhance the probability of selecting and picking the best possible colonies expressing ChR2, hyper resistant or "jackpot" colonies.

Hence, electroporated cells were plated on YPD-Zeocin plates with different and growing concentration of antibiotic (0 µg/ml, 100 µg/ml, 1000 µg/ml and 2000 µg/ml), as direct selection of positives recombinants (Figure 21a). The YPD-Zeocin plates were grown for 48 hours until clones were perceptible (Figure 21b).

Consequently, X-33 strain colonies were selected based on their growth in high Zeocin concentration in YPD plates associated with higher levels of protein expression. Colonies were preferentially picked from the 2000ug/ml Zeocin plates. Colony selection from plates with less concentrated antibiotic happened only if there were no visible colonies in 2000ug/ml plates and as a comparative control to the hyper resistant colonies (from 2000 Zeocin) (Figure 21a).

In fact, compared to all other plates, highest concentrated plates presented a very noticeable reduction in the number of grown colonies, usually with 1-10 colonies. The 100ug/ml and 1000ug/ml plates always presented a large number of colonies through all YPD surface, being more disperse on 1000ug/ml Zeocin plates. Therefore, hyper resistant colonies can be considered the colonies that integrated in their genome more copies of the vector through

repeated cycles of homologous recombination. As such, they contain not only multi-copies of the mutated DNA sequence but also from the Zeocin resistance cassette.

First, the 2000ug/ml Zeocin plate positive clones were re-picked to a fresh 2000ug/ml Zeocin plate (screening plate) (Figure 21c) and then grown in yeast complex media. Afterwards, a small-scale induction was performed (Figure 21d) to find the best possible colony expressing ChR2. To do this small scale the widest possible, several colonies were screened and analyzed, usually more than 10, from all variable electroporation plates. This small-scale induction was implemented with final 50 mL of growth culture. This protocol is original and created optimized for the purpose of this project. Each culture volumes, induction time and defined step in this protocol were optimized specifically for ChR2.

Briefly, 1-10 clones were first grown in BMGY, a medium containing glycerol as the carbon source, until an O.D.$_{600}$ between 4 and 6 is reached (usually 5 was used as the optimal O.D.). Then, clones grown in BMGY were centrifuged to discard the glycerol medium and ressuspended in BMMY, a medium containing 2,5% methanol and also supplemented with retinal (Bruun *et al.*, 2011) to induce ChR2 expression (methanol added to the complex medium acted as the activator of the AOX1 promoter). The 50 mL cultures were induced for 24 hours and then centrifuged to obtain a cell pellet, to further extract and isolate the expressed protein.
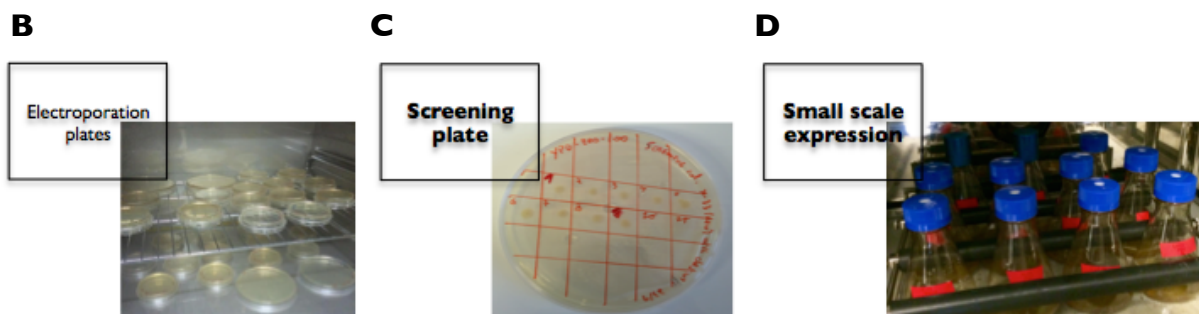
A

| 100 | 1000 | 2000 ug /ml Zeocin |
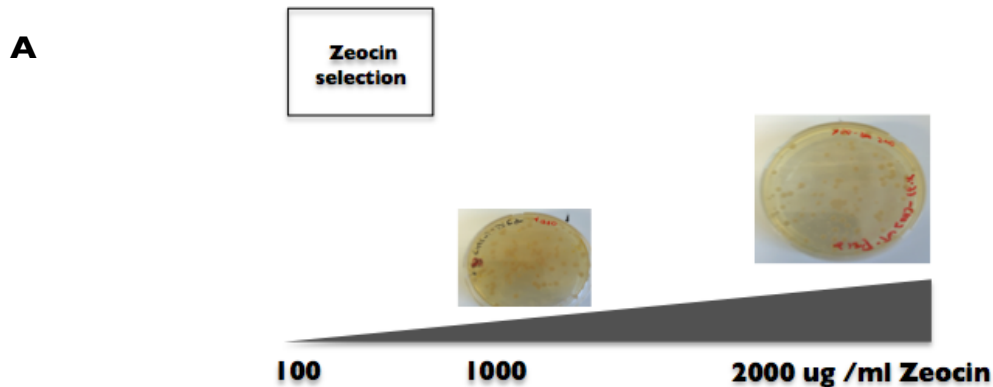
Zeocin selection

Figure 21 – Channelrhodopsin-2 expression strategy in *Pichia pastoris*. (**a**) ChR2 colony selection method based on growing Zeocin concentration. (**b**) Full range variety of YPD/Zeocin electroporation plates. (**c**) Screening plate with isolated selected colonies from original 2000ug/ml Zeocin plates. (**d**) 50 ml cultures of ChR2 small- scale induction screening in *Pichia pastoris* X-33.

Next, western-blot and silver staining techniques were performed to confirm ChR2 expression (Figure 22). First, an induction test was done comparing ChR2 expression in *Pichia pastoris* against the same yeast strain with no protein transfected (Figure 22a). This experiment confirmed that ChR2 was successfully and exclusively expressed and that the X-33 strain had no similar size endogenous protein recognized by his tag antibody.

Small scale screened colonies expression was also tested using western-blot (Figure 22b) and silver staining (Figure 22c). In these cases the protein expression in clarified cell lysate (removed of cell debris) was isolated from the membrane fraction and analyzed. It was also compared the expression of colonies from 1000ug/ml (control) against the ones in the highest 2000ug/ml antibiotic plates.

Analyses of these results showed the presence of ChR2 double band, one with 31 kDa and another one with 34 kDa (Figure 22). These bands are known to correspond to a glycosylated and non-glycosylated form of the protein (Ernst *et al.*, 2008). However, all the positions and amount of glycosylation in ChR2 remain undetermined (Kirsch, 2008). The glycosylations have an important role, as they are responsible for proper folding and targeting of channelrhodopsins.

We also observed that ChR2 presented a certain tendency to aggregate (Figure 22), a common feature in membrane proteins (Lin e Guidotti, 2009). Many published studies also witnessed that most opsins have a high tendency to aggregate in eukaryotic systems (Bamann *et*

al., 2010; Gradinaru *et al.*, 2010; Lin, 2011). Our decision of adding 2,5% methanol to the yeast culture buffered medium, contrarily to the 0,5% methanol commonly used in similar studies (Govorunova *et al.*, 2013), also proved to enable a high yield of expressed ChR2.

These results also corroborate the successful ChR2 expression as we observed stronger bands in isolated membrane fractions than in the respective cells lysate (Figure 22 b, c). Hence, from this point on, only isolated membrane fraction samples were presented and analyzed in the following experiments. Furthermore, it is clear that ChR2 presented stronger bands when isolated from 2000ug/ml colonies, compared to colonies from lower antibiotic plates.

Finally, the results obtained allowed the selection of a single colony (named as "1" in Figure 22b), the highest expressing one, to express in large-scale induction protocol and to be used as a control in the following ChR2 mutants experiments. This chosen hyper resistant colony was also tested using silver staining, and showed the same strong double band patterns, alongside with the presence of naturally occurring endogenous *Pichia* proteins (Figure 22c), commonly present due to the highest sensitivity of silver staining technique and the lacking of protein purification so far. The large-scale experiment included the scale up of the previously done small scale, from 50 ml to 3L culture, with each step being proportionally increased in terms of quantities. Colony 1 was successfully expressed in large scale (Figure 22d) and its membrane fraction was isolated to posterior purification of ChR2.

It is important to mention that the cell pellet obtained from large-scale induction was lysed with a EmulsiFlex-C5 system, instead of the French Press, due to the high amount of pellet obtained. The EmulsiFlex-C5 system made it possible to lyse a high amount of cells in large sample volumes and to achieve maximum ChR2 recovery.

We attained a considerable yield of channelrhodopsin using the *Pichia pastoris* system, as reported and established by other groups working on the same protein (Bamann *et al.*, 2008; Bruun *et al.*, 2011; Govorunova *et al.*, 2013; Müller *et al.*, 2015; Yizhar *et al.*, 2011), allowing further channelrhodopsin-2 purification.
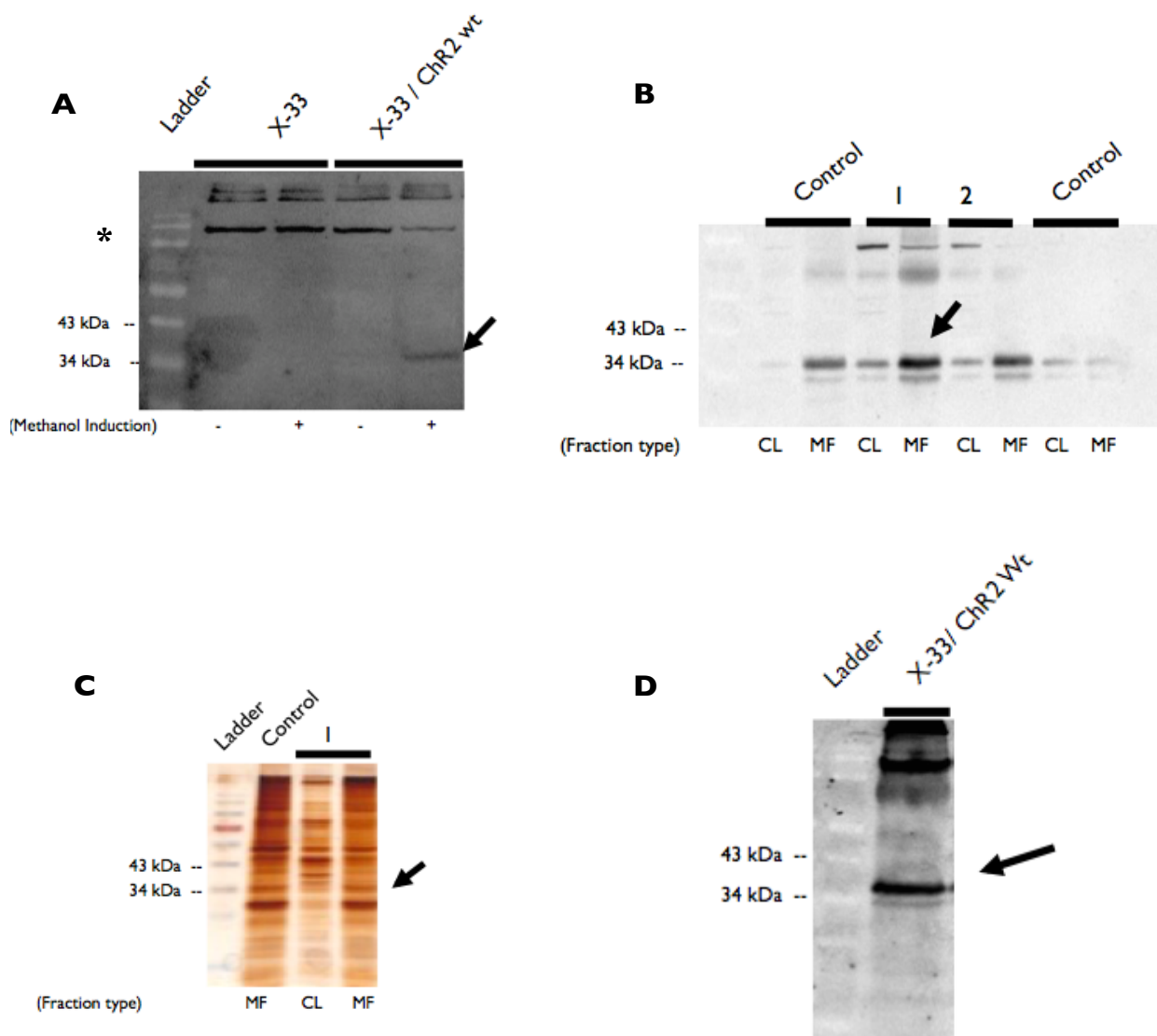
Figure 22 – Channelrhodopsin-2 expression tests. (a) Western-blot image for ChR2 wild type methanol induction test. (b) Western-blot results from small-scale screening identifying positive hyper resistant ChR2 colonies. Used controls are selected colonies from less concentrated YPD/Zeocin plates (1000ug/ml). 1 and 2 are the two best expressing colonies from previous wider small-scale screening (data not shown). CL represents cell lysate and MF represents membrane fraction samples. (c) Image from silver staining gel of CL and MF samples of chosen ChR2 wt best expressing clone, designated "colony 1" (from (b)). (d) Western-blot result representing successful scale up of ChR2 expression through large-scale protocol. (*) All western-blot membranes were incubated with rabbit anti-histidine primary antibody and anti-rabbit secondary antibody.

III.5 – Channelrhodopsin-2 purification

After ChR2 was isolated from yeast cells, the cell membrane fraction was solubilized with n-Dodecyl β-D-maltoside (DDM), a detergent formerly reported to stabilize ChR2 (Bruun *et al.*, 2011; Ernst *et al.*, 2008; Govorunova *et al.*, 2013; Kato *et al.*, 2012, 2015; Stehfest *et al.*, 2010), as well as comparable membrane proteins like type II (animal) opsins (Filipek *et al.*, 2003; Palczewski, 2006).

We then proceeded to the purification of ChR2. Initially, we performed this step using "in batch" purification technique, that is, incubating the protein extract with IMAC resin (immobilized metal affinity chromatography), outside a column. After that incubation time, the protein/resin mixture was inserted into an empty column and posteriorly eluted. Despite the fact that this technique has been used to purify several proteins (Chang, Chen e Ho, 2015; Chong *et al.*, 2009), in our hands this technique did not work, given that no specific ChR2 bands appeared in silver staining and comassie gels (data not shown). To overcome this obstacle, ChR2 was purified using pre-packed nickel columns suitable for nickel affinity chromatography, as used in similar experiments for channelrhodopsins (Kato *et al.*, 2012, 2015).

Following protein injection in the columns with a peristaltic pump, with a flow of 1 ml per minute, the system used for chromatography was the AKTA system. Our initial binding buffer composition contained 20 mM sodium phosphate pH 7,4, 200 mM NaCl, 5% (v/v) glycerol, 0,03% (w/v) DDM, 10 mM Imidazole and 250mM Arginine. This buffer was also based on channelrhodopsin published studies (Ernst *et al.*, 2008; Kato *et al.*, 2012), and was optimized to increase the purity of ChR2. After equilibration of the column with binding buffer, the protein extract was diluted 1:10 in the same buffer and then transferred in the nickel column, containing a resin with selectivity and high affinity for histidine-tagged proteins. In the AKTA system, ChR2 was automatically eluted with increasing concentration of imidazole, providing a specific chromatogram to indicate where and in which fraction the protein was eluted (Figure 23a).

After analysis of the obtained chromatogram UV peak, fractions samples were run on a SDS-PAGE. Also, silver staining was performed to the same gel to detect the purified ChR2 (Figure 23b). The presence of the same double band pattern observed in previous experiments showed again the existence of aggregates. Minimum contaminants were also observed in the silver staining gel but they were not significant to interfere with the following absorption spectra

determination. Samples 16-18 (Figure 23) were selected for the following experiments.

We achieved successful purification of ChR2 by nickel affinity chromatography, analogously to Kato's channelrhodopsin studies (Kato *et al.*, 2012, 2015) and by other groups (Berthold *et al.*, 2008; Bruun *et al.*, 2011; Govorunova *et al.*, 2013). The AKTA purifier system that we used to perform the affinity chromatography also proved to be suitable for imidazole gradient elution and an accurate final purification, as reported for other channelrhodopsin variants development (Bruun *et al.*, 2011).
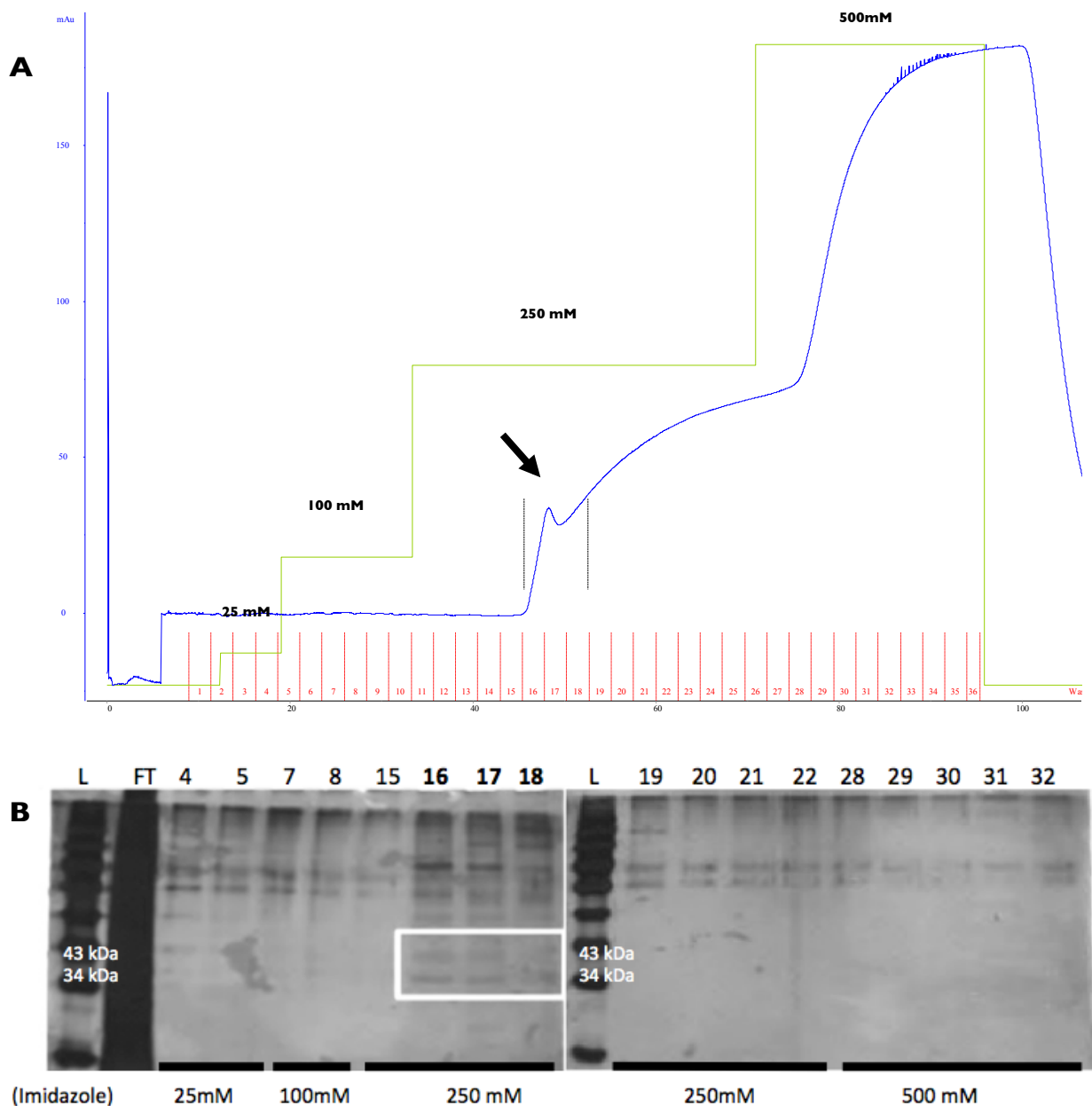

Figure 23 – ChR2 wt purification with nickel affinity chromatography. (a) ChR2 wt purification chromatogram. Absorbance at 260 nm is represented in blue, imidazole concentration in green,

collected fractions in red and black arrow indicates positive eluted fractions. (**b**) Silver staining of collected protein samples from imidazole elution range. Positive samples for ChR2 purified are indicated in white box.

III.6 – Determination of ChR2 wt absorption spectra

With the successful purification of ChR2, the next step was to determine its absorption spectrum. Respective measurements were obtained using a spectrophotometer, as done by other groups (Ernst *et al.*, 2008; Kato *et al.*, 2012; Ritter *et al.*, 2008). However, the device that we used was somehow less advanced than the ones used in other published studies. For example, other devices present more spectral resolution (2 nm (cite) vs. 10nm) and a more advanced illumination (with LED).

To achieve higher concentrations of ChR2 and to generate the most reliable absorption spectra, positive samples 16-18 were mixed together and concentrated by centricon centrifugation. The selected samples presented high concentration of imidazole (250 nM), naturally essential to elute the protein from the column. Before concentration, mixed samples were diluted three times to reduce imidazole concentration, detrimental to the centricon membrane.

Additionally, because concentrated protein fractions still presented some imidazole that could possibility interfere with the final absorption spectrum, we performed dialysis of the samples, in the same centricon used for sample concentration. Centrifuging the concentrated sample resulting in a simple salts buffer exchange (dialysis). An additional second concentration step was done to a final volume of 500 microliters. Final sample was achieved (Figure 24a), in a final buffer similar to the used binding buffer, with less imidazole (5mM).

After this process, the amount of purified protein was sufficient to produce absorption spectra (Figure 24b), similar to what has been observed in other published channelrhodopsin structural studies (Ernst *et al.*, 2008; Govorunova *et al.*, 2013; Kato *et al.*, 2012; Muders *et al.*, 2014; Ritter *et al.*, 2008).

The wild type of ChR2 presented a very noticeable peak, in the blue light region of the spectra, as predicted and expected as a main feature from ChR2. However, the maximal peak

was centered at 510 nm, a slight red shift compared to the 470 nm established for wild type ChR2 (Nagel *et al.*, 2003; Ritter *et al.*, 2008; Zhang *et al.*, 2010). This may be explained by the fact that pH and imidazole, especially the pH, affect the spectral properties of ChR2 (Ernst *et al.*, 2008; Scholz *et al.*, 2012) and even ChR1 (Berthold *et al.*, 2008), specifically causing red-shifts in the final output. In our case, the absorption spectra was measured with wild type ChR2 in a final buffer of pH 7, against the 7,4-7,5 pH of other published spectra (Ernst *et al.*, 2008; Ritter *et al.*, 2008). Additionally, the buffer used in this output also contained imidazole (5mM).

This first valid absorption spectrum of wild type ChR2 obtained was the primary goal and achievement of this work, crucial to the following experiments, as it demonstrated it was possible to achieve an absorption output from ChR2 with the strategy we defined. It was also used as the main control for experiments using each ChR2 mutant, and the first step to validate TDDFT predictions. More importantly, wild type ChR2 successful absorption spectra enabled the possibility to compare and determine the predicted and desirable shifts of the new variants. Further optimizations are presented below regarding the new ChR2 variants.
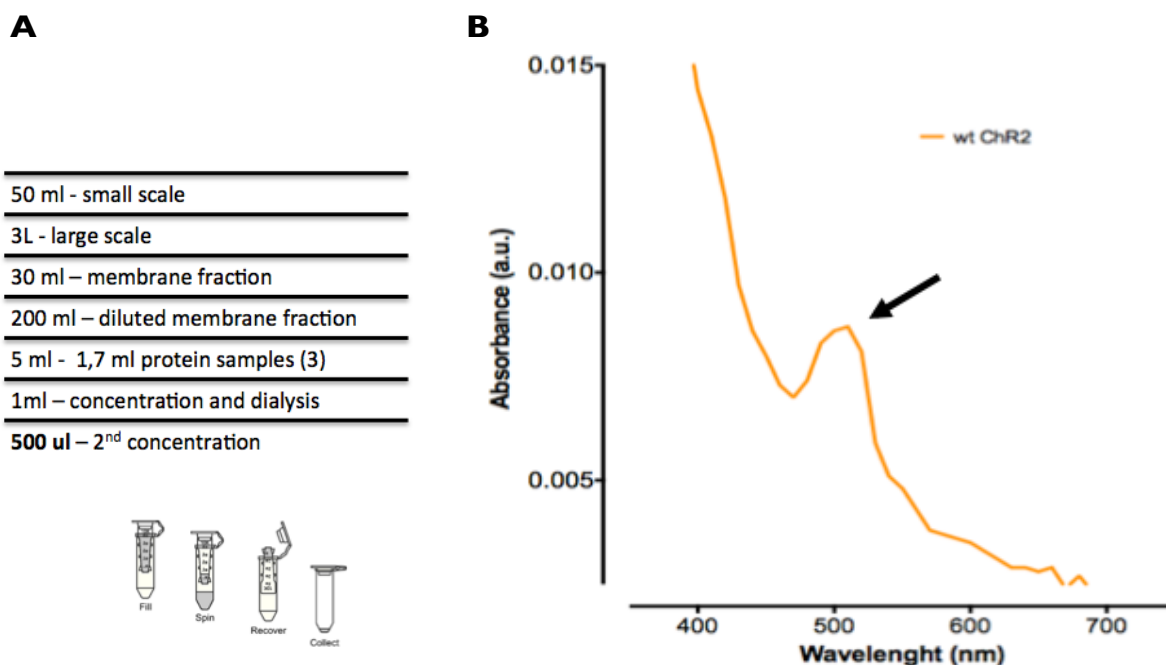

Figure 24 – UV-visible spectroscopy of purified ChR2 wild type. (**a**) Complete steps of adopted strategy to achieve final sample of purified and concentrated ChR2 wt. (**b**) Absorption spectra of purified ChR2 wt in dodecyl maltoside solution at pH 7.

III.7 – Protocol optimization

After the validation of the spectral properties of wild type ChR2, we proceeded to the experiments using the four new ChR2 mutants with the same strategy used for the wild type protein. Hence, following the determination of wild type ChR2 absorption spectra, a few steps in the protocol were optimized to achieve better results with the mutants, such as higher yields of expression for all ChR2 forms.

Particularly, two main optimizations were tested: the use of a new strain of *Pichia pastoris* and the use of new vectors, suitable for the heterologous protein expression in the yeast system. The protein purification protocol was also optimized, as shown below.

III.7.1 – *Pichia pastoris* SMD1168H strain

After the purification of ChR2 from *P. pastoris*, we aimed at obtaining higher yields of ChR2 expression from this system, as superior amounts of extracted protein enhance purification and to obtain better and accurate absorption spectra. We therefore used a different strain of *Pichia pastoris* to induce and express ChR2: instead of the X-33 wild type strain previously used and that have been shown to present low expression levels in ChR1 (Berthold *et al.*, 2008), we followed the identical protocol of protein induction and extraction exploiting the SMD1168 strain, a protease-deficient strain lacking key protease activity, described to led to a higher expression of recombinant proteins .

ChR2 expression in *P.pastoris* have been reported to be enhanced with the use of proteinase A (pep4) deficient strains and the SMD1168H strain in particular was already successfully used in channelrhodopsin heterologous expression (Govorunova *et al.*, 2013; Hou *et al.*, 2012; Yizhar *et al.*, 2011). Hence, to test this new strain and to obtain better results with the ChR2 variants, we performed a high-throughput small-scale induction as a wide screening to compare X-33 vs. SMD1168H protein expression, but also to select the best ChR2 mutant colonies to use in large scale and further purify.

We electroporated all ChR2 forms, wild type and four mutants, in both X-33 and SMD

yeast cells. Afterwards, we picked several colonies from 2000ug/ml antibiotic plates and a few ones from 1000ug/ml for additional control. Then, we compared by western-blot all the screened isolated membrane fractions, attaining a very expressive output of X-33 vs. SMD expression capability. We also used as a control, the "colony 1" that was used in the previous experiments to achieve our first absorption spectra. These results are shown in Figure 25.

We obtained positive clones for all ChR2 forms in both *Pichia* strains. However, as reported on published literature (Govorunova *et al.*, 2013; Hou *et al.*, 2012; Yizhar *et al.*, 2011), when analyzing these results, it is clear that SMD1168H clones accomplished significantly higher expression levels of ChR2 than the ones from X-33. This showed that enhanced expression efficiency can be obtained for all protein variants in SMD and even when comparing the oldest "colony 1" to new wild type and mutant clones. SMD clones also tended to present less aggregation than X-33 clones.

The output from these experiments led us to choose SMD1168H strain to express the ChR2 mutants in large scale and also the wild type form of ChR2 as an additional and accurate control for these new optimizations. The best expressing colonies were selected for each protein form based on these results.
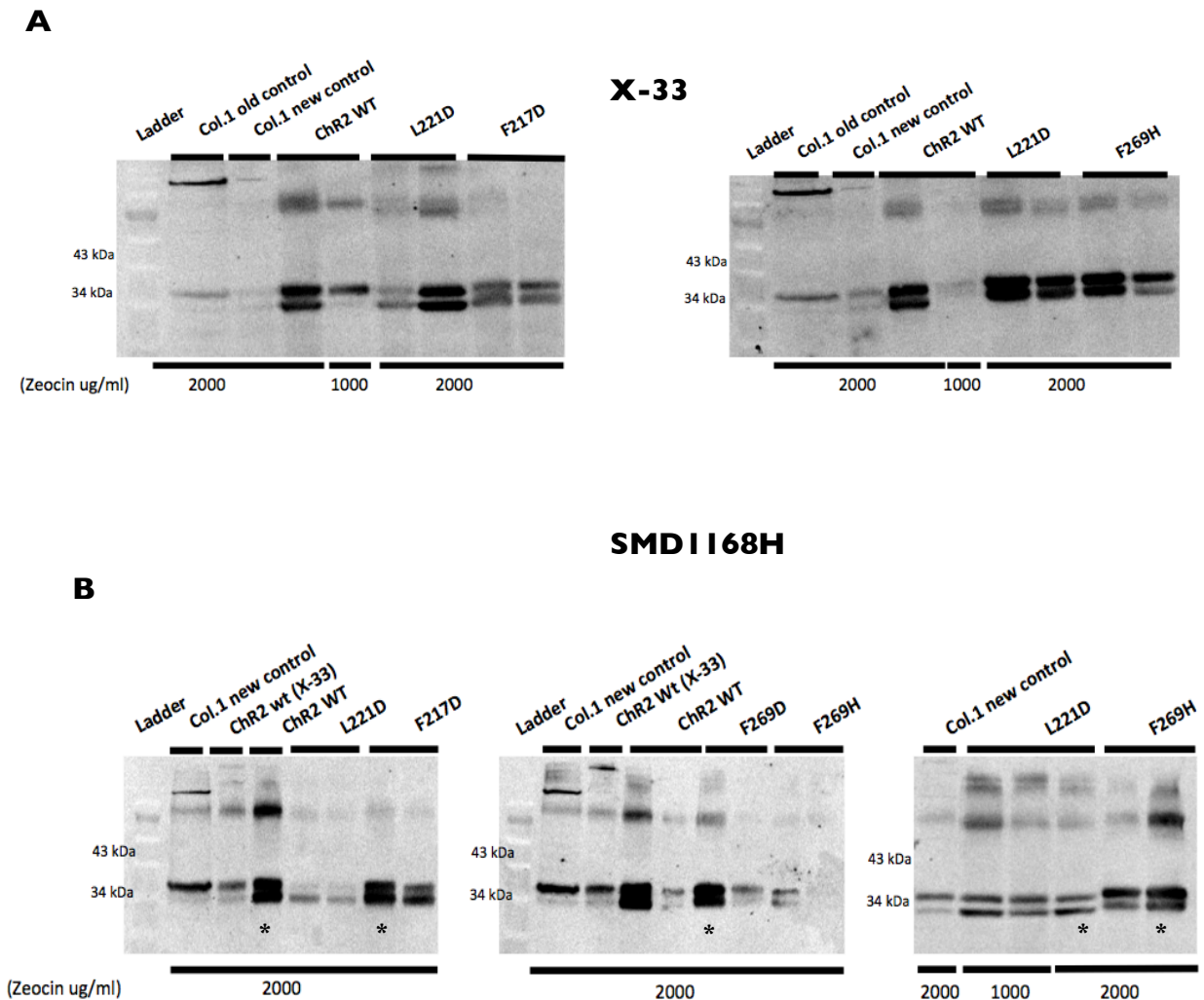
A

X-33

SMD1168H

B

Figure 25 – SMD1168H vs. X-33 ChR2 expression. (a) Western-blot image of small-scale screening of ChR2 wild type and four new variants, expressed in X-33 *Pichia pastoris* strain. Colony 1 was used as control from previous expressed ChR2 wt in X-33. Double control with ran samples of first/old induction and new induction in parallel with other presented clones. **(b)** Western-blot image of mall-scale screening of ChR2 wild type and mutants, expressed in SMD1168H *Pichia pastoris* strain. Same double control with Colony 1, with additional control of ChR2 wt expressed in X-33. * Represents selected clones for posterior large-scale induction. All western-blot membranes were incubated with rabbit anti-histidine primary antibody and anti-rabbit secondary antibody.

The results obtained after small scale screening (Figure 25) allowed the selection of the best expressing clones and to perform large scale induction to each one. After lysis of the yeast cells and isolation of the membrane fractions, an additional test was done before proceding for protein purification. Samples from the large scale induction of each ChR2 variant were

compared with the same ones from respective small scale using western blot analysis to confirm successful scaling up of protein expression (Figure 26). Three samples were compared for each ChR2 variant: one from the 50mL culture small-scale, an intermidate from both scales, 50mL removed from the 3L large-scale, representing the exact same amount of pellet from the small-scale, and a third one, from the 3L large-scale.

All four channelrhodopsin-2 new mutants presented clear double pattern bands, when expressed in large scale culture with *Pichia pastoris* SMD1168H, corrorobating again the known efficacy of this specifc yeast strain for channelrhodopsin expression (Govorunova *et al.*, 2013; Hou *et al.*, 2012; Yizhar *et al.*, 2011). The ChR2 specific bands in large-scale samples are clearly stronger than the ones resulted from expression in small scale cultures, validating our scale-up strategy.
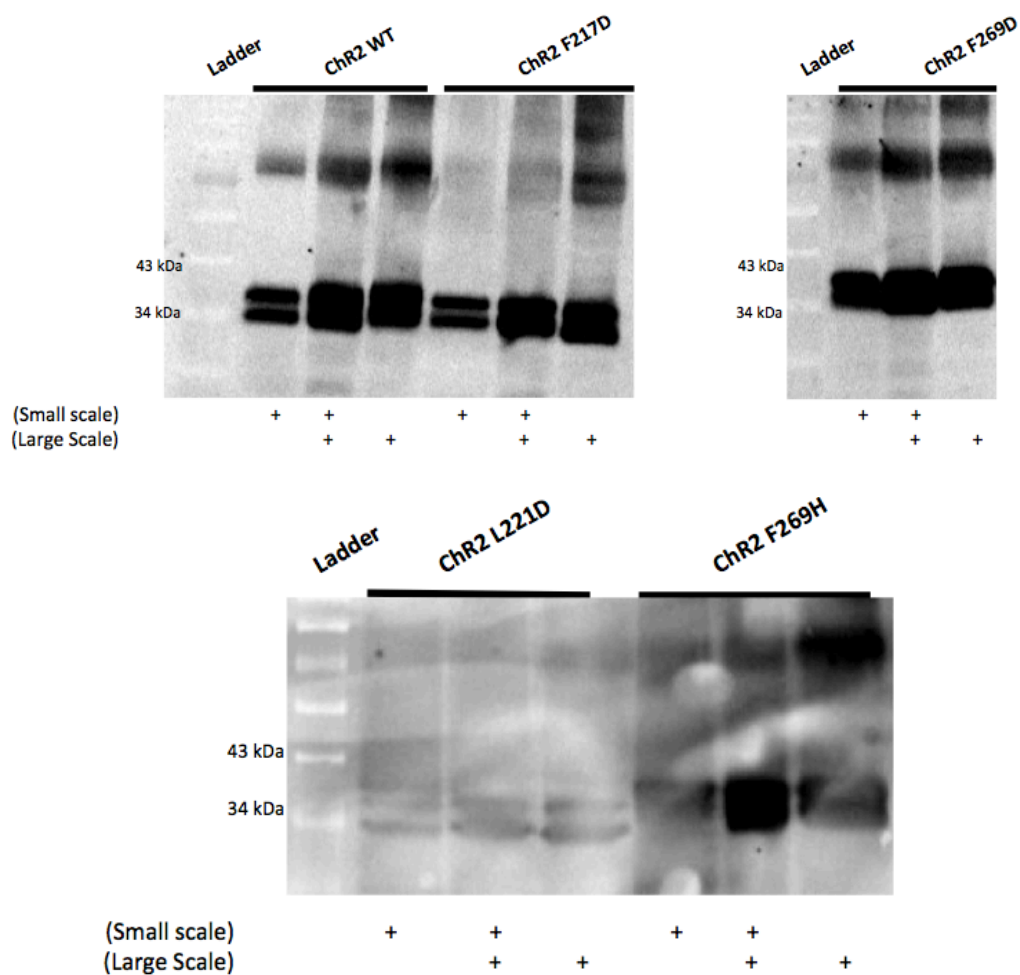

Figure 26 – ChR2 large-scale induction test. (**a**) Western-blot image of large-scale vs. small scale of selected ChR2 clones to purify. All western-blot membranes were incubated with rabbit anti-histidine primary antibody and anti-rabbit secondary antibody.

III.7.2 – Alternative expression vectors for *Pichia pastoris*

III.7.2.1 – ChR2 constitutive expression

The heterologous *Pichia pastoris* system presents multiple suitable commercial vectors for convenient protein expression. *Pichia pastoris* harbours several stronger or weaker promoters that can be exploited to drive heterologous expression of recombinant genes, both in an inducible or constitutive fashion. Our gene of interest, ChR2, was cloned into the pPICZ vector, as previously shown. With this vector we achieved successful ChR2 expression. However, to achieve higher amounts of expressed protein, we decided to test alternative vectors, specifically the pGAPZ vector for constitutive expression.

With the same cloning strategy used for the pPICZ vector, we cloned wild type ChR2 in frame with the *GAP* promoter, the histidine tag and a Kozak sequence (Figure 27). Cloning was successful, as confirmed by PCR screening (Figure 28a) and sequencing (Figure 28b).
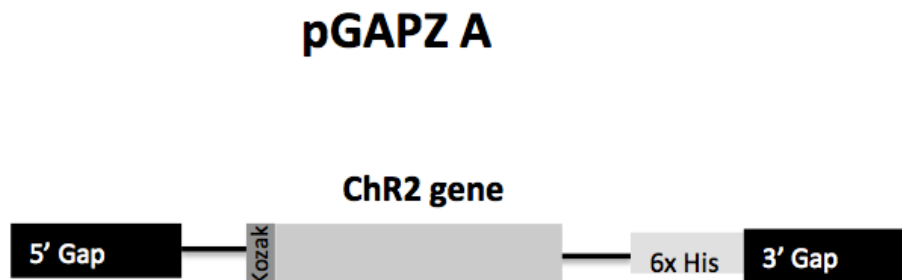

Figure 27 – Cloning strategy for constitutive expression of ChR2 wt. Illustration of final expected fragment from cloning strategy used to transfer ChR2 protein forms from pcDNA 3.1 vector to pGAPZ A. GAP promoter is presented in black, Kozak sequence is shown in dark grey, ChR2 inserted sequence is presented in regular grey and 6x histidine Tag is presented in light grey.
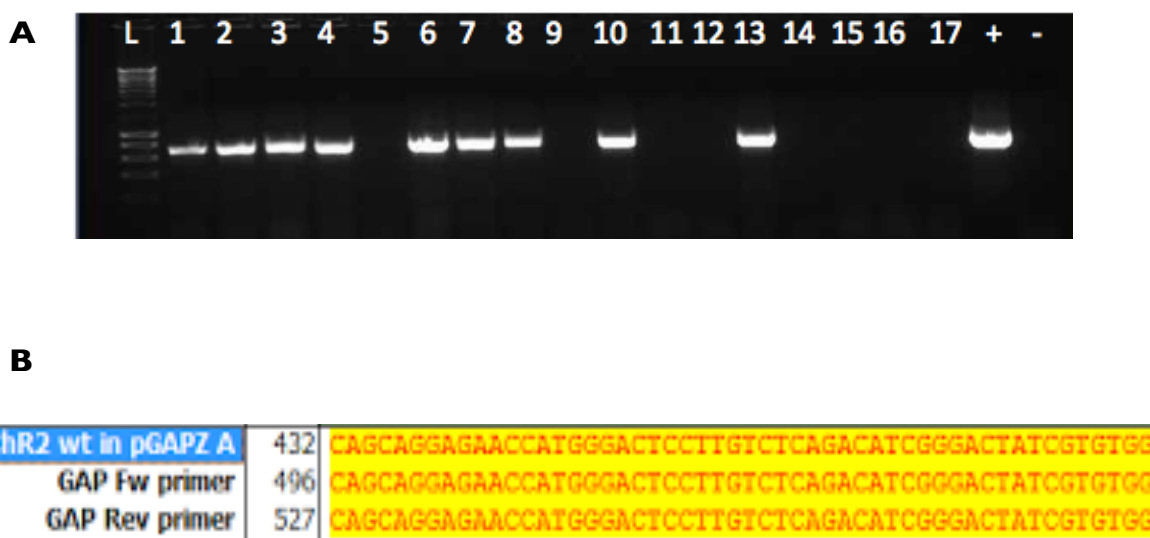
Figure 28 – PCR screening and sequence results of ChR2 wt cloning into pGAPZ A vector. (**a**) PCR screening of ligation product of ChR2 wild type cloning into pGAPZ A vector. Expected band of ~700bp. Used primers on table 3 (Gap_scr_fw and Aox_rev). (**b**) Alignment of sequencing results from positive colony 4. Gap_scr_fw and Aox_rev primers were used to sequencing purposes.

Inducible expression is usually the preferred strategy, since it allows a convenient control of the experimental conditions applied before expression and is ideally adapted for the production of proteins that are toxic to the host. We used the promoter mostly used for the alcohol oxidase-encoding gene (*AOX1*). This promoter is tightly repressed by glucose and strongly induced by methanol (Hartner e Glieder, 2006), allowing cells to use methanol as their sole carbon source.

So far, there are no reports of the constitutive expression of channelrhodopsins, which increases the interest of our approach. However, there are numerous cases where constitutive expression performs as well as inducible expression, in particular when using the strong glyceraldehyde-3-phosphate dehydrogenase (*GAP*) promoter (Cos *et al.*, 2006; Qin *et al.*, 2011; Zhang *et al.*, 2009). In addition, constitutive expression is more straightforward to manage since no switch in the carbon source is required, which can be particularly convenient when running fermentation procedures.

Constitutive expression eases process handling, omits the use of potentially hazardous inducers and provides continuous and slower transcription of the gene of interest. For this purpose, the GAP promoter is commonly used and, on glucose, reaches almost the same

expression levels as methanol-induced AOX1 (Waterham *et al.*, 1997). Expression levels from GAP vectors drop to about one half on glycerol and to one third when cells are grown on methanol (Cereghino e Cregg, 2000). However, only reasonable protein levels were reached after optimizing cultivation conditions (Várnai *et al.*, 2014), normally less than with inducible promoters.

We electoporated the linearized wild type pGAPZ/ChR2 construct into SMD1168H and X-33 yeast cells, proceeding to small scale screening and selecting the best expressing clone, the only SMD colony that grew in 2000ug/ml Zeocin plates.

Afterwards, to optimize ChR2 expression and to compare with the pPICZ vector, a time point induction test was performed using that selected colony (Figure 29a). A successful constitutive expression of ChR2 wild type was achieved. All samples were normalized, with the same amount of loaded protein (250mg), all grown from 50 mL small-scale culture and with the same weight of the final cell pellet. After western blot analysis, it is possible to conclude that the optimized time for constitutive wild typ ChR2 expression was 36h (Figure 29b). When comparing 24h induction (time used for inducible expression) from both vectors, we confirmed that, according to the literature, constitutive expression yields less amount of protein than inducible expression (Figure 29c).

Interestingly, when constitutively expressed, ChR2 presents an initial pattern of two bands. With the increasing of induction time, after 24 hours, it presents a single band. This noticeable fact contrasts with the double band pattern shown after inducible expression. Consequently, it is possible to speculate that constitutively expressing ChR2 enhances its glycosylation, which becomes more efficient and more complete than with inducible expression. As a result, ChR2 is more prevalent at the membrane. This fact is probably due to the simpler and slower induction and expression with the GAPZ vector, with no need to change the carbon source during the experiment.

These results allow the comparison between both types of induction. However, to achieve even more accurate information, the time point test required further replication and the western blot quantification to be performed with a loading control (for example, beta-tubulin). Unfortunately, these experiments were not performed due to time constraints.

Finally, after obtaining higher amounts of expressed protein, the pPICZ vector was used in the following experiments with the ChR2 mutants.
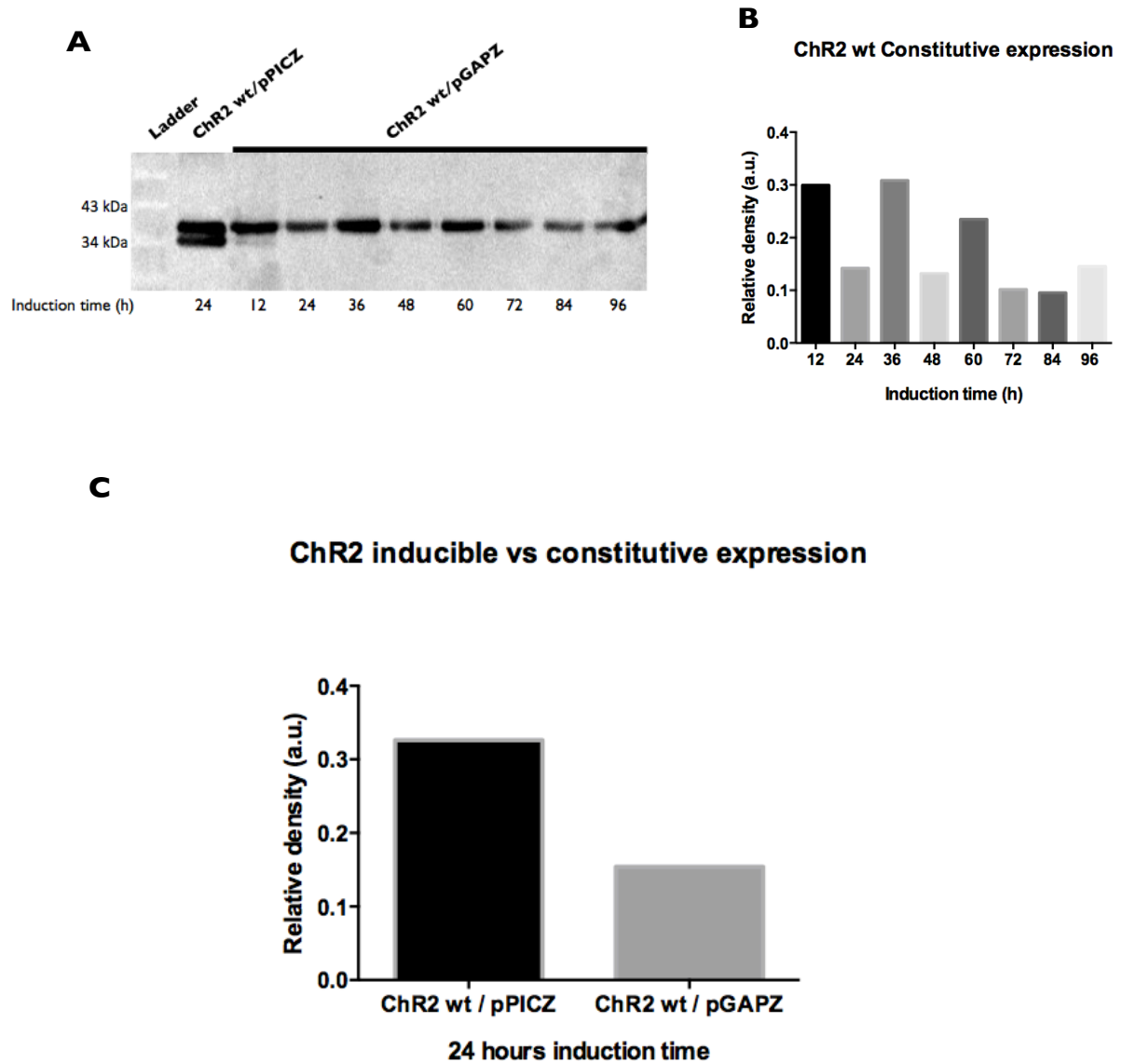
Figure 29 – Inducible vs. constitutive expression in ChR2. (**a**) Representative western-blot of ChR2 wild type constitutive expression. Inducible expression is presented as a control. All samples were quantified and normalized. It was loaded 250mg of protein per well. (**b**) Relative quantification results of ChR2 wild type time-point induction test. (**c**) Relative quantification of protein amount in 24 hours of constitutive expression and 24 hours of inducible expression.

III.7.2.2 – ChR2 secreted expression

Having successfully expressed channelrhodopsin with an inducible and constitutive strategy, the next test was to express this protein with a secretion strategy. The secretion of recombinant proteins to the culture medium, outside the cell, may present some advantages: soluble protein expression may be induced for longer periods of time, since they do not accumulate in the limited volume of the cytoplasm where they might become toxic for the host. This can lead to an increase in the expression yield. Furthermore, no cell lysis is required and secreted proteins can be recovered directly from the culture media, which contains far fewer contaminating proteins than the cells, thus simplifying the purification process. One limitation is the frequent degradation of the secreted proteins by extracellular proteases and proteases released from lysed cells. In addition, proteins that are not naturally secreted, like Ch22, may not be properly folded outside the cell. In this regard, intracellular expression is a valuable alternative (Delroisse *et al.*, 2005; Fantoni *et al.*, 2007), as successfully proved by our experiments.

When choosing a secretion strategy, the target protein needs to be recognized for the secretion pathway by the presence of a signal sequence. Successful secretion of many proteins from *P. pastoris* has been reported using a range of different signal sequences. These include a protein's native secretion signal, the *Saccharomyces cerevisiae* α-factor secretion signal. The vector that we used for this approach, pPICZ (Alpha) A contains the same AOX1 promoter with the additional feature of including this secretion signal.

In the case of integral membrane proteins, adding a secretion sequence may be highly beneficial for expression in *P. pastoris*. Such an approach has proved highly effective for the production of some proteins, such as G- protein coupled receptors (Grünewald *et al.*, 2004; Weiss *et al.*, 1995). Interestingly, these proteins are type II opsins, which is a good indicator of this type of expression in channelrhodopsins.

There are no reports of ChR2 being expressed with the pPICZ(alpha) vector. However, some structural studies of this protein reported secretory expression with the use of an alternative vector, pPIC9K (Govorunova *et al.*, 2013; Scholz *et al.*, 2012). This vector is similar to the one we chose, with the same secretory function and with exactly the same secretion signal as pPICZ(alpha) vector. The only differences are that pPIC9K does not present the Zeocin resistance gene, but resistance to Geneticin. Regarding this antibiotic difference, pPIC9K

is genetically modified to enhance multiple plasmid integration into the yeast genome. In other words, this permits the use of high antibiotic concentration (until 4mg/m) to select hyper resistant clones containing multiple copies of the gene of interest. Interestingly, that is the approach we used for selection of a ChR2 clone (2mg/ml) in pPICZ and pGAPZ vectors. However, these two vectors are not specifically engineered for this multicopy integration strategy, thus it is possible to say that we developed a successful strategy with the vectors used in our experiments.

To perform this secretory approach, wild type ChR2 was shuttled into the commercial pPICZ(alpha) A vector with the cloning strategy (Figure 30) used for pPICZ and pGAPZ vectors. We designed a specific set of primers to amplify wild type ChR2 to insert into the pPICZ(alpha) vector (Table 3).

The cloning strategy was effective and the final construct was achieved, as shown by PCR screening and respective DNA sequencing (Figure 31). However, due to time constraints, the final construct was not linearized and electroporated in *Pichia pastoris* cells to perform a small-scale screening. Thus, it was not possible to confirm if wild type ChR2 was also successfully expressed in a secretory way. In the future, the completion of this experiment will make it possible to compare the inducible vs. constitutive vs. secretory expression of ChR2.
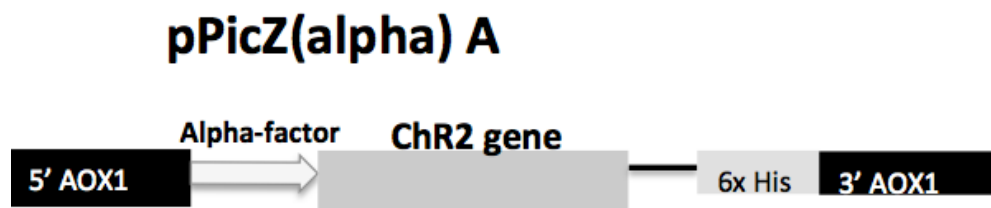

Figure 30 – Cloning strategy for secretory expression of ChR2 wt. Illustration of final expected fragment from cloning strategy used to transfer ChR2 protein forms from pcDNA 3.1 vector to pPICZ(alpha) A. AOX1 promoter is presented in black, white arrow represents alpha-factor secretion signal, ChR2 inserted sequence is presented in grey and 6x histidine Tag is presented in light grey.

A
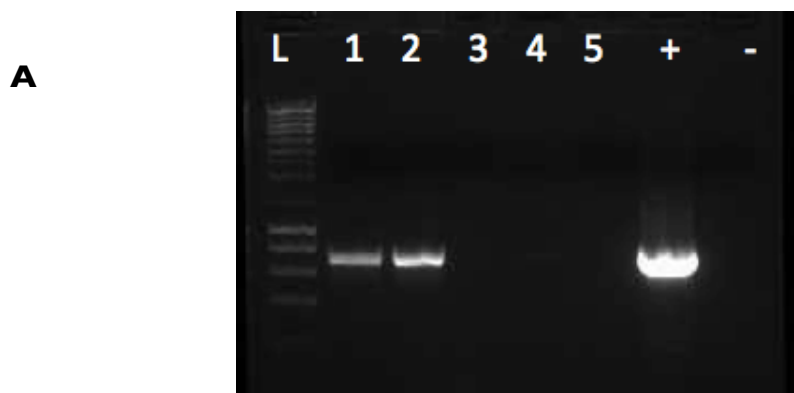
B

ChR2 wt in pPICZ(alpha) A	831	CACATTTTTTCACGCCGCCAAAGCATATATCGAGGGTTATCATACTGTGCCAAAGGGTCGGTGC
AOX Fw primer	873	CACATTTTTTCACGCCGCCAAAGCATATATCGAGGGTTATCATACTGTGCCAAAGGGTCGGTGC
AOX Rev primer	737	CACATTTTTTCACGCCGCCAAAGCATATATCGAGGGTTATCATACTGTGCCAAAGGGTCGGTGC

Figure 31 – PCR screening and sequence results of ChR2 wt cloning into pPICZ(alpha) A vector. (**a**) PCR screening of ligation product of ChR2 wild type cloning into pPICZ(alpha) A vector. Expected band of ~700bp. Used primers on table 3 (Aox_fw and Aox_rev). (**b**) Alignment of sequencing results from positive colony 2. Aox _fw and Aox_rev primers were used to sequencing purposes.

III.8 – Purification and determination of absorption spectra of new ChR2 variants

The full and complete optimization of the protocol concerning wild type ChR2, described in the previous sections, led us to choose the pPICZ vector and the *P. pastoris* SMD1168H strain to express the four ChR2 mutants as well.

After establishing the crucial issues and perform large-scale expression (Figure 28), the membrane fraction of each ChR2 mutant was isolated and ressuspended before proceeding to protein purification and subsequent determination of the absorption spectra.

Despite the chromatography and absorption spectra of wild type ChR2 were performed in the wild type X-33 strain, here we took advantage of the new selected and optimized strain

(SMD1168H) of *Pichia pastoris* in order to improve the rate of expression and obtain higher levels of the protein (Govorunova *et al.*, 2013). Also, we optimized the composition of the purification buffers and the final dialyzed buffer where purified ChR2 was when its absorption spectrum was determined. These optimizations are specific to each ChR2 mutant purification and spectral determination. We also aimed to perform a new purification and absorption spectra of wild type ChR2, in SMD1168H strain, as a new and accurate control in the same conditions as the protein mutants.
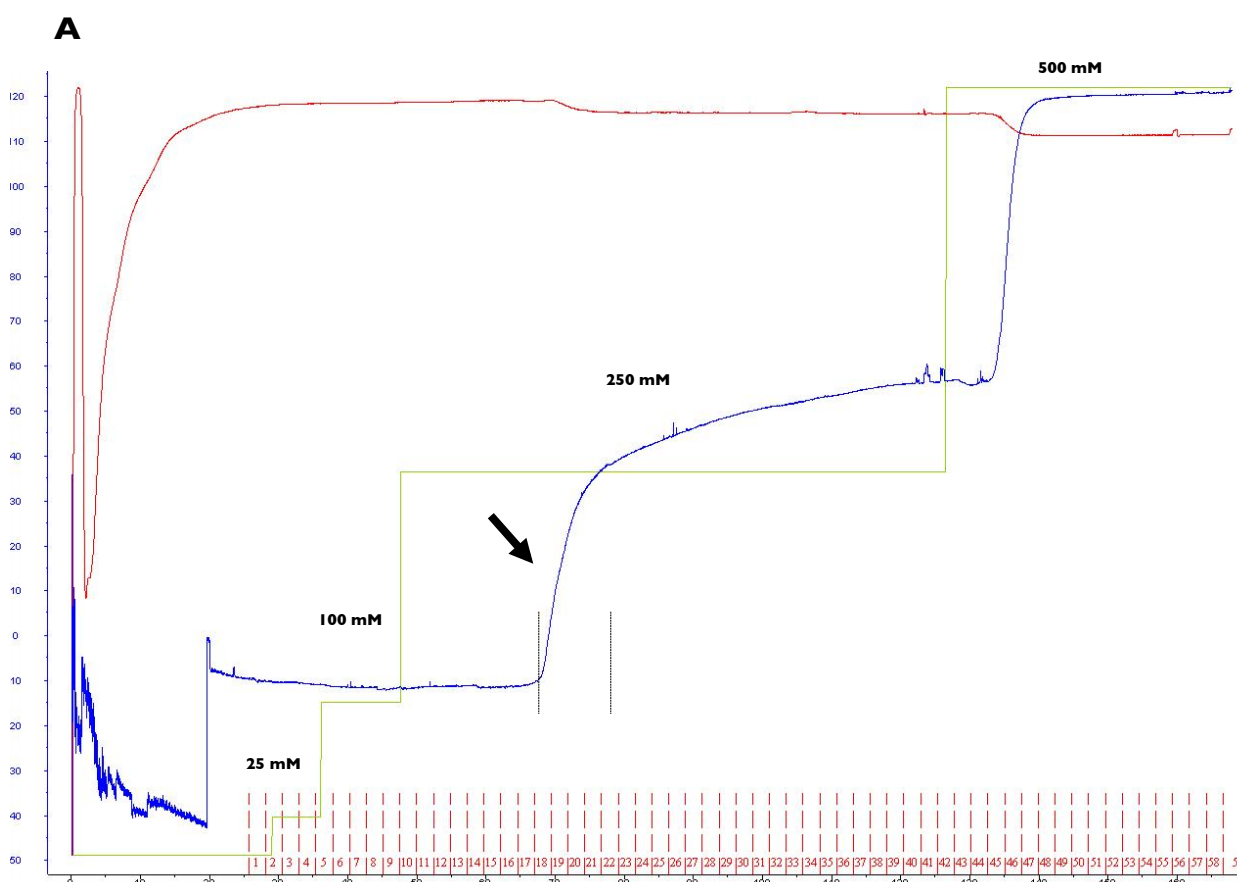
III.8.1 – ChR2 F217D

After obtaining the first valid results of the wild type ChR2 purification, we started by using the same strategy for the first mutant, the F217D. In particular, we used the same composition for the binding and elution buffers, and the same flow when injecting the protein extract into the 1ml HisTrap column (Bruun, 2013). However, this first attempt to purify the mutant protein was not successful and no purified ChR2 F217D protein was observable in any eluted fraction, when analysing silver staining gels (data not shown). Therefore, it was obvious that an optimization on this purification step was necessary.

The concentration of glycerol had already been decreased to avoid excessive pressure on the column and it has been reported that increasing the concentration of salt and imidazole may reduce non-specific protein binding (Block *et al.*, 2009; Bornhorst e Falke, 2000). We then decided to increase the concentration of NaCl from 0,2M to 0,3M and sodium phosphate from 20mM to 50mM. However, we decided not to increase imidazole concentration but instead to decrease, from 10mM to 7,5mM. This decrease was included to free the column resin of imidazole and render it more available to bind ChR2, since there was poor protein binding. As such, these changes were established, the protein membrane fraction was solubilized and purification by nickel affinity chromatography was performed. To enable a slower and effective protein binding to the resin, we also decreased the flow on protein injection into the column, from 1mL/min to 0,5mL/min. Furthermore, from this point on, we started to pass the flow-through a second time through the column.

Analysis of the obtained chromatogram (Figure 32, a) and the eluted fractions (Figure 32b) showed that the protein was successfully purified and eluted in the fractions corresponding

to the marked peak/increasing (250mM imidazole) of absorbance at 260nm and presented the characteristic double band patterns in the silver staining. Some contaminants, protein aggregation or endogenous protein from *P.pastoris* are seen in the silver staining gel, a natural occurring issue probably resulting from the necessary reduction in imidazole that, in an inverse way, increased non-specific protein binding. A size exclusion chromatography could be a solution to this issue as performed in other channelrhodopsin studies (Kato *et al.*, 2012, 2015); however, the probability of these contaminants to interfere with the determination of the absorption spectra by presenting meaningful absorbance in the full range of the visible light spectrum is very small. In fact, this circumstance was confirmed in the following results.

A positive sample, with successful purified ChR2 F217D, was also tested by western blot, before and after concentration of samples 19-22 (Figure 32 c,d). Once again, these results confirmed the successful purification of ChR2 F217D and the efficient concentration procedure, after which the protein absorption spectrum was measured.

A

B

| L | FT | L | W | I | 3 | 4 | 6 | 7 | 19 | L | 20 | 21 | 22 | 23 | 24 | 25 | 26 | 27 |

43 kDa

34 kDa

43 kDa

34 kDa

(Imidazole) 25mM 100mM 250mM 250 mM

C

Ladder   ChR2 F217D

Before concentration

43 kDa

34 kDa

FT   W   I   7   19   20   21   22   45

D

Ladder   ChR2 F217D

After concentration

43 kDa

34 kDa

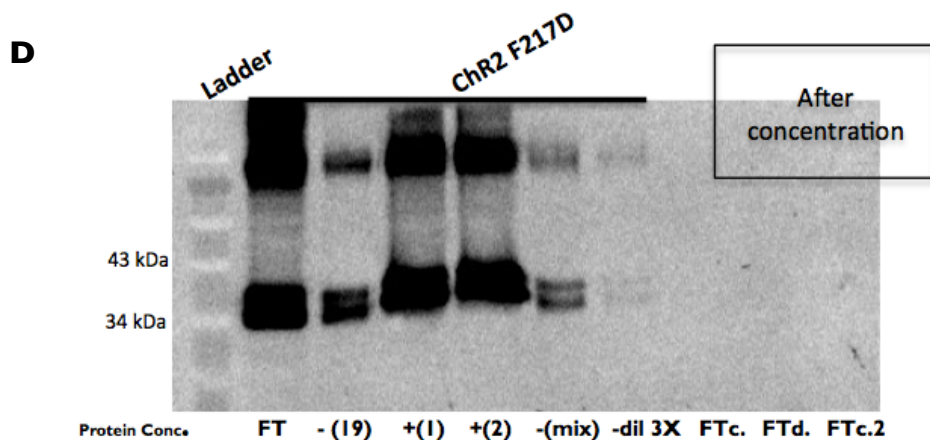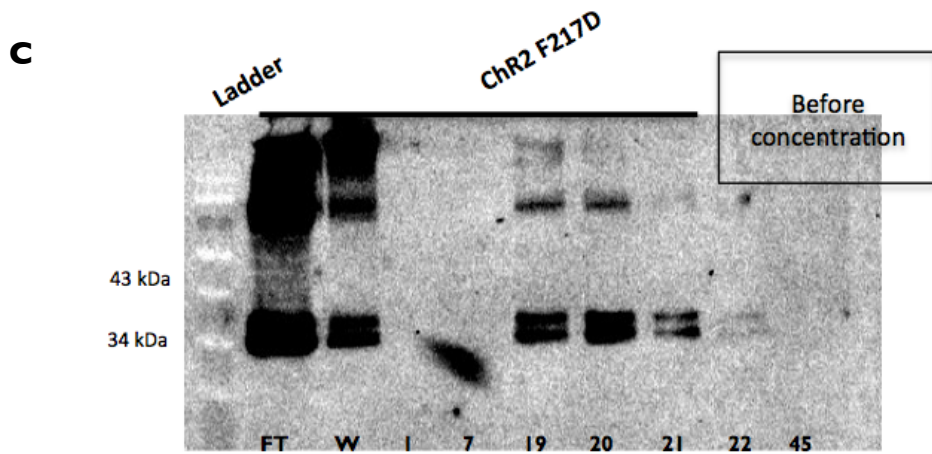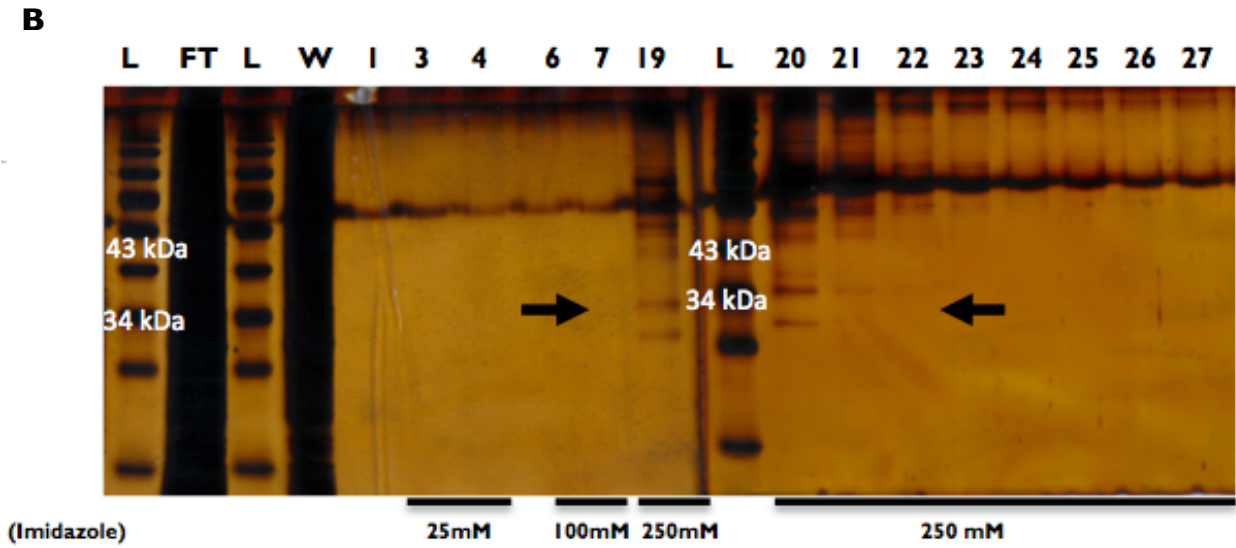Protein Conc.   FT   -(19)   +(1)   +(2)   -(mix)   -dil 3X   FTc.   FTd.   FTc.2

Figure 32 – ChR2 F217D purification with nickel affinity chromatography. (a) ChR2 F217D purification chromatogram. Absorbance at 260 nm is represented in blue, imidazole concentration in green, collected fractions in red and black arrow indicates positive eluted fractions. (**b**) Silver staining of collected protein

samples from imidazole elution range. Two black arrows indicate positive samples for purified ChR2 F217D. Note: Black pattern across both gels are SDS-PAGE buffer contaminant and not specific contaminants from purification procedure. (**c**) Western-blot of ChR2 F217D positive and negative samples. FT is flow-through and W is wash. (**d**) Western blot of ChR2 F217D positive mixed samples after concentration. 1 and 2 represent first and second concentration, respectively. Mix represents all positive samples mixture before concentration; dil 3x is the mix sample diluted 3 times to reduce prejudicial imidazole; FTc, FTd and FTc2 are flow-through from first concentration, dialysis and second concentration, respectively.

We observed a clear spectral absorbance of ChR2 F217D, with a noticeable red-shifted peak around 600 nm (Figure 33). Hence, observe that TDDFT prediction was confirmed, as this mutant presented a clear red-shifted comparing to the spectrum of wild type ChR2. This was the first step to a complete corroboration of TDDFT predictions and the characterization of our first ChR2 red-shifted mutant.

We also observed that the final concentrated sample containing ChR2 F217D presented a very strong yellowish colour (Figure 33), which is an additional confirmation that ChR2 F217D was present in the sample. This has been previously shown by other groups as proof of a successfully ChR2 purification (Li, 2013).

However, to achieve the most accurate absorption spectrum possible, we decided to investigate and test the final concentrated and dialysed buffer, where the protein was when the absorption spectra was measured. This decision was also based on the fact that, in short wavelengths measurements (from 300nm), protein absorption is highly saturated (Figure 33).

A

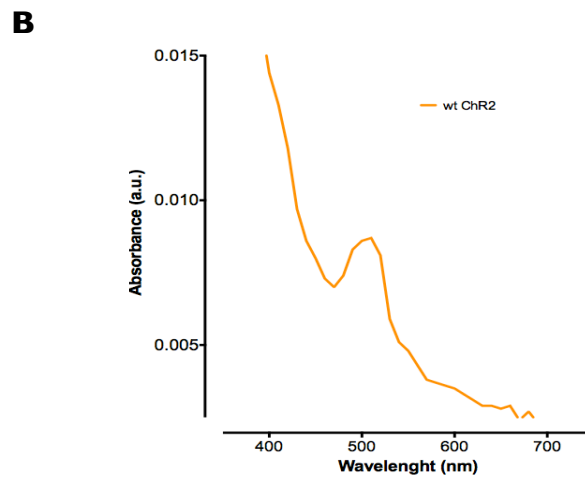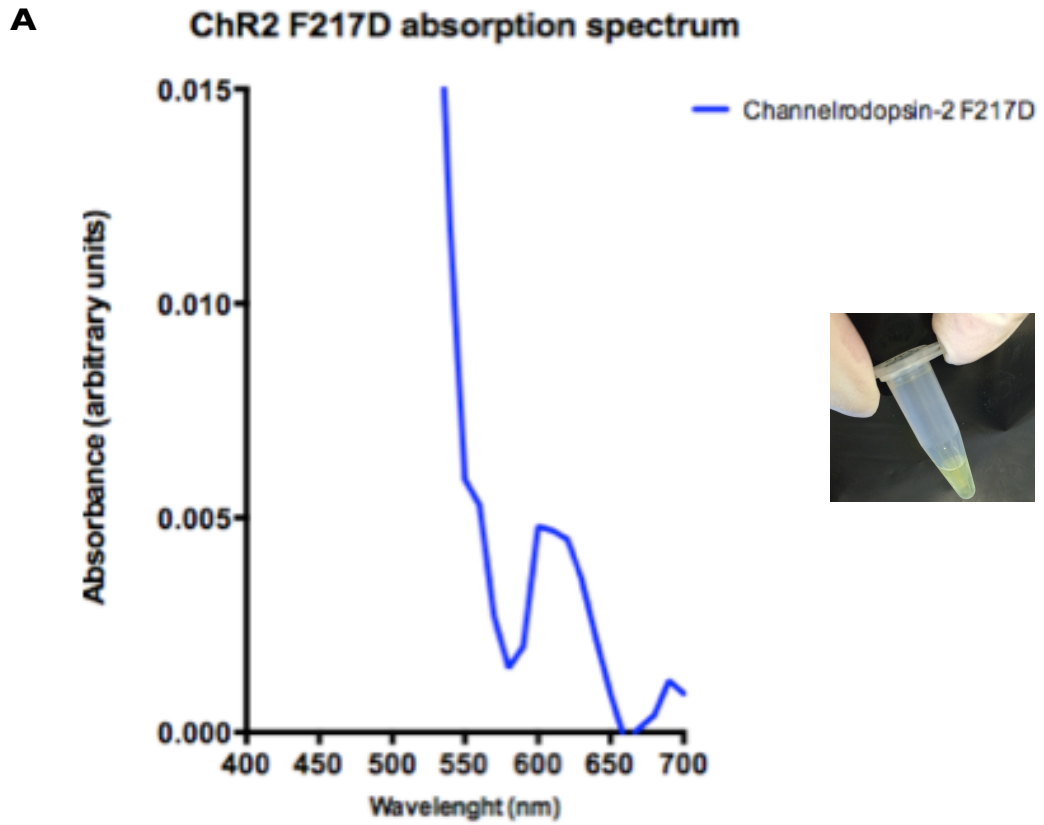**ChR2 F217D absorption spectrum**

B

Figure 33 – UV-visible spectroscopy of purified ChR2 F217D. (**a**) Absorption spectra of purified ChR2 F217D in dodecyl maltoside solution at pH 7. (**b**) Absorption spectra of purified ChR2 wt in dodecyl maltoside solution at pH 7.

III.8.1.1 – Channelrhodopsin buffer test

To study the influence of the final buffer on the absorption spectra output for all the ChR2 variants, we measured the absorption of different buffer compositions.

The final buffer composition used so far contained sodium phosphate, NaCl, DDM, retinal, glycerol and PMSF. The imidazole was only present in the first spectrum for wild type ChR2. Based on the previously mentioned fact that imidazole affects spectral properties of ChR2 (Scholz *et al.*, 2012), this component was removed for experiments concerning ChR2 F217D as well as the remaining variants.

There is a theoretical explanation for the initially saturated and high absorbance values and the strong yellowish color in the final purified, concentrated and dialyzed sample. DDM is a micelle-forming detergent that has been shown to maintain many membrane proteins in a stable state over prolonged periods of time (Gutmann *et al.*, 2007) and is widely used to stabilize our protein (Bruun *et al.*, 2011; Kato *et al.*, 2012). It is known that DDM stabilizes ChR2, forming a protein-detergent complex with a micelle around the protein. The retinal is covalently linked to ChR2 structure, working as its chromophore, and in solution presents a yellow color. However, after observing high lower wavelength absorption we questioned if free retinal and free DDM, unbounded from protein, formed a similar micelle complex with each other. We hypothesize that the retinal-DDM complex would not able to pass through the Centricon membrane device, and thus concentrate with ChR2 and enhance the yellowish color and the saturated absorbance in the beginning of the spectrum.

To test this, we measured the absorption spectrum of the final buffer, protein free, with four different compositions: final buffer without imidazole (Figure 34a), without imidazole and without retinal (Figure 34b), without imidazole and without DDM (Figure 34c) and finally without imidazole, without DDM and without retinal (Figure 34d). Each buffer composition was concentrated and the absorption spectra were measured before and after this process, with samples from non-concentrated buffer and from the centricon membrane and flow-through.

In fact, when analyzing the output of this different absorption spectrum, it is possible to confirm that, in the buffer with retinal and DDM together (no imidazole, Figure 34a), there is a large peak of saturated absorbance around 350nm. This peak is initially present before concentration and it is even higher in the sample from the centricon membrane (the membrane turned yellow), contrarily to the flow-through sample where there is no peak anymore. These

results suggest that retinal in the presence of DDM is not able to pass through the membrane and was therefore concentrated. Additionally, none of the other buffers, when retinal and DDM were not mixed together, presented the same issue.

Taken together, these results validate our hypothesis of a retinal-DDM complex that interferes with the protein absorption spectra in the 350-400 nm range.

Thus, to achieve more accurate ChR2 absorptions spectra, we decided to remove retinal from the final buffer, since DDM can be considered to have a more crucial role as it stabilized ChR2. The retinal useful for ChR2 was already bound to the protein structure, with the free one being considered unessential. Consequently, for the rest of our experiments, the binding buffer added to the columns in protein purification was the last step where vitamin-A aldehyde was added.

A
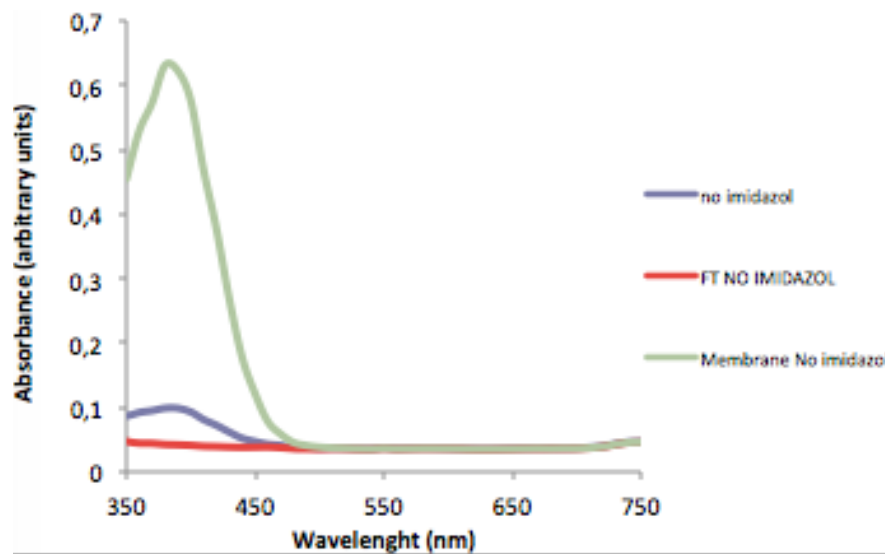
B
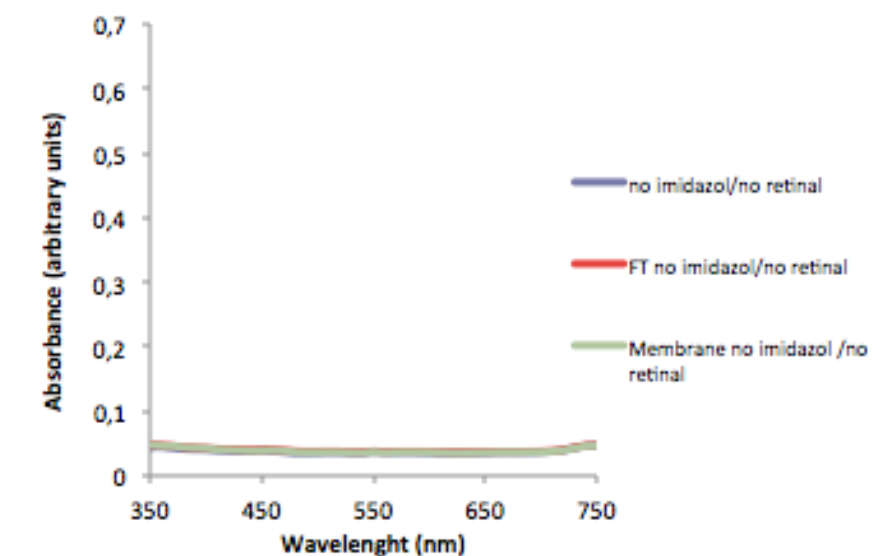
C
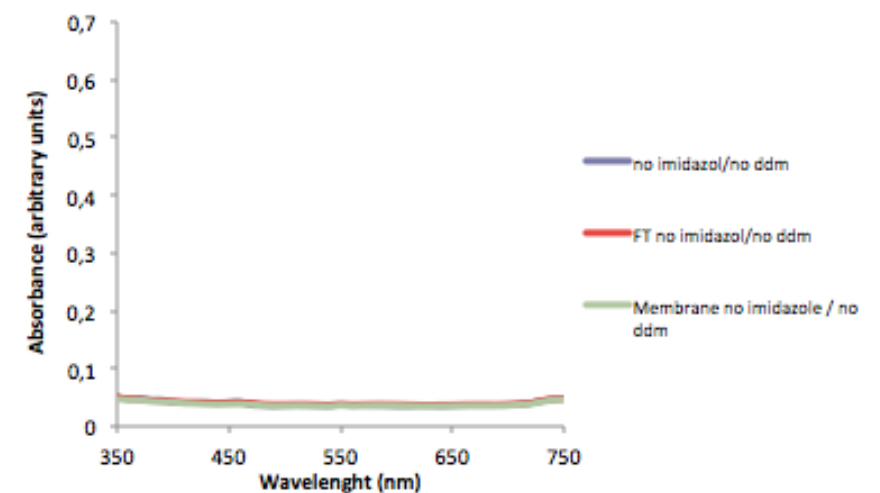
D
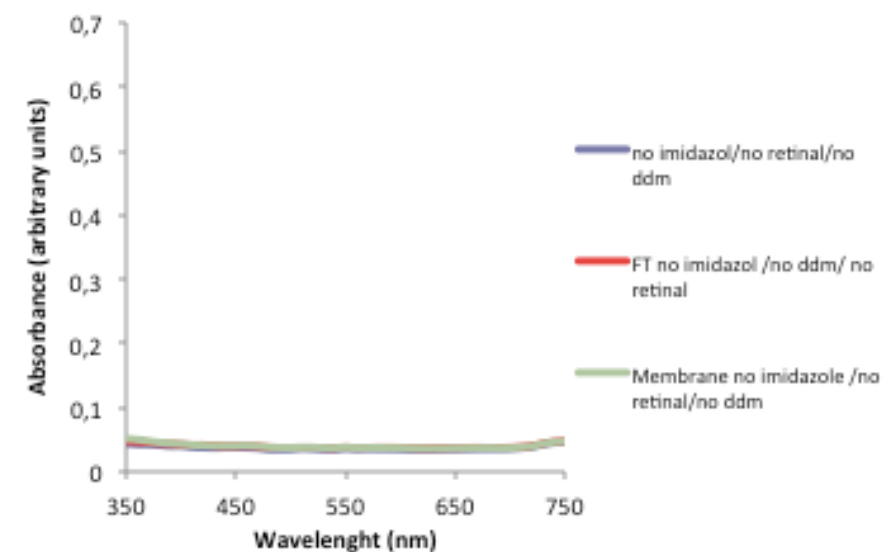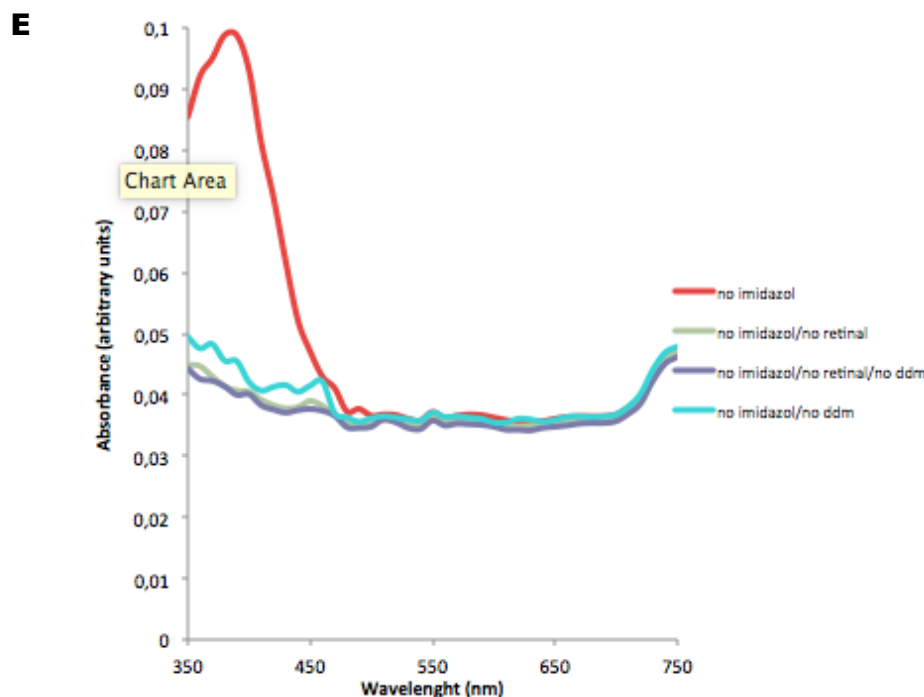
Figure 34 – UV-visible spectroscopy of different candidates to final buffer to measure ChR2 absorption spectra. Each graphic presents samples from pre-concentration and after concentration (membrane and flow-through). (**a**) Absorption spectra of final buffer without imidazole (**b**) Absorption spectra of final buffer without imidazole and without retinal. (**c**) Absorption spectra of final buffer without imidazole and without DDM. (**d**) Absorption spectra of final buffer without imidazole, without retinal and without DDM. (**e**) Absorption spectra of all four final buffers in pre-concentration. All measurements were performed in solution at pH 7.

III.8.2 – ChR2 wild type (2)

A second set of identical experiments was performed to obtain new absorption spectra for wild type ChR2. Similarly to other channelrhodopsin studies, our protein of interest was purified again by nickel affinity chromatography (Govorunova *et al.*, 2013; Kato *et al.*, 2012, 2015), concentrated and dialyzed (Berthold *et al.*, 2008; Ernst *et al.*, 2008; Kianianmomeni *et al.*, 2009; Ritter *et al.*, 2008) to finally measure its absorption spectrum. These results were obtained after expression of wild type ChR2 in the *Pichia pastoris* SMD1168H strain, with the optimized buffers, as an additional and more accurate control to the absorption spectra of all

the ChR2 mutants.

The purification results are presented in wild type ChR2 (2) chromatogram (Figure 35a) and in silver staining of eluted fractions (Figure 35b). As in previously obtained purifications, the protein was eluted in fractions corresponding to the absorbance peak noticed in 250 mM imidazole elution.

To confirm the presence of the purified protein (samples 21-23), before (Figure 35c) and after concentration (Figure 35d) we used western blot analysis. In both cases, the wild type ChR2 characteristic double band pattern was clearly visible (*even after 20 days at 4°C), which validates the purification and concentration processes.

A

B

L 21 22 23 24 25 26 40 41 42

43 kDa

34 kDa

(Imidazole)   250mM   500mM

C

Ladder   ChR2 WT

Before concentration

43 kDa

34 kDa

FT   W   19   20   21   22   23   24   41

D

Ladder   ChR2 WT

After concentration

Protein conc.   - (22)   +   +(*)   -(mix)   -(dil 3x)   -FTc.   - FTd.
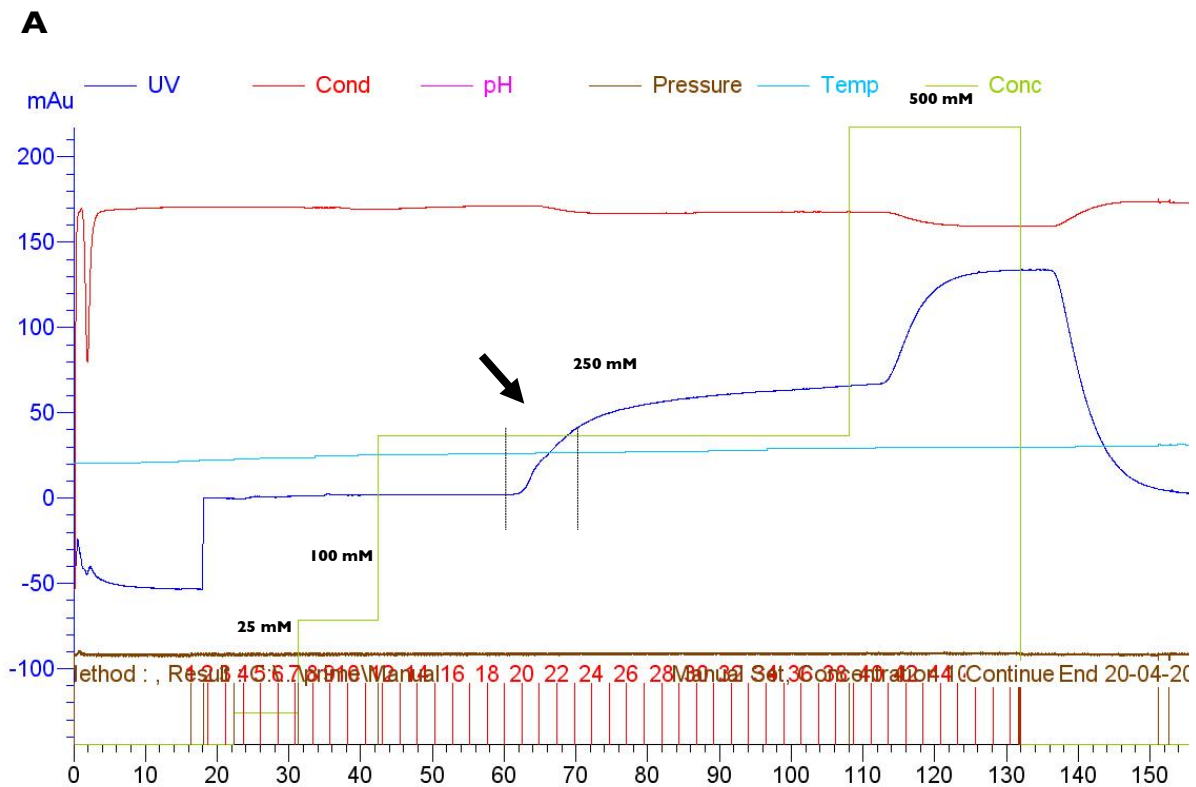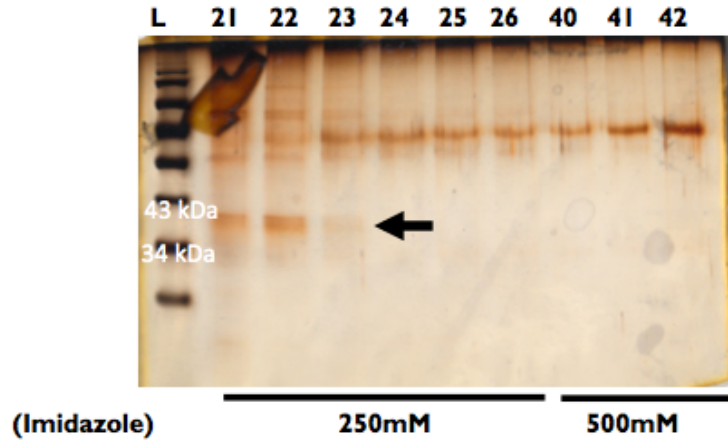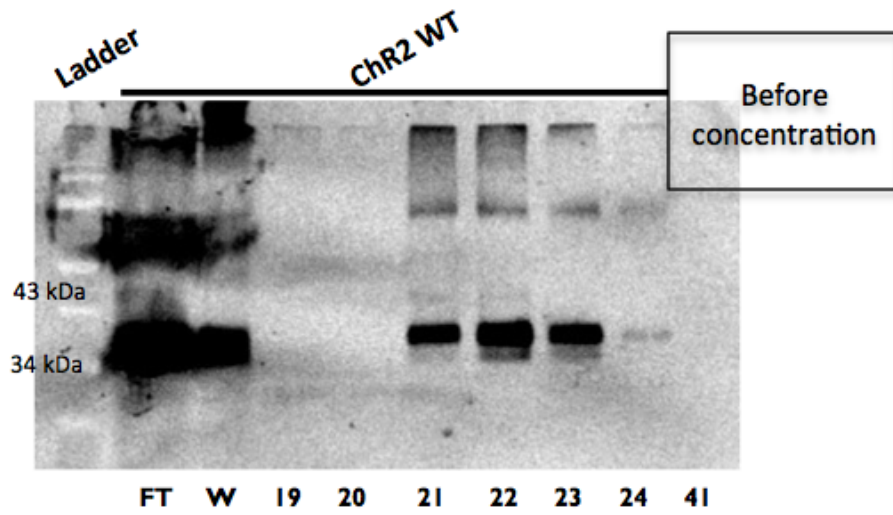
*20 days at 4°C

Figure 35 – ChR2 wt (2) purification with nickel affinity chromatography. (**a**) ChR2 wt purification chromatogram. Absorbance at 260 nm is represented in blue, imidazole concentration in green, collected fractions in red and black arrow indicates positive eluted fractions. (**b**) Silver staining of collected protein samples from imidazole elution range. Black arrow indicates positive samples for purified ChR2 F217D. Note: Black pattern across the gel are SDS-PAGE buffer contaminant and not specific contaminants from purification procedure. (**c**) Western-blot of ChR2 wt positive and negative samples. FT is flow-through and W is wash. (**d**) Western blot of ChR2 F217D positive mixed samples after concentration. Mix represents all positive samples mixture before concentration; dil 3x is the mix sample diluted 3 times to reduce prejudicial imidazole; FTc, FTd and flow-through from concentration and dialysis, respectively.

The absorption spectrum was determined and once again it was possible to see the absorption peak around 510 nm (Figure 36a), in line with the first absorption spectra of wild type ChR2 (510nm) and the known published peak (470nm) (Nagel *et al.*, 2003). As previously mentioned and discussed, this difference in the peak is a result of pH variation (Ernst *et al.*, 2008; Scholz *et al.*, 2012) (470nm→ pH 7,5; 510nm→ pH 7).

A second valid and clear spectral absorbance of wild type ChR2 was also observed. This control was another step to further compare and complete validate TDDFT predictions.

A

ChR2 WT absorption spectrum (2)

B
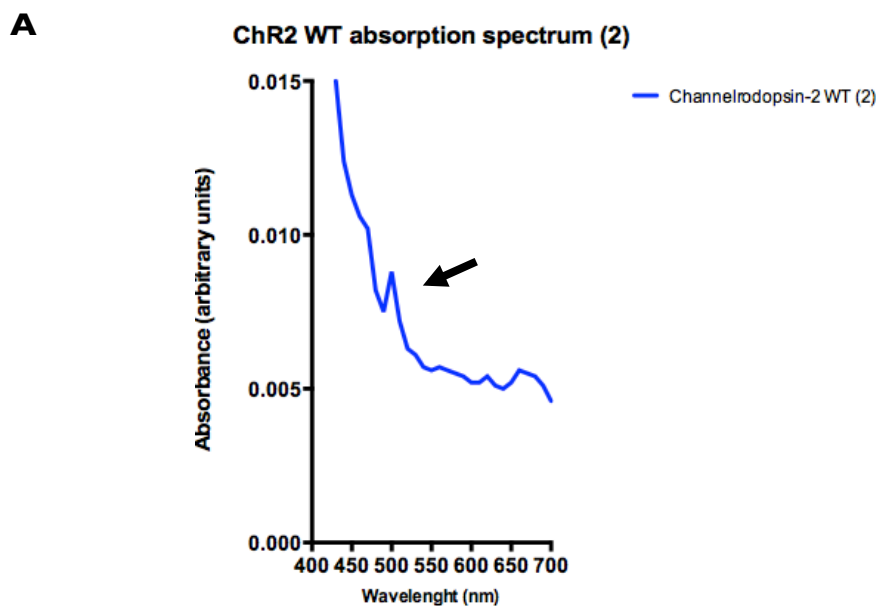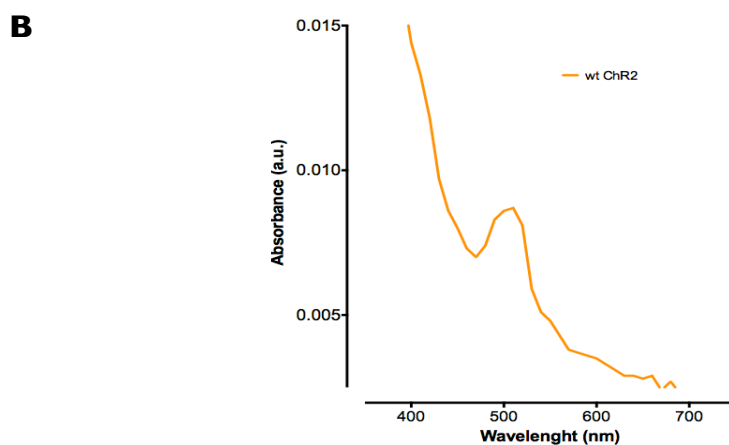
Figure 36 – UV-visible spectroscopy of purified ChR2 wt (2). (**a**) Absorption spectra of purified ChR2 wt (2) in dodecyl maltoside solution at pH 7. (**b**) Absorption spectra of purified ChR2 wt in dodecyl maltoside solution at pH 7.

III.8.3 – ChR2 F269D

The second mutant we tested was ChR2 F269D. All experiments for this variant were done in parallel with the wild type ChR2 (2) control, with the exact same conditions.

Concordant with the previous successful and validated outputs for wild type ChR2 (1 and 2) and ChR2 F217D, the ChR2 F269D purification results are presented in the respective chromatogram (Figure 37a) and in silver staining of eluted fractions (Figure 37b). The protein was eluted in fractions corresponding to the noticed absorbance peak, but contrarily to the other purifications, elution of this mutant occurred in 100 mM imidazole elution. This fact is explained by the re-use of a 1mL HisTrap column (Bruun, 2013), which created a poorly binding of the protein to the resin.

We also used western blot analysis to confirm the presence of the purified protein (samples 7-9), before (Figure 37c) and after concentration (Figure 37d). In both cases, the wild type ChR2 characteristic double band pattern was clearly visible, which corroborates the purification and concentration processes.

A

B

C

Before concentration

D

After concentration

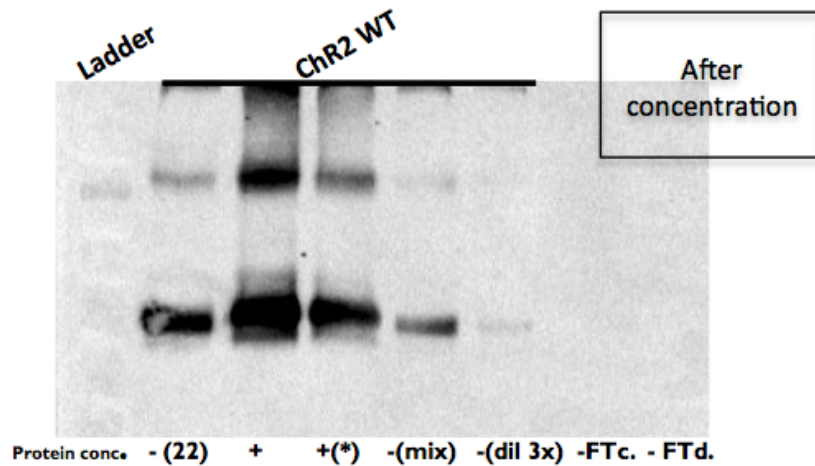Protein Conc.   - (8)   +   +(*) -(mix) -FTc. - FTd.

*20 days at 4°C
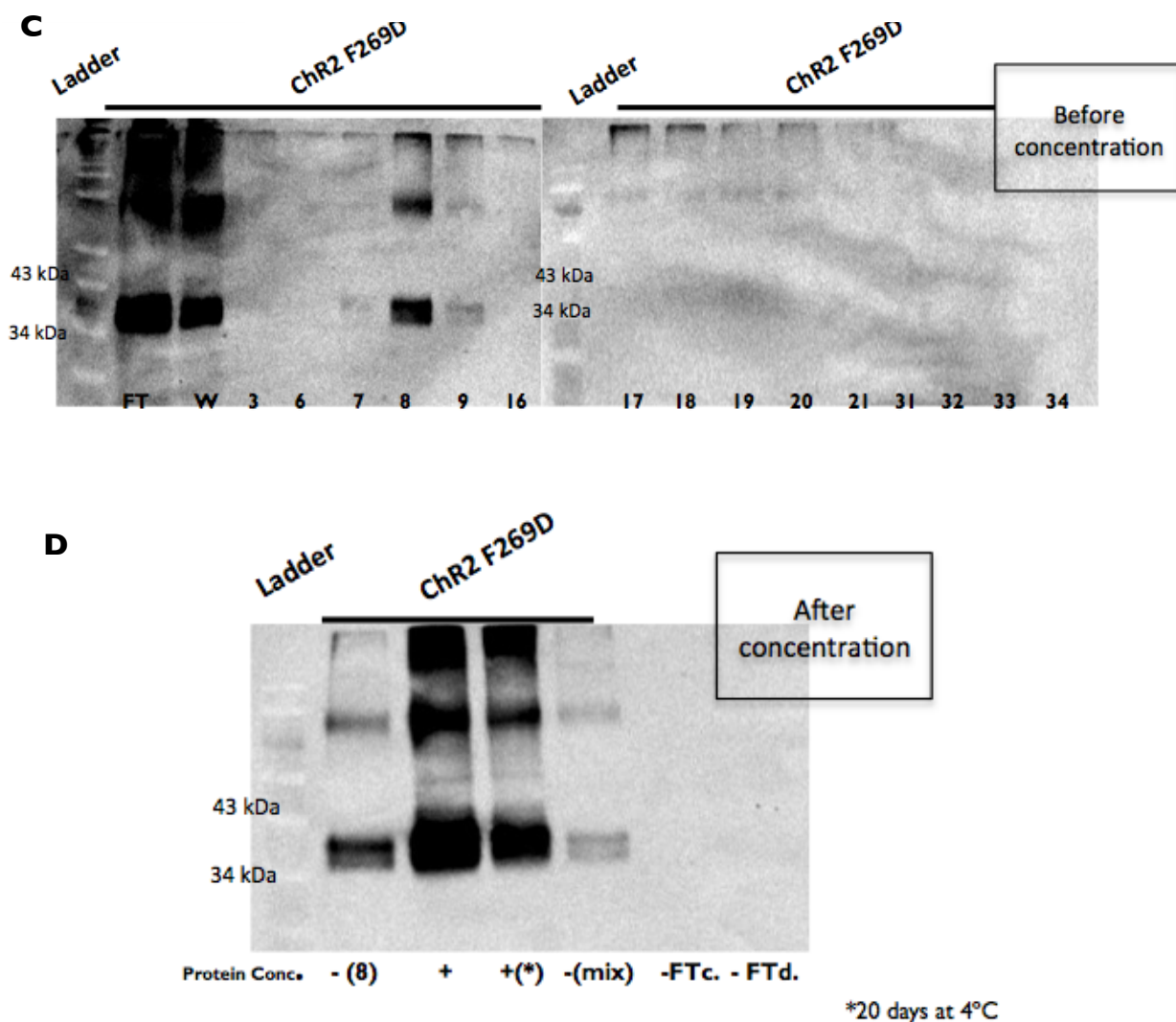
Figure 37 – ChR2 F269D purification with nickel affinity chromatography. (a) ChR2 F269D purification chromatogram. Absorbance at 260 nm is represented in blue, imidazole concentration in green, collected fractions in red and black arrow indicates positive eluted fractions. (b) Silver staining of collected protein samples from imidazole elution range. Black arrow indicates positive samples for purified ChR2 F269D. Note: Black pattern across the gel are SDS-PAGE buffer contaminant and not specific contaminants from purification procedure. (c) Western-blot of ChR2 wt positive and negative samples. FT is flow-through and W is wash. (d) Western blot of ChR2 F269D positive mixed samples after concentration. Mix represents all positive samples mixture before concentration; dil 3x is the mix sample diluted 3 times to reduce prejudicial imidazole; FTc, FTd and flow-through from concentration and dialysis, respectively.

After determination of the ChR2 F269D absorption spectrum, it was possible to see a clear red shifted absorption peak around 600 nm (Figure 38a). Compared to the absorption

spectrum of the wild type protein (Figure 38b), this had a red-shift around 100 nm, similar to the previous validated ChR2 F217D. Both of these two novel red-shifted variants have their spectral peak close to the red-shifted variant Chrimson (Klapoetke *et al.*, 2014). However, the kinetic parameters of Chrimson are undesirable when compared to ChR2 and it is also activated at 470nm on a fraction of its peak currents (Klapoetke *et al.*, 2014). Consequently, our new red-shifted variants, F217D and F269D will need characterization in neuronal tissue to evaluate their kinetic properties in comparison to published red-shifted variants.

Taken together, these results support a second valid red-shifted ChR2 mutant, as predicted by TDDFT. This output was another crucial step towards the complete validation of the physics theory, and the creation of one more new desired variant of ChR2.
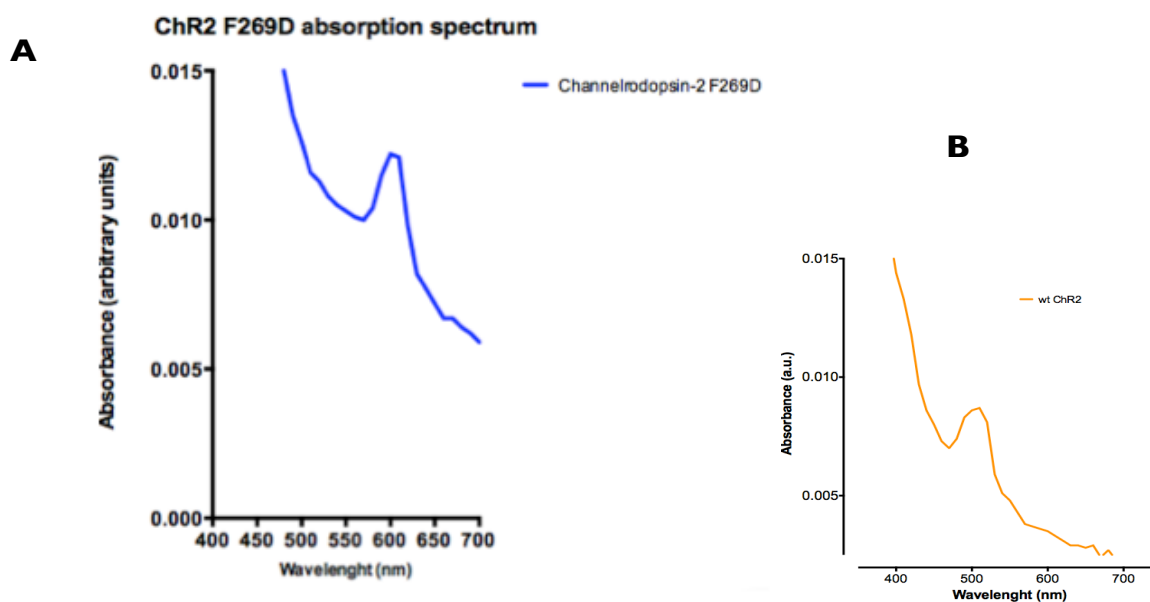

Figure 38 – UV-visible spectroscopy of purified ChR2 F269D. (**a**) Absorption spectra of purified ChR2 F269D in dodecyl maltoside solution at pH 7. (**b**) Absorption spectra of purified ChR2 wt in dodecyl maltoside solution at pH 7.
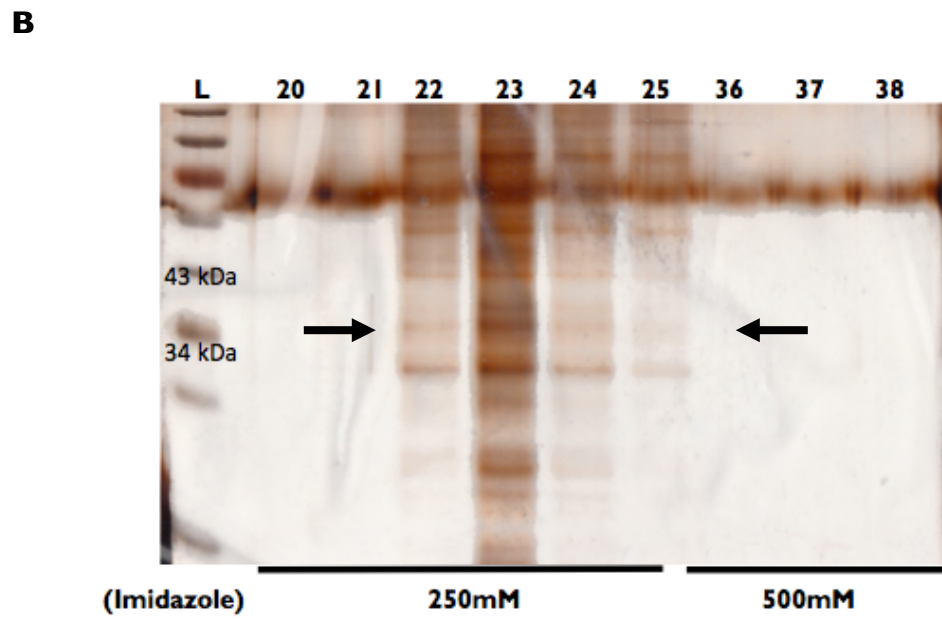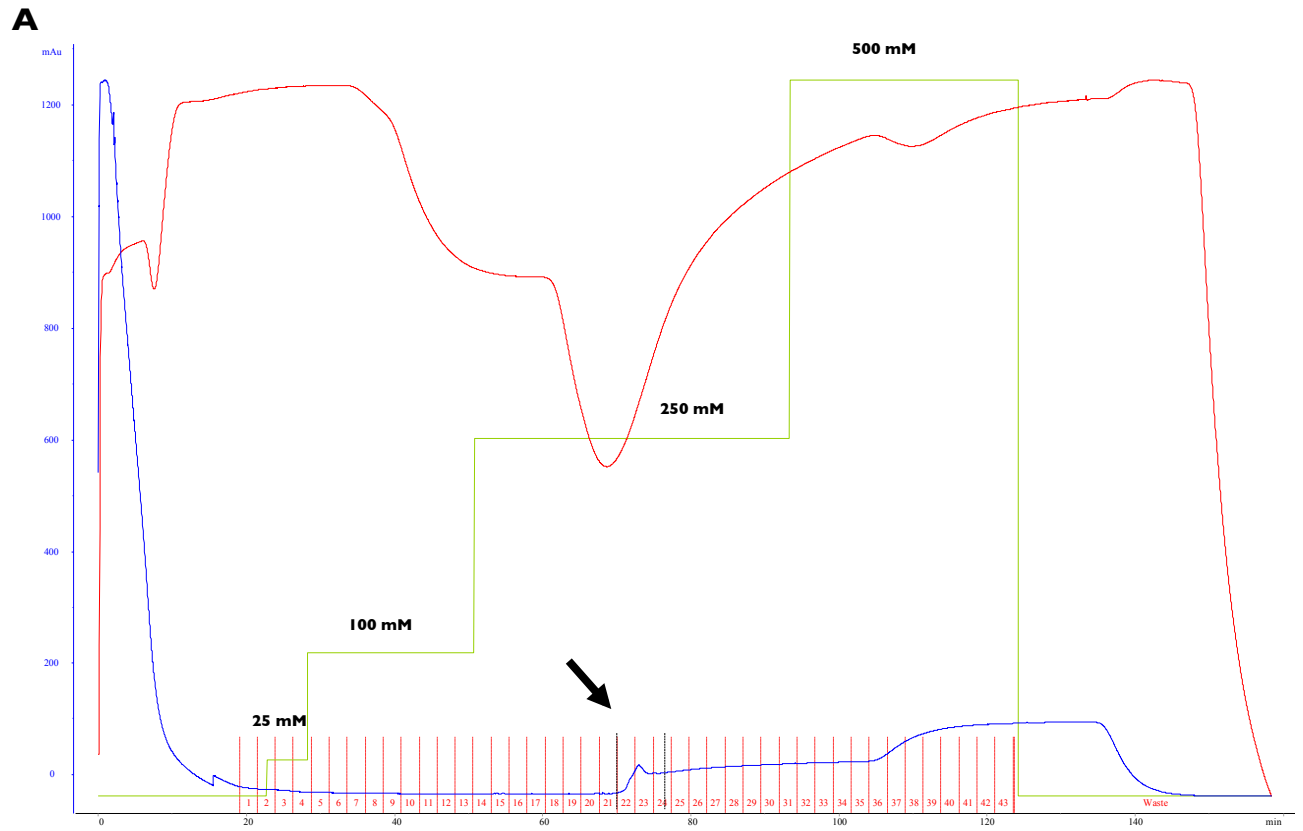
III.8.4 – ChR2 L221D

At this point we obtained successful absorption spectra of wild type ChR2 (two independent experiments), ChR2 F217D and ChR2 2F69. Hence, our strategy to achieve these outputs was successful. However, we aimed at achieving higher amounts of purified protein and clearer absorption spectra. Consequently, we decided to scale up our purification strategy, using new 5mL HisTrap columns (Bruun *et al.*, 2015) instead of the 1mL columns. This way, we increased the binding surface with five times more available resin.

The third mutant to be studied was ChR2 L221D and we applied the same strategy used so far, with the aforementioned change. The purification results are again presented in the respective chromatogram (Figure 39a) and in silver staining of eluted fractions (Figure 39b). The protein was eluted in fractions corresponding to the very noticed absorbance peak, in the elution gradient of imidazole 250mM. Analyses of the silver staining showed that, when using the 5mL columns, the amount of purified protein was higher than all the previous ones, where 1mL columns were used. However, it is clear that the increased amount of purified protein was proportional to the increase of endogenous protein and contaminants, as shown by the visible unspecific bands in this "dirtier" gel.

In the silver staining gel it was possible to identify the same double band pattern, as in the previous western blots and staining, with some contaminants. However, due to the nature of the assays needed to be performed after the purification, the absorption spectra measurements, it was not necessary to execute any further optimization, since the chances that these contaminants present significant absorbance in the 300-800nm window is negligeble. This fact was confirmed in the following measurements of the absorption spectra.

Positive purified samples were also confirmed by western blot (samples 23-25), before (Figure 39c) and after concentration (Figure 39d). In both cases, the wild type ChR2 characteristic double band pattern was visible, corroborating the purification and concentration processes. In this particular case, the double band pattern was less visible than on the same test to the other ChR2 variants. We ascribe this discrepancy to deficient primary antibody incubation during western blot, regardless; this result will require future investigation.

A

B

| L | 20 | 21 | 22 | 23 | 24 | 25 | 36 | 37 | 38 |

43 kDa

34 kDa

(Imidazole)   250mM   500mM

C

Ladder	ChR2 L221D		Before concentration

43 kDa

34 kDa

FT   W   10   21   22   23   24   25   38

D

Ladder	ChR2 L221D	After concentration

43 kDa

34 kDa

Protein conc.   FT   - (25)   +   +(2)   -(mix) -(dil 3x) -FTc.- FTd.
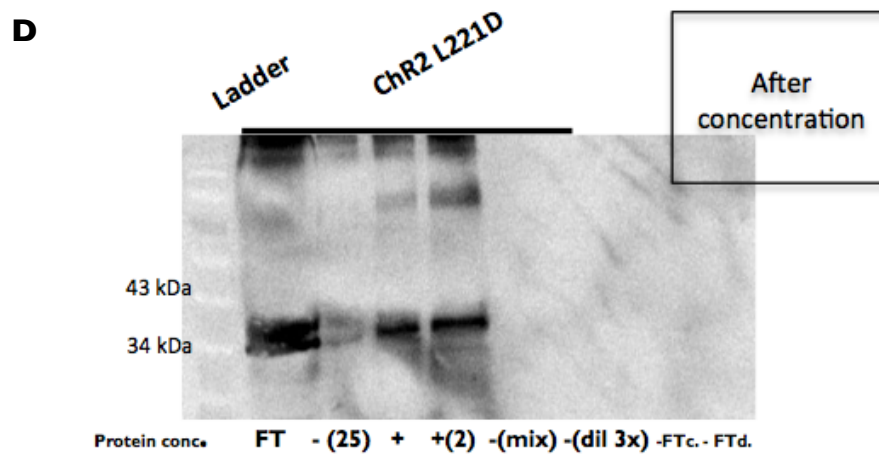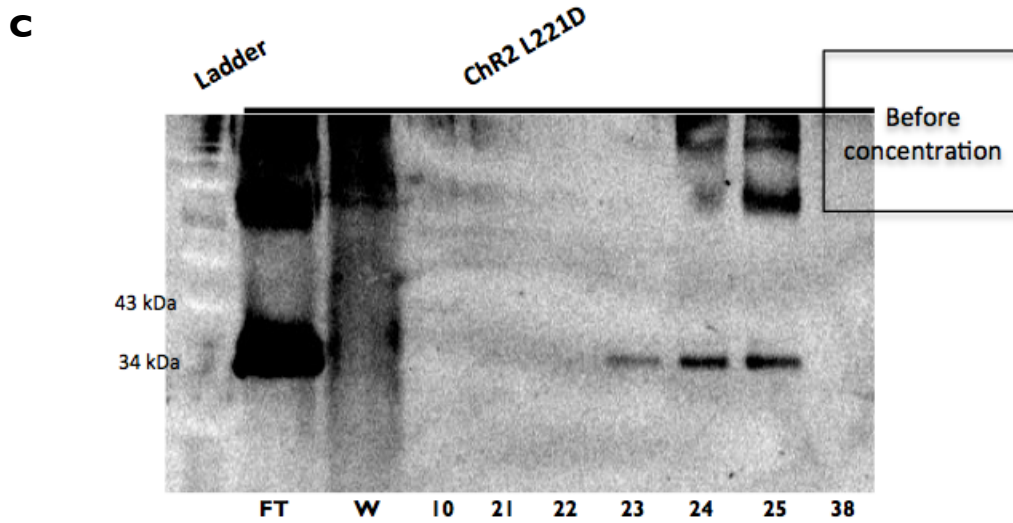
Figure 39 – ChR2 L221D purification with nickel affinity chromatography. (a) ChR2 L221D purification chromatogram. Absorbance at 260 nm is represented in blue, imidazole concentration in green, collected fractions in red and black arrow indicates positive eluted fractions. (**b**) Silver staining of collected protein samples from imidazole elution range. Black arrow indicates positive samples for purified ChR2 L221D. Note: Black pattern across the gel are SDS-PAGE buffer contaminant and not specific contaminants from purification procedure. (**c**) Western-blot of ChR2 L221D positive and negative samples. FT is flow-through and W is wash. (**d**) Western blot of ChR2 L221D positive mixed samples after first and second concentration. Mix represents all positive samples mixture before concentration; dil 3x is the mix sample diluted 3 times to reduce prejudicial imidazole; FTc, FTd and flow-through from concentration and dialysis, respectively.

After measurement of the ChR2 L221D absorption spectrum, it was possible to observe the most significant red shift from all of the ChR2 mutants. This absorption peak was visible around 690 nm (Figure 40a), a 190 nm red shift when compared to the wild type protein (Figure 40b). ChR2 L221D absorption peak is significantly more red-shifted than the characteristic peak in ReaChR, the most red-shifted available variant thus far (Lin *et al.*, 2013). Furthermore, ReaChR spectral shift resulted from several known point mutations combined with swapping of different chimeras domains (Lin *et al.*, 2013) . With these present results, we achieved a bigger red shift with an original single point mutation in the wild-type ChR2 sequence.

We also note that the present shift is more accentuated and clear than the previous ones (leading to absorbance scale adjustment). This can be a consequence of the purification scale up, from 1mL to 5 mL column. However, the increased "dirtiness" of the analyzed silver staining, and the fact that this was an output from the first time we used 5mL columns, led us to conclude that an optimization to these columns was needed. This optimization will be discussed in the next sections for the ChR2 mutant.

Importantly, ChR2 L221D was the third red-shift variant of ChR2 created, and the one with the superior shift. Once again, this validates the TDDFT prediction
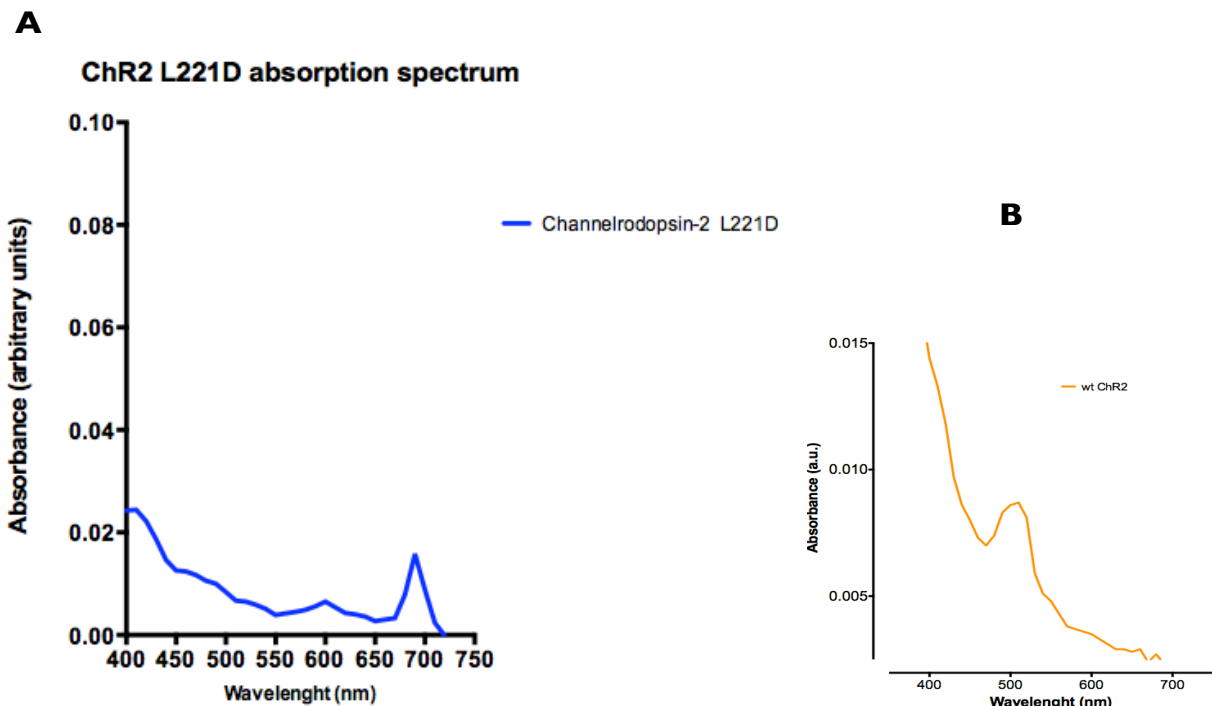
A

B

Figure 40 – UV-visible spectroscopy of purified ChR2 L221D. (**a**) Absorption spectra of purified ChR2 L221D in dodecyl maltoside solution at pH 7. (**b**) Absorption spectra of purified ChR2 wt in dodecyl maltoside solution at pH 7.

III.8.5 – ChR2 F269H

The fourth and last ChR2 mutant that we studied was ChR2 F269H. This specific mutation has the same target residue, phenylalanine (F) 269, as the previously validated red-shifted ChR2 F269D. However, rather than substituting the non-polar target residue for a negative amino acid like aspartate (D), in this mutation the F269 is substituted by the positively charged amino acid histidine.

The TDDFT theory predicts that this opposite rationale results into a blue-shifted ChR2. Hence, ChR2 F269H experiments were fundamental to completely validate the putative physics predictions that already demonstrate to be accurate with the three new and *Ab-iniitio* designed ChR2 red-shifted variants.

Once again, we aimed at further achieving higher amounts of purified protein, to reach even clear abortion spectra. Accordingly, we maintained the previous scale up in our purification strategy, using new 5mL HisTrap column (Bruun *et al.*, 2015) instead of the regular 1mL column.

However, it became clear that we needed to optimize the use of 5mL columns to purify this protein. More precisely, we needed to reduce non-specific binding and increase the concentration of salts and imidazole, that are known to produce that desired effect (Block *et al.*, 2009; Bornhorst e Falke, 2000). The concentration of salts was already increased in the previous purifications but the imidazole concentration was reduced to enhance general binding. Thus, for this purification with five times scale-up, we increased the concentration of imidazole from 7.5mM to 12,5mM.

The ChR2 F269H purification results are displayed in the respective chromatogram (Figure 41a) and in silver staining of eluted fractions (Figure 41b). The protein was eluted in fractions corresponding to the elution step gradient of imidazole 250mM. An earlier peak in the elution step on 100 mM was observed, corresponding to unspecific protein, as demonstrated in silver staining (Figure 41b). The silver staining results turned it possible to see that, when using the 5mL columns, the amount of purified columns is in fact superior than all the past ones

where 1mL columns was used. In this case, the purification was more efficient than before, with strong and clear bands showing in the silver staining gel. The imidazole ratio balance should be optimized and settled depending on the used column volume and the binding capacity of our protein of interest.

Hence, it was observed that the increasing imidazole concentration led to reduced non-specific binding and we also settled the most optimized purification for the protein, with 5mL HisTrap columns with high concentration of salts (50mM sodium phosphate and 0,3M NaCl) and 12,5mM of imidazole.

Positive purified samples were also confirmed in western blot (samples 23-25), before (Figure 41c) and after concentration (Figure 41d). In both cases, the wild type ChR2 characteristic double band pattern was visible, corroborating the purification and concentration process. In this particular case, the double band pattern was again less visible than on the same test to the other ChR2 variants

B

C

D
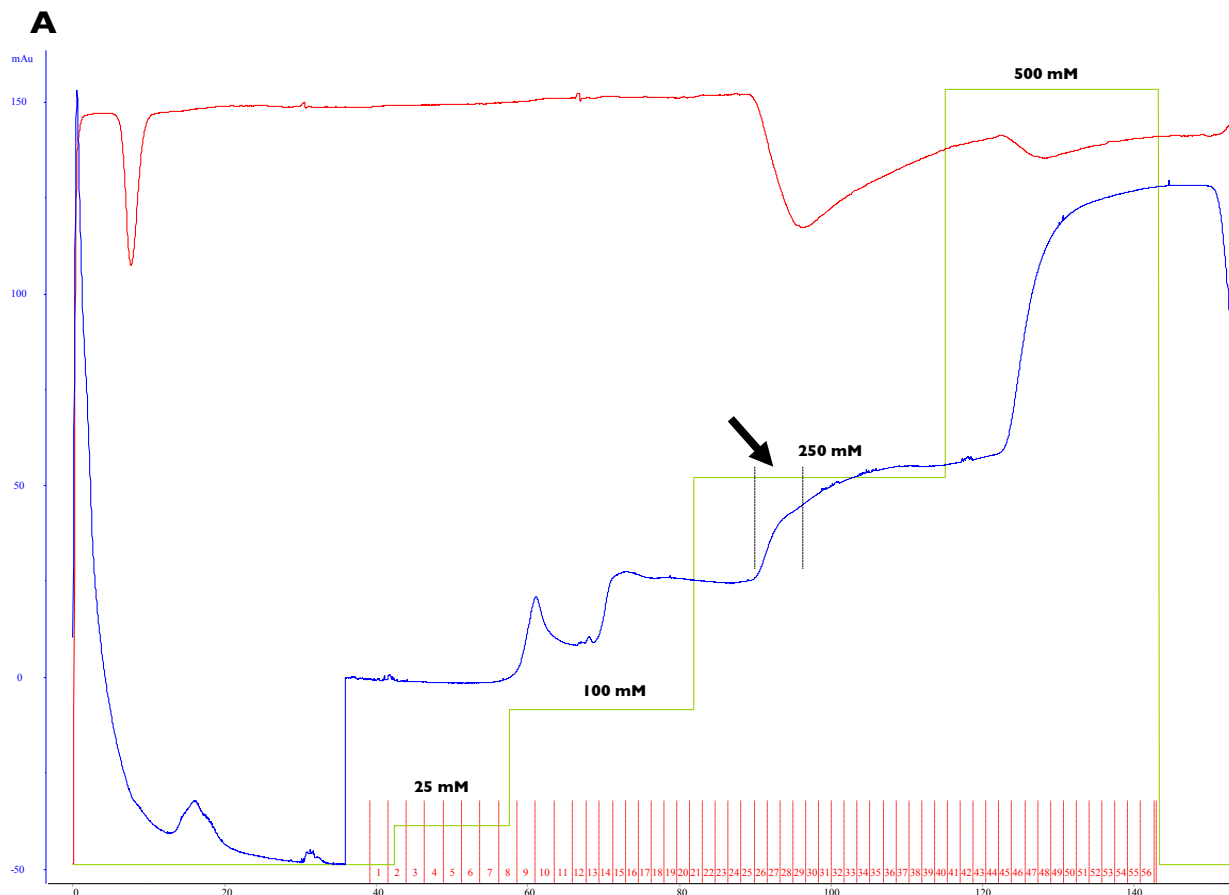
Figure 41 – ChR2 F269H purification with nickel affinity chromatography. (a) ChR2 F269H purification chromatogram. Absorbance at 260 nm is represented in blue, imidazole concentration in green,
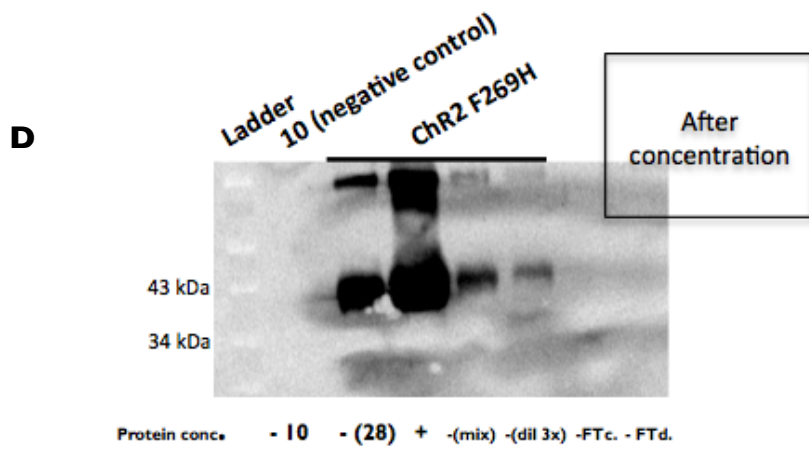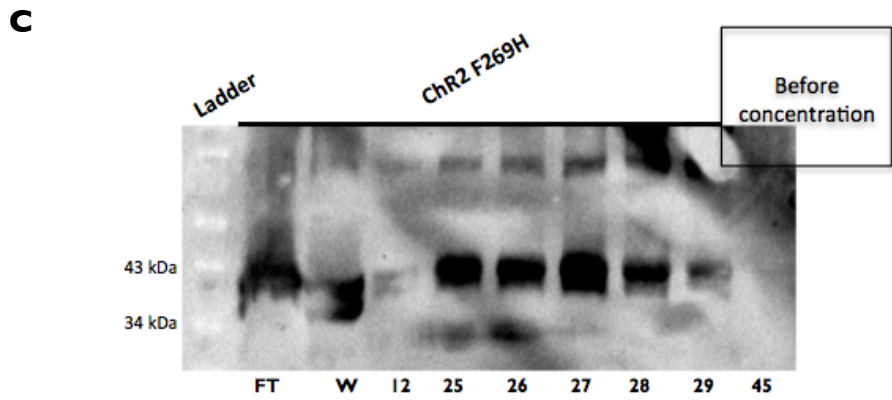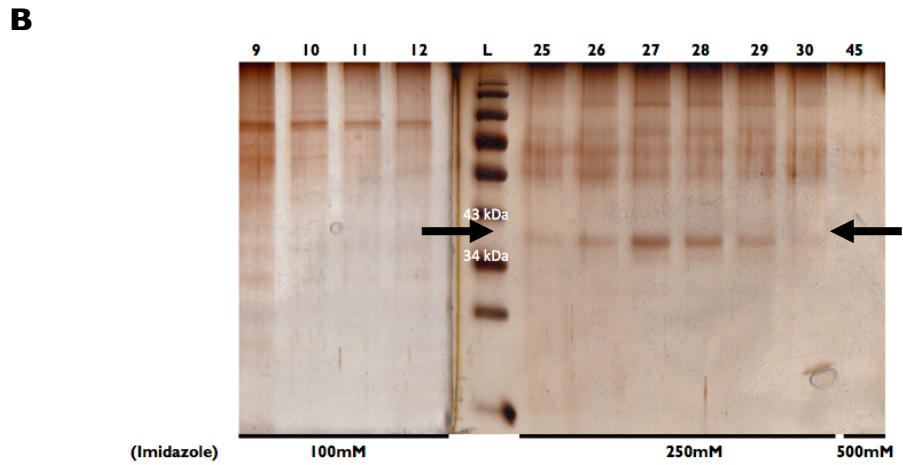
collected fractions in red and black arrow indicates positive eluted fractions. (**b**) Silver staining of collected protein samples from imidazole elution range. Black arrows indicate positive samples for purified ChR2 L221D. Note: Black pattern across the gel are SDS-PAGE buffer contaminant and not specific contaminants from purification procedure. (**c**) Western-blot of ChR2 F269H positive and negative samples. (**d**) Western blot of ChR2 F269H positive mixed samples after concentration. Mix represents all positive samples mixture before concentration; dil 3x is the mix sample diluted 3 times to reduce prejudicial imidazole; FTc, FTd and flow-through from concentration and dialysis, respectively.

After measurement of the ChR2 F269H absorption spectrum, it was possible to see the strongest and clearest peak so far, specifically in the blue light zone of the spectrum. ChR2 F269H absorption peak was visible around 490 nm (Figure 42a), a 20 nm blue shift when compared to the wild type protein (Figure 42b).

Interestingly, when mutating the non-polar F269 residue for a positive amino acid (histidine), it enables a blue shift on the ChR2 absorbance spectrum. Mutating the exact same residue for a negative charged amino acid (aspartate) leads to a very noticeable red shift absorption. These outputs validate TDDFT predictions as an original and noteworthy rationale to apply to ChR2 sequence in the creation of novel desirable mutations. Furthermore, our new variants, ChR2 F269D and F269H, have the potential to form a pair of ChR2 that have non-overlapping absorption spectrum, for optical excitation of distinct neural populations. This specific goal was already achieved by expressing both Chronos and Chrimson, two red-shifted channelrhodopsins, in mouse brain slice (Klapoetke *et al.*, 2014). These two actuators present a gap of 90nm between its respective absorption spectra (Klapoetke *et al.*, 2014), while our new variants ChR2 F269D and F269H display an absorption difference of 110nm between each other. Consequently, these results highlight the potential of our novel ChR2 variants. This potential can be further increased it if we consider ChR2 L221D to form pair with ChR2 F269H, resulting in an interesting absorption difference of 200nm.

For ChR2 L221D, the accentuated absorbance peak was now proved to be a consequence of the purification scale up, from 1mL to 5 mL column. These results also corroborate the efficacy of increasing the imidazole concentration in the purification process, leading to more purified protein with less contaminants and non-specifying binding. The optimization used in this respective mutant was the most suitable for our goal of attaining clear and accurate ChR2 absorption spectra.

Finally, ChR2 F269H was the fourth and last variant of ChR2 created and the first blue

shift protein. This was a crucial result since it fully and extensively validates the TDDFT predictions, and supported the possibility of creating red and blue shifted variants of ChR2. We successfully designed and produced three red-shifted and one blue-shifted new ChR2 variants.
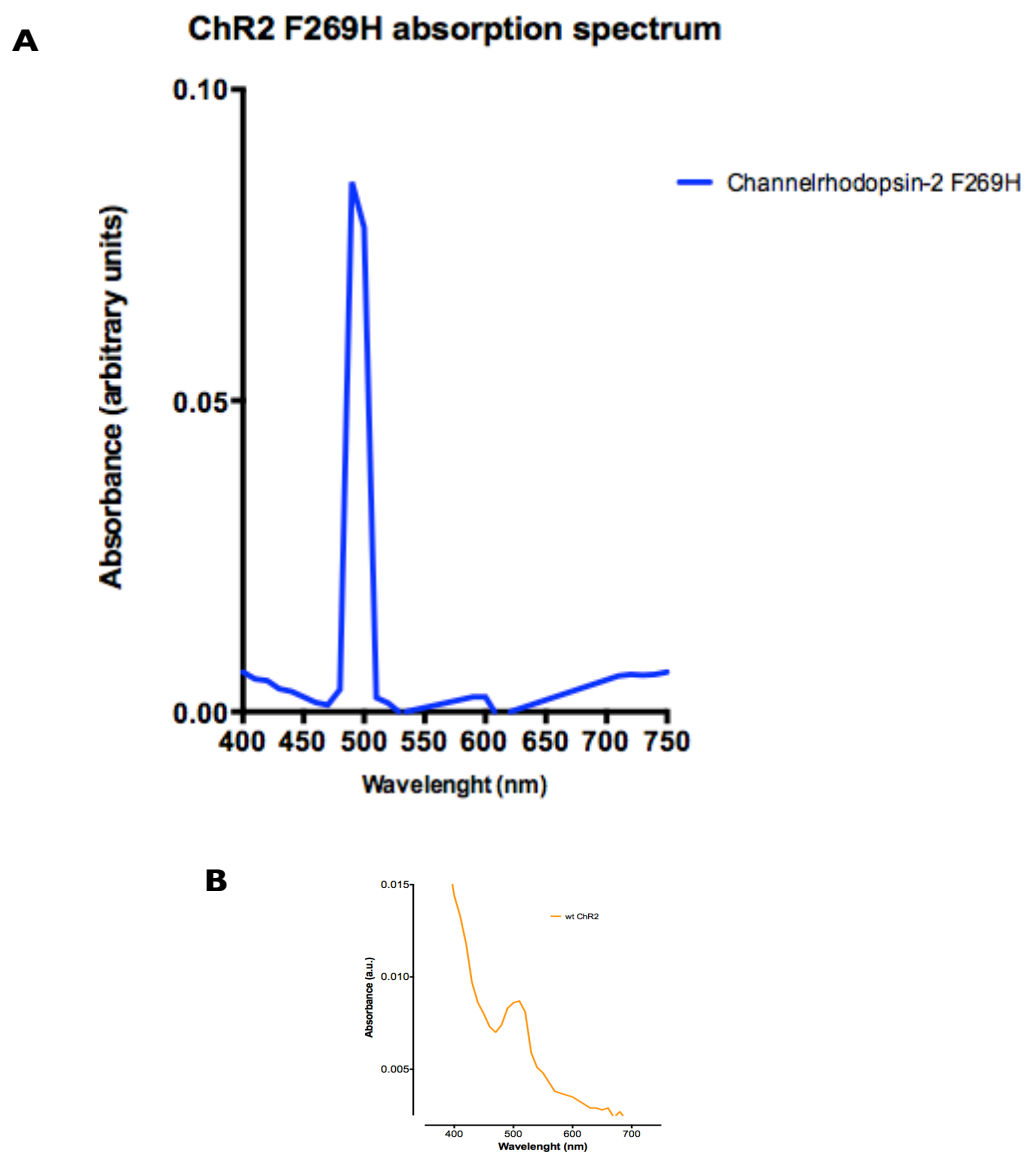
Figure 42 – UV-visible spectroscopy of purified ChR2 F269H. (a) Absorption spectra of purified ChR2 F269H in dodecyl maltoside solution at pH 7. (b) Absorption spectra of purified ChR2 wt in dodecyl maltoside solution at pH 7.

III.9 – *Ab-initio* designed new ChR2 optogenetic toolbox

In this project, we successfully designed and created four new ChR2 variants: ChR2 L221D, ChR2 F217D, ChR2 F269D and ChR2 F269H. We next normalized the absorption spectra of all these proteins and plotted them together in the same graphic (Figure 43).
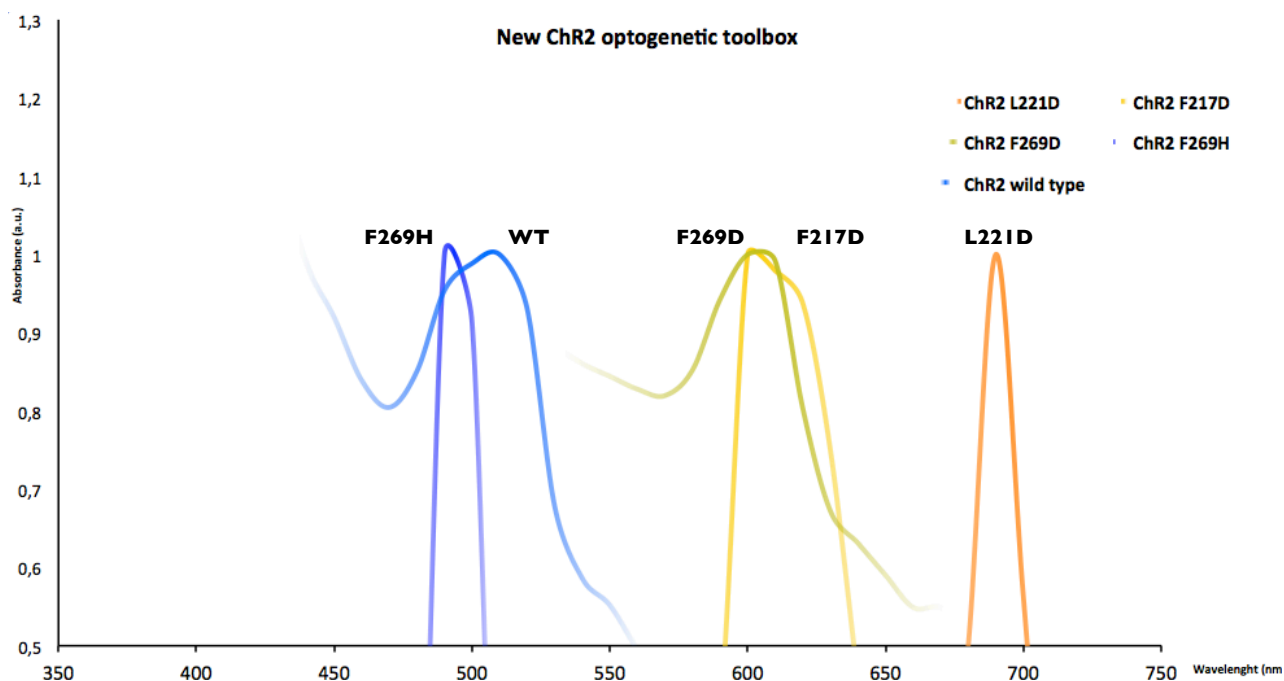
Figure 43 – UV-visible spectroscopy of purified new ChR2 optogenetic toolbox. Absorption spectra of four purified ChR2 new variants in dodecyl maltoside solution at pH 7. All measured absorbance values were normalized.

We were able to produce three red-shifted variants and one blue-shifted protein. Our wild type protein absorption peak was established at 510 nm, at pH 7.

The ChR2 F269D and F217D mutants present their own peaks at 600nm, consequently presenting very substantial red shift absorption of 90 nm. Both these variants presented even higher red shift output than the shifts predicted by TDDFT. Particularly, the F269D mutation resulted in an increased shift of 40nm relatively to TDDFT predictions, 90nm vs. 50nm,

respectively. The ChR2 F217D was predicted to induce a significant shift of 60nm, 30nm less than our scrutinized outputs of 90nm shift.

The substitution of the non-polar leucine residue 221 by the negative charged aspartate turned ChR2 L221D in our highest red-shifted variant, with a characteristic absorption peak at 690nm. This variant grants a shift of 180 nm when compared to the wild type ChR2, rendering ChR2 L221D the protein with the biggest potential to achieve desirable red-shifted absorptions, higher than any published variant so far. Once again, the TDDFT prediction was smaller than the final output, 45nm and 180nm respectively.

The ChR2 L221D 180nm red shift is higher than the two most red-shifted depolarizing variants so far, Chrimson (Klapoetke *et al.*, 2014) and ReaChR (Lin *et al.*, 2013), with 120nm and 160nm, respectively.

Wild type ChR2 has a small single-channel conductance and is optimally excitable at a wavelength of 470 nm, naturally not extended over 520 nm, limiting in this way its use in high-light scattering medium as the brain (Hegemann e Möglich, 2011). Long-wavelength excitation light decreases the scatter produced by biological tissues and it will avoid the absorption by haemoglobin. The more red-shifted channelrhodopsins absorbing red or even near infra-red light would be more desirable for relatively deep tissue penetration. Hence, our three new ChR2 red-shifted variants can be good candidates to solve this issue.

Finally, the fourth mutant we created presents an absorption peak at 490nm. Hence, F269H displays a 20nm blue shifted variance respectively to wild type ChR2. The theoretical physics output predicted a shift of 30nm, against our experimental 20nm shift. ChR2 F269H is just less 5nm than the biggest channelrhodopsin blue shift published so far (Govorunova *et al.*, 2013).

The ChR2 F269H blue-shift variant can be interesting to use in combination with red shifted variants, leading to the separation of the maxima peaks of the two mutants. This will generate two distinct peaks of absorption and avoid the overlapping of neuronal activation. This can enhance the possibility of a distinct activation of two ChR2 mutants with different light, and if expressed in two different classes of neurons, it will result in the distinct excitation of specific types of neurons. Particularly, this combination brings the possibility of controlling a defined subset of cells intermixed in the multitudes of neuronal tissue, as already exhibited through the combination of ChR2 and NpHR, activated with blue and yellow light, respectively (Zhang *et al.*, 2007). However, this published approach led to parallel depolarization and hyperpolarization (NpHR). As such, we propose that an optogenetic approach using a pair of mutants obtained in

our work, for instance ChR2 F269H and L221D, would enhance the possibility of depolarizing two different populations of neurons with non-overlapping (Klapoetke *et al.*, 2014) blue and red lights, respectively. This possible application may show great interest in optogenetics, based on the inexistence of protein variants with distinct absorption spectrum.

There is still room for improvement and optimization for future experiments, such as the study of the effect of pH in the absorption spectra of the proteins we obtained, as performed in a similar study (Scholz *et al.*, 2012). It is also possible to increase the number of outputs to enhance the accuracy of the protein characterization, in a more sensible spectrophotometer.

Although we designed single mutations, it would be interesting to combine modifications and produce a double mutant with a potential synergistic effect. This approach could achieve even bigger shifts than the outputs resulting from single mutations.

TDDFT rationale has full and wide applicability to produce new variants of ChR2, the main protein used in optogenetics and potentially other optogenetic proteins such as Halo or ArchT. The basis for the four new ChR2 variants could also result in a method to generate, on demand, a platform of colour-tuned ChR2 and other rhodopsin mutants with scientific and biomedical applications. A creation of a viral vector encoding the created variants for animal delivery could also be a following step.

We successfully completed protein production and purification, as well as the initial and crucial biophysical characterization of the engineered mutants. However, an enhanced study of the new proteins is still required, such as the analysis of the kinetic properties of the channel using electrophysiology experiments and protein membrane trafficking in neurons.

In fact, we have already started experiments concerning membrane trafficking in cortical neurons transfected with the four proteins cloned into a mammalian vector fused with YFP (intracellularly on the protein c-terminal).

With the approach of changing non-polar residues by polar ones in the retinal environment, the colour-tuned mutations could affect the kinetics properties of the ChR2 channel. Hence, the determination of the functional properties of these mutations is crucial, as it is known that, concerning depolarizing tools, there is a tradeoff between kinetics and peak activation (Berndt *et al.*, 2011; Mattis *et al.*, 2012; Pan *et al.*, 2014) . Besides, this fact it is still not fully understood and explained, as there is a noted deficiency of depolarizing optogenetics tools with fast kinetics and red-shifted absorption.

The present study revealed that biophysical and biomolecular simulation predictions, based on Time-dependent Density Functional theory, accomplished accurate creation of novel ChR2 variants. This specific protein design and rationale can be a powerful and reliable approach to engineer several biotechnological protein tools that compel detailed control of the protein molecular structure by mutations. Our original and final outputs presented in this thesis show high potential for future optogenetic application.

Chapter IV – Conclusions and Future Perspectives

Channelrhodopsin-2 is a light-gated cation channel initially isolated from the microalgae *Chlamydomonas reinhardtii*. For the last decade, ChR2 has become the central paradigm of optogenetics and its main tool, with wide biomedical and neuroscience applications.

The relevance of ChR2 in neuroscience arose from discorering that its heterologous expression in mammalian brain allows a millisecond precise and selective control of specific genetically targeted neurons, without the need to add exogenous factors. Hence, the optogenetics technique allowed that, for the first time, it is conceivable to depolarize and/or hyperpolarize a specific group of neural cells to map and study the brain complexity, with a breakthrough efficacy.

With honours like "method of the year" and "breakthrough of the decade," it's comfortable to assume that optogenetics, and its ability for turning neurons on and off using light, is indeed, a game-changing technology.

The optogenetic toolbox is being under continuous development, based on protein engineering with strategies as site-directed mutagenesis and chimeras construction with domain swapping between different channelrhodopsin species. However, there are still opportunities for further enhancements in channelrhodopsin action.

Despite the broad application and development of optogenetics and ChR2, there are still some limitations precluding the required effect of channelrhodopsin in the depolarization of neurons, such as unsuitable kinetics, low expression levels, rapid inactivation, small conductance and undesired absorption peak light sensitivity. In fact, in terms of spectral properties, few variants were successfully generated and fully characterized.

In this present work, based on biophysical computational theory predictions, we established the successful creation of color-tuned variants of ChR2, by radical directed-site mutagenesis on target residues on the electrostatic environment of the protein chromophore.

Four new mutants were effectively *Ab-initio* designed, produced and characterized. We originally created three red-shifted variants. F217D and F269D were characterized with a 90nm red-shifted absorption peak, relatively to the wild type protein. L221D protein presents even a higher red-shifter, of 180nm. We were also proficient to create a fourth new variant, F269H, a 20nm blue-shifted ChR2.

Although we designed single mutations and achieved very significant shifts, it is possible to try the use of combined modifications and challenge to produce a double mutant with a potential synergistic effect between. This approach could achieve even bigger shifts than the outputs from single mutations.

To achieve our final fruitful outputs, we completed a series of molecular biology designed constructs, in both mammalian and yeast suitable vectors. Furthermore, we entirely settled and optimized the laboratory production of recombinant protein in the heterologous system *of Pichia pastoris*. More precisely, we were able to generate ChR2 by inducible and constitutive expression in two different strains, X-33 and SMD1168H. We selected and defined the combination of inducible expression in SMD1168H strain as the one with higher yields of ChR2. Molecular constructs aimed at secretory expression were also completed, but required experimental investigation.

Protein purification by nickel affinity chromatography was also achieved and continuously optimized, in both 1 mL and scale-up 5 mL columns. Protein concentration and spectral characterization of all ChR2 variants and wild type was also fully achieved. The study of pH effect on our proteins absorption spectra is a future optimization process. It can also be possible to increase the number of wavelength points to enhance the accuracy of the protein characterization, using a more sensitive spectrophotometer.

The electrophysiological characterization of our new proteins is the following step of this project. This characterization includes analysis of the kinetic properties of the channel and the efficacy of protein trafficking in neurons. A creation of a viral vector encoding our created mutants for *in vivo* delivering could also be a next step.

The functional purification and spectroscopic characterization of our four novel ChR2 variants we report on this dissertation signifies a significant step towards a detailed structural and functional exploration of ChR2.

Concluding, we were able to produce a successful colour tuning of ChR2, to create four new desired ChR2 mutants and validate theoretical TDDFT predictions. The continuous study of our proteins will be essential for its development and potential optogenetic implementation.

The present study open the prospect of tailoring channelrhodopsins for biomedical and neuroscience applications, based on biophysical and biomolecular simulation predictions, based on Time-dependent Density Functional theory. The creation of intelligently designed ChR2 variants using protein design can be a consistent method to engineer other numerous biotechnological proteins, based on a reliable control of the protein molecular structure.

Chapter V – References

ADAMANTIDIS, Antoine R. *et al.* - Neural substrates of awakening probed with optogenetic control of hypocretin neurons. **Nature**. . ISSN 1476-4687. 450:7168 (2007) 420–4. doi: 10.1038/nature06310.

AHMAD, Mudassar *et al.* - Protein expression in Pichia pastoris: recent achievements and perspectives for heterologous protein production. **Applied microbiology and biotechnology**. . ISSN 1432-0614. 98:12 (2014) 5301–17. doi: 10.1007/s00253-014-5732-5.

AIRAN, Raag D. *et al.* - Temporally precise in vivo control of intracellular signalling. **Nature**. . ISSN 1476-4687. 458:7241 (2009) 1025–9. doi: 10.1038/nature07926.

ALILAIN, Warren J. *et al.* - Light-induced rescue of breathing after spinal cord injury. **The Journal of neuroscience : the official journal of the Society for Neuroscience**. . ISSN 1529-2401. 28:46 (2008) 11862–70. doi: 10.1523/JNEUROSCI.3378-08.2008.

ARENKIEL, Benjamin R. *et al.* - In vivo light-induced activation of neural circuitry in transgenic mice expressing channelrhodopsin-2. **Neuron**. . ISSN 0896-6273. 54:2 (2007) 205–18. doi: 10.1016/j.neuron.2007.03.005.

ARENKIEL, Benjamin R.; PECA, Joao - Using light to reinstate respiratory plasticity. **Journal of neurophysiology**. . ISSN 0022-3077. 101:4 (2009) 1695–8. doi: 10.1152/jn.00009.2009.

AZIMIHASHEMI, N. *et al.* - Synthetic retinal analogues modify the spectral and kinetic characteristics of microbial rhodopsin optogenetic tools. **Nature communications**. . ISSN 2041-1723. 5:2014) 5810. doi: 10.1038/ncomms6810.

BAMANN, Christian *et al.* - Spectral characteristics of the photocycle of channelrhodopsin-2 and its implication for channel function. **Journal of molecular biology**. . ISSN 1089-8638. 375:3 (2008) 686–94. doi: 10.1016/j.jmb.2007.10.072.

BAMANN, Christian *et al.* - Structural guidance of the photocycle of channelrhodopsin-2 by an interhelical hydrogen bond. **Biochemistry**. . ISSN 1520-4995. 49:2 (2010) 267–78. doi: 10.1021/bi901634p.

BAMBERG, E.; TITTOR, J.; OESTERHELT, D. - Light-driven proton or chloride pumping by halorhodopsin. **Proceedings of the National Academy of Sciences of the United States of America**. . ISSN 0027-8424. 90:2 (1993) 639–43.

BARLOWE, Charles K.; MILLER, Elizabeth A. - Secretory protein biogenesis and traffic in the early secretory pathway. **Genetics**. . ISSN 1943-2631. 193:2 (2013) 383–410. doi: 10.1534/genetics.112.142810.

BARON, Michel *et al.* - A selectable bifunctional β-galactosidase::phleomycin-resistance fusion protein as a potential marker for eukaryotic cells. **Gene**. . ISSN 03781119. 114:2 (1992) 239–243. doi: 10.1016/0378-1119(92)90581-9.

BARRETT, John Martin; BERLINGUER-PALMINI, Rolando; DEGENAAR, Patrick - Optogenetic approaches to retinal prosthesis. **Visual neuroscience**. . ISSN 1469-8714. 31:4-5 (2014) 345–54. doi: 10.1017/S0952523814000212.

BECKWITH, Jonathan - Fifty years fused to lac. **Annual review of microbiology**. . ISSN 1545-3251. 67:2013) 1–19. doi: 10.1146/annurev-micro-092412-155732.

BÉJÀ, O. *et al.* - Bacterial rhodopsin: evidence for a new type of phototrophy in the sea. **Science (New York, N.Y.)**. . ISSN 0036-8075. 289:5486 (2000) 1902–6.

BERNDT, Andre *et al.* - Structure-guided transformation of channelrhodopsin into a light-activated chloride channel. **Science (New York, N.Y.)**. . ISSN 1095-9203. 344:6182 (2014) 420–4. doi: 10.1126/science.1252367.

BERNDT, André *et al.* - Bi-stable neural state switches. **Nature neuroscience**. . ISSN 1546-1726. 12:2 (2009) 229–34. doi: 10.1038/nn.2247.

BERNDT, André *et al.* - Two open states with progressive proton selectivities in the branched channelrhodopsin-2 photocycle. **Biophysical journal**. . ISSN 1542-0086. 98:5 (2010) 753–61. doi: 10.1016/j.bpj.2009.10.052.

BERNDT, André *et al.* - High-efficiency channelrhodopsins for fast neuronal stimulation at low light levels. **Proceedings of the National Academy of Sciences of the United States of America**. . ISSN 1091-6490. 108:18 (2011) 7595–600. doi: 10.1073/pnas.1017210108.

BERNSTEIN, Jacob G.; BOYDEN, Edward S. - Optogenetic tools for analyzing the neural circuits of behavior. **Trends in cognitive sciences**. . ISSN 1879-307X. 15:12 (2011) 592–600. doi: 10.1016/j.tics.2011.10.003.

BERTHOLD, Peter *et al.* - Channelrhodopsin-1 initiates phototaxis and photophobic responses in chlamydomonas by immediate light-induced depolarization. **The Plant cell**. . ISSN 1040-4651. 20:6 (2008) 1665–77. doi: 10.1105/tpc.108.057919.

BI, Anding *et al.* - Ectopic expression of a microbial-type rhodopsin restores visual responses in mice with photoreceptor degeneration. **Neuron**. . ISSN 0896-6273. 50:1 (2006) 23–33. doi: 10.1016/j.neuron.2006.02.026.

BLOCK, Helena *et al.* - Immobilized-metal affinity chromatography (IMAC): a review. **Methods in enzymology**. . ISSN 1557-7988. 463:2009) 439–73. doi: 10.1016/S0076-6879(09)63027-5.

BOGOMOLNI, R. A.; SPUDICH, J. L. - Identification of a third rhodopsin-like pigment in phototactic Halobacterium halobium. **Proceedings of the National Academy of Sciences of the United States of America**. . ISSN 0027-8424. 79:20 (1982) 6250–4.

BORNHORST, J. A.; FALKE, J. J. - Purification of proteins using polyhistidine affinity tags. **Methods in enzymology**. . ISSN 0076-6879. 326:2000) 245–54.

BOYDEN, Edward S. *et al.* - Millisecond-timescale, genetically targeted optical control of neural activity. **Nature neuroscience**. . ISSN 1097-6256. 8:9 (2005) 1263–8. doi: 10.1038/nn1525.

BRUUN, Sara *et al.* - The chromophore structure of the long-lived intermediate of the C128T channelrhodopsin-2 variant. **FEBS letters**. . ISSN 1873-3468. 585:24 (2011) 3998–4001. doi: 10.1016/j.febslet.2011.11.007.

BRUUN, Sara - **Raman spectroscopy on microbial rhodopsins** [Em linha] [Consult. 13 ago. 2015]. Disponível em WWW:<URL:file:///Users/joaocalmeiro/Downloads/bruun_sara.pdf>.

BRUUN, Sara *et al.* - Light-Dark Adaptation of Channelrhodopsin Involves Photoconversion Between the all-trans and 13-cis Retinal Isomers. **Biochemistry**. . ISSN 1520-4995. 2015). doi: 10.1021/acs.biochem.5b00597.

BURKE, Kieron; WERSCHNIK, Jan; GROSS, E. K. U. - Time-dependent density functional theory: past, present, and future. **The Journal of chemical physics**. . ISSN 0021-9606. 123:6 (2005) 62206. doi: 10.1063/1.1904586.

BYRNE, Bernadette - Pichia pastoris as an expression host for membrane protein structural biology. **Current opinion in structural biology**. . ISSN 1879-033X. 32C:2015) 9–17. doi: 10.1016/j.sbi.2015.01.005.

CATTERALL, W. A. - Structure and function of voltage-gated ion channels. **Annual review of biochemistry**. . ISSN 0066-4154. 64:1995) 493–531. doi: 10.1146/annurev.bi.64.070195.002425.

CEREGHINO, J. - Heterologous protein expression in the methylotrophic yeast Pichia pastoris. **FEMS Microbiology Reviews**. . ISSN 01686445. 24:1 (2000) 45–66. doi: 10.1016/S0168-6445(99)00029-7.

CEREGHINO, J. L.; CREGG, J. M. - Heterologous protein expression in the methylotrophic yeast Pichia pastoris. **FEMS microbiology reviews**. . ISSN 0168-6445. 24:1 (2000) 45–66.

CHANG, Yaw-Jen; CHEN, Sheng-Zheng; HO, Ching-Yuan - Crystallographic structure of Ni-Co coating on the affinity adsorption of histidine-tagged protein. **Colloids and surfaces. B, Biointerfaces**. . ISSN 1873-4367. 128:2015) 55–60. doi: 10.1016/j.colsurfb.2015.02.018.

CHONG, Fui Chin *et al.* - Purification of histidine-tagged nucleocapsid protein of Nipah virus using immobilized metal affinity chromatography. **Journal of chromatography. B, Analytical technologies in the biomedical and life sciences**. . ISSN 1873-376X. 877:14-15 (2009) 1561–7. doi: 10.1016/j.jchromb.2009.03.048.

CHOW, Brian Y. *et al.* - High-performance genetically targetable optical neural silencing by light-driven proton pumps. **Nature**. . ISSN 1476-4687. 463:7277 (2010) 98–102. doi: 10.1038/nature08652.

CHOW, Brian Y. *et al.* - Synthetic physiology strategies for adapting tools from nature for genetically targeted control of fast biological processes. **Methods in enzymology**. . ISSN 1557-7988. 497:2011) 425–43. doi: 10.1016/B978-0-12-385075-1.00018-4.

CHOW, Brian Y.; BOYDEN, Edward S. - Optogenetics and translational medicine. **Science translational medicine**. . ISSN 1946-6242. 5:177 (2013) 177ps5. doi: 10.1126/scitranslmed.3003101.

COS, Oriol *et al.* - Operational strategies, monitoring and control of heterologous protein production in the methylotrophic yeast Pichia pastoris under different promoters: a review. **Microbial cell factories**. . ISSN 1475-2859. 5:1 (2006) 17. doi: 10.1186/1475-2859-5-17.

CREGG, J. M. *et al.* - Pichia pastoris as a host system for transformations. **Molecular and cellular biology**. . ISSN 0270-7306. 5:12 (1985) 3376–85.

CREGG, J. M. *et al.* - Functional characterization of the two alcohol oxidase genes from the yeast Pichia pastoris. **Molecular and cellular biology**. . ISSN 0270-7306. 9:3 (1989) 1316–23.

CREGG, James M. *et al.* - Expression in the yeast Pichia pastoris. **Methods in enzymology**. . ISSN 1557-7988. 463:2009) 169–89. doi: 10.1016/S0076-6879(09)63013-5.

CRICK, F. H. - The Brain. **San Francisco, W. H. Freeman.** (1979).

CRICK, F. H. - Thinking about the brain. **Scientific American**. . ISSN 0036-8733. 241:3 (1979) 219–32.

DALY, Rachel; HEARN, Milton T. W. - Expression of heterologous proteins in Pichia pastoris: a useful experimental tool in protein engineering and production. **Journal of molecular recognition : JMR**. . ISSN 0952-3499. 18:2 (2005) 119–38. doi: 10.1002/jmr.687.

DAWYDOW, Alexej *et al.* - Channelrhodopsin-2-XXL, a powerful optogenetic tool for low-light applications. **Proceedings of the National Academy of Sciences of the United States of America**. . ISSN 1091-6490. 111:38 (2014) 13972–7. doi: 10.1073/pnas.1408269111.

DEISSEROTH, K. *et al.* - Next-Generation Optical Technologies for Illuminating Genetically Targeted Brain Circuits. **Journal of Neuroscience**. . ISSN 0270-6474. 26:41 (2006) 10380–10386. doi: 10.1523/JNEUROSCI.3863-06.2006.

DEISSEROTH, Karl - Controlling the Brain with Light. **Scientific American**. . ISSN 0036-8733. 303:5 (2010) 48–55. doi: 10.1038/scientificamerican1110-48.

DEISSEROTH, Karl - Optogenetics. **Nature methods**. . ISSN 1548-7105. 8:1 (2011) 26–9. doi: 10.1038/nmeth.f.324.

DELROISSE, Jean-Marc *et al.* - Expression of a synthetic gene encoding a Tribolium castaneum carboxylesterase in Pichia pastoris. **Protein expression and purification**. . ISSN 1046-5928. 42:2 (2005) 286–94. doi: 10.1016/j.pep.2005.04.011.

DIESTER, Ilka *et al.* - An optogenetic toolbox designed for primates. **Nature neuroscience**. . ISSN 1546-1726. 14:3 (2011) 387–97. doi: 10.1038/nn.2749.

DOROUDCHI, M. Mehdi *et al.* - Virally delivered channelrhodopsin-2 safely and effectively restores visual function in multiple mouse models of blindness. **Molecular therapy : the journal of the American Society of Gene Therapy**. . ISSN 1525-0024. 19:7 (2011) 1220–9. doi: 10.1038/mt.2011.69.

DROCOURT, D. *et al.* - Cassettes of the Streptoalloteichus hindustanus ble gene for transformation of lower and higher eukaryotes to phleomycin resistance. **Nucleic acids research**. . ISSN 0305-1048. 18:13 (1990) 4009.

EHLENBECK, Sabine *et al.* - Evidence for a light-induced H(+) conductance in the eye of the green alga Chlamydomonas reinhardtii. **Biophysical journal**. . ISSN 0006-3495. 82:2 (2002) 740–51. doi: 10.1016/S0006-3495(02)75436-2.

EISENHAUER, Kirstin *et al.* - In channelrhodopsin-2 Glu-90 is crucial for ion selectivity and is deprotonated during the photocycle. **The Journal of biological chemistry**. . ISSN 1083-351X. 287:9 (2012) 6904–11. doi: 10.1074/jbc.M111.327700.

ELLIS, S. B. *et al.* - Isolation of alcohol oxidase and two other methanol regulatable genes from the yeast Pichia pastoris. **Molecular and cellular biology**. . ISSN 0270-7306. 5:5 (1985) 1111–21.

ERNST, Oliver P. *et al.* - Photoactivation of channelrhodopsin. **The Journal of biological chemistry**. . ISSN 0021-9258. 283:3 (2008) 1637–43. doi: 10.1074/jbc.M708039200.

ERNST, Oliver P. *et al.* - Microbial and animal rhodopsins: structures, functions, and molecular mechanisms. **Chemical reviews**. . ISSN 1520-6890. 114:1 (2014) 126–63. doi: 10.1021/cr4003769.

ESSEN, Lars-Oliver - Halorhodopsin: light-driven ion pumping made simple? **Current opinion in structural biology**. . ISSN 0959-440X. 12:4 (2002) 516–22.

FANTONI, Adele *et al.* - Improved yields of full-length functional human FGF1 can be achieved using the methylotrophic yeast Pichia pastoris. **Protein expression and purification**. . ISSN 1046-5928. 52:1 (2007) 31–9. doi: 10.1016/j.pep.2006.10.014.

FELDBAUER, Katrin *et al.* - Channelrhodopsin-2 is a leaky proton pump. **Proceedings of the National Academy of Sciences of the United States of America**. . ISSN 1091-6490. 106:30 (2009) 12317–22. doi: 10.1073/pnas.0905852106.

FILIPEK, Sławomir *et al.* - G protein-coupled receptor rhodopsin: a prospectus. **Annual review of physiology**. . ISSN 0066-4278. 65:2003) 851–79. doi: 10.1146/annurev.physiol.65.092101.142611.

FOSTER, K. W.; SMYTH, R. D. - Light Antennas in phototactic algae. **Microbiological reviews**. . ISSN 0146-0749. 44:4 (1980) 572–630.

GASSER, Brigitte *et al.* - Pichia pastoris: protein production host and model organism for biomedical research. **Future microbiology**. . ISSN 1746-0921. 8:2 (2013) 191–208. doi: 10.2217/fmb.12.133.

GOSHEN, Inbal *et al.* - Dynamics of retrieval strategies for remote memories. **Cell**. . ISSN 1097-4172. 147:3 (2011) 678–89. doi: 10.1016/j.cell.2011.09.033.

GOVORUNOVA, Elena G. *et al.* - New channelrhodopsin with a red-shifted spectrum and rapid kinetics from Mesostigma viride. **mBio**. . ISSN 2150-7511. 2:3 (2011) e00115–11. doi: 10.1128/mBio.00115-11.

GOVORUNOVA, Elena G. *et al.* - New channelrhodopsin with a red-shifted spectrum and rapid kinetics from Mesostigma viride. **mBio**. . ISSN 2150-7511. 2:3 (2011) e00115–11. doi: 10.1128/mBio.00115-11.

GOVORUNOVA, Elena G. *et al.* - Characterization of a highly efficient blue-shifted channelrhodopsin from the marine alga Platymonas subcordiformis. **The Journal of biological chemistry**. . ISSN 1083-351X. 288:41 (2013) 29911–22. doi: 10.1074/jbc.M113.505495.

GRADINARU, Viviana *et al.* - Optical deconstruction of parkinsonian neural circuitry. **Science (New York, N.Y.)**. . ISSN 1095-9203. 324:5925 (2009) 354–9. doi: 10.1126/science.1167093.

GRADINARU, Viviana *et al.* - Molecular and cellular approaches for diversifying and extending optogenetics. **Cell**. . ISSN 1097-4172. 141:1 (2010) 154–65. doi: 10.1016/j.cell.2010.02.037.

GRADINARU, Viviana; THOMPSON, Kimberly R.; DEISSEROTH, Karl - eNpHR: a Natronomonas halorhodopsin enhanced for optogenetic applications. **Brain cell biology**. . ISSN 1559-7113. 36:1-4 (2008) 129–39. doi: 10.1007/s11068-008-9027-6.

GRADMANN, Dietrich *et al.* - Rectification of the channelrhodopsin early conductance. **Biophysical journal**. . ISSN 1542-0086. 101:5 (2011) 1057–68. doi: 10.1016/j.bpj.2011.07.040.

GRÜNEWALD, Sylvia *et al.* - Production of the human D2S receptor in the methylotrophic yeast P. pastoris. **Receptors & channels**. . ISSN 1060-6823. 10:1 (2004) 37–50.

GUNAYDIN, Lisa A. *et al.* - Ultrafast optogenetic control. **Nature Neuroscience**. . ISSN 1097-6256. 13:3 (2010) 387–392. doi: 10.1038/nn.2495.

GUNAYDIN, Lisa A. *et al.* - Natural neural projection dynamics underlying social behavior. **Cell**. . ISSN 1097-4172. 157:7 (2014) 1535–51. doi: 10.1016/j.cell.2014.05.017.

GUTMANN, Daniel A. P. *et al.* - A high-throughput method for membrane protein solubility screening: The ultracentrifugation dispersity sedimentation assay. **Protein Science**. . ISSN 09618368. 16:7 (2007) 1422–1428. doi: 10.1110/ps.072759907.

HAN, Xue *et al.* - A high-light sensitivity optical neural silencer: development and application to optogenetic control of non-human primate cortex. **Frontiers in systems neuroscience**. . ISSN 1662-5137. 5:2011) 18. doi: 10.3389/fnsys.2011.00018.

HAN, Xue; BOYDEN, Edward S. - Multiple-color optical activation, silencing, and desynchronization of neural activity, with single-spike temporal resolution. **PloS one**. . ISSN 1932-6203. 2:3 (2007) e299. doi: 10.1371/journal.pone.0000299.

HARTNER, Franz S.; GLIEDER, Anton - Regulation of methanol utilisation pathway genes in yeasts. **Microbial cell factories**. . ISSN 1475-2859. 5:1 (2006) 39. doi: 10.1186/1475-2859-5-39.

HARZ, Hartmann; HEGEMANN, Peter - Rhodopsin-regulated calcium currents in Chlamydomonas. **Nature**. . ISSN 0028-0836. 351:6326 (1991) 489–491. doi: 10.1038/351489a0.

HATTAR, S. *et al.* - Melanopsin and rod-cone photoreceptive systems account for all major accessory visual functions in mice. **Nature**. . ISSN 1476-4687. 424:6944 (2003) 76–81. doi: 10.1038/nature01761.

HAUPTS, U. *et al.* - General concept for ion translocation by halobacterial retinal proteins: the isomerization/switch/transfer (IST) model. **Biochemistry**. . ISSN 0006-2960. 36:1 (1997) 2–7. doi: 10.1021/bi962014g.

HEGEMANN, P. - Vision in microalgae. **Planta**. . ISSN 0032-0935. 203:3 (1997) 265–74.

HEGEMANN, P.; OESTERBELT, D.; STEINER, M. - The photocycle of the chloride pump halorhodopsin. I: Azide-catalyzed deprotonation of the chromophore is a side reaction of photocycle intermediates inactivating the pump. **The EMBO journal**. . ISSN 0261-4189. 4:9 (1985) 2347–50.

HEGEMANN, Peter; EHLENBECK, Sabine; GRADMANN, Dietrich - Multiple photocycles of channelrhodopsin. **Biophysical journal**. . ISSN 0006-3495. 89:6 (2005) 3911–8. doi: 10.1529/biophysj.105.069716.

HEGEMANN, Peter; MÖGLICH, Andreas - Channelrhodopsin engineering and exploration of new optogenetic tools. **Nature methods**. . ISSN 1548-7105. 8:1 (2011) 39–42. doi: 10.1038/nmeth.f.327.

HEGEMANN, Peter; NAGEL, Georg - From channelrhodopsins to optogenetics. **EMBO molecular medicine**. . ISSN 1757-4684. 5:2 (2013) 173–6. doi: 10.1002/emmm.201202387.

HIGGINS, D. R. - Overview of protein expression in Pichia pastoris. **Current protocols in protein science / editorial board, John E. Coligan ... [et al.]**. . ISSN 1934-3663. Chapter 5:2001) Unit5.7. doi: 10.1002/0471140864.ps0507s02.

HOLLAND, E. M. *et al.* - Control of phobic behavioral responses by rhodopsin-induced photocurrents in Chlamydomonas. **Biophysical journal**. . ISSN 0006-3495. 73:3 (1997) 1395–401. doi: 10.1016/S0006-3495(97)78171-2.

HOLMES, S. J. - Light and the Behavior of Organisms. **Science**. . ISSN 0036-8075. 33:860 (1911) 964–966. doi: 10.1126/science.33.860.964.

HOU, Jin *et al.* - Metabolic engineering of recombinant protein secretion by Saccharomyces cerevisiae. **FEMS yeast research**. . ISSN 1567-1364. 12:5 (2012) 491–510. doi: 10.1111/j.1567-1364.2012.00810.x.

HOU, Sing-Yi *et al.* - Diversity of Chlamydomonas channelrhodopsins. **Photochemistry and photobiology**. . ISSN 1751-1097. 88:1 (2012) 119–28. doi: 10.1111/j.1751-1097.2011.01027.x.

IDIRIS, Alimjan *et al.* - Engineering of protein secretion in yeast: strategies and impact on protein production. **Applied microbiology and biotechnology**. . ISSN 1432-0614. 86:2 (2010) 403–17. doi: 10.1007/s00253-010-2447-0.

INADA, Kengo *et al.* - Optical dissection of neural circuits responsible for Drosophila larval locomotion with halorhodopsin. **PloS one**. . ISSN 1932-6203. 6:12 (2011) e29019. doi: 10.1371/journal.pone.0029019.

Introduction - [Em linha] [Consult. 11 ago. 2015]. Disponível em WWW:<URL:https://cuvillier.de/uploads/preview/public_file/8536/Leseprobe.pdf>.

INVITROGEN - **Pichia expression vectors for constitutive expression and purification of recombinant proteins** [Em linha] [Consult. 22 jul. 2015]. Disponível em WWW:<URL:https://tools.lifetechnologies.com/content/sfs/manuals/pgapz_man.pdf>.

ISHIZUKA, Toru *et al.* - Kinetic evaluation of photosensitivity in genetically engineered neurons expressing green algae light-gated channels. **Neuroscience research**. . ISSN 0168-0102. 54:2 (2006) 85–94. doi: 10.1016/j.neures.2005.10.009.

JUNG, Kwang-Hwan; TRIVEDI, Vishwa D.; SPUDICH, John L. - Demonstration of a sensory rhodopsin in eubacteria. **Molecular microbiology**. . ISSN 0950-382X. 47:6 (2003) 1513–22.

KATERIYA, Suneel *et al.* - «Vision» in single-celled algae. **News in physiological sciences : an international journal of physiology produced jointly by the International Union of Physiological Sciences and the American Physiological Society**. . ISSN 0886-1714. 19:2004) 133–7.

KATO, Hideaki E. *et al.* - Crystal structure of the channelrhodopsin light-gated cation channel. **Nature**. . ISSN 1476-4687. 482:7385 (2012) 369–74. doi: 10.1038/nature10870.

KATO, Hideaki E. *et al.* - Atomistic design of microbial opsin-based blue-shifted optogenetics tools. **Nature communications**. . ISSN 2041-1723. 6:2015) 7177. doi: 10.1038/ncomms8177.

KIANIANMOMENI, Arash *et al.* - Channelrhodopsins of Volvox carteri are photochromic proteins that are specifically expressed in somatic cells under control of light, temperature, and the sex inducer. **Plant physiology**. . ISSN 0032-0889. 151:1 (2009) 347–66. doi: 10.1104/pp.109.143297.

KIM, Jong-Myoung *et al.* - Light-driven activation of beta 2-adrenergic receptor signaling by a chimeric rhodopsin containing the beta 2-adrenergic receptor cytoplasmic loops. **Biochemistry**. . ISSN 0006-2960. 44:7 (2005) 2284–92. doi: 10.1021/bi048328i.

KIRSCH, Taryn - Functional expression of Channelrhodopsin-2 (ChR2) in the methylotrophic yeast Pichia pastoris and biophysical characterization. 2008).

KLAPOETKE, Nathan C. *et al.* - Independent optical excitation of distinct neural populations. **Nature methods**. . ISSN 1548-7105. 11:3 (2014) 338–46. doi: 10.1038/nmeth.2836.

KLEINLOGEL, Sonja *et al.* - Ultra light-sensitive and fast neuronal activation with the $Ca^{2}+$-permeable channelrhodopsin CatCh. **Nature neuroscience**. . ISSN 1546-1726. 14:4 (2011) 513–8. doi: 10.1038/nn.2776.

KOBAYASHI, T.; SAITO, T.; OHTANI, H. - Real-time spectroscopy of transition states in bacteriorhodopsin during retinal isomerization. **Nature**. . ISSN 0028-0836. 414:6863 (2001) 531–4. doi: 10.1038/35107042.

KOHN, W.; SHAM, L. J. - Self-Consistent Equations Including Exchange and Correlation Effects. **Physical Review**. . ISSN 0031-899X. 140:4A (1965) A1133–A1138. doi: 10.1103/PhysRev.140.A1133.

KOLBE, M. *et al.* - Structure of the light-driven chloride pump halorhodopsin at 1.8 A resolution. **Science (New York, N.Y.)**. . ISSN 0036-8075. 288:5470 (2000) 1390–6.

KOUTZ, P. *et al.* - Structural comparison of the Pichia pastoris alcohol oxidase genes. **Yeast (Chichester, England)**. . ISSN 0749-503X. 5:3 (1989) 167–77. doi: 10.1002/yea.320050306.

KOZAK, M. - An analysis of 5'-noncoding sequences from 699 vertebrate messenger RNAs. **Nucleic acids research**. . ISSN 0305-1048. 15:20 (1987) 8125–48.

KOZAK, M. - Downstream secondary structure facilitates recognition of initiator codons by eukaryotic ribosomes. **Proceedings of the National Academy of Sciences of the United States of America**. . ISSN 0027-8424. 87:21 (1990) 8301–5.

KOZAK, M. - An analysis of vertebrate mRNA sequences: intimations of translational control. **The Journal of cell biology**. . ISSN 0021-9525. 115:4 (1991) 887–903.

KRAVITZ, Alexxai V *et al.* - Regulation of parkinsonian motor behaviours by optogenetic control of basal ganglia circuitry. **Nature**. . ISSN 1476-4687. 466:7306 (2010) 622–6. doi: 10.1038/nature09159.

KREIMER, Georg - The green algal eyespot apparatus: a primordial visual system and more? **Current genetics**. . ISSN 1432-0983. 55:1 (2009) 19–43. doi: 10.1007/s00294-008-0224-8.

KUHNE, Jens *et al.* - Early formation of the ion-conducting pore in channelrhodopsin-2. **Angewandte Chemie (International ed. in English)**. . ISSN 1521-3773. 54:16 (2015) 4953–7. doi: 10.1002/anie.201410180.

LAGALI, Pamela S. *et al.* - Light-activated channels targeted to ON bipolar cells restore visual function in retinal degeneration. **Nature neuroscience**. . ISSN 1097-6256. 11:6 (2008) 667–75. doi: 10.1038/nn.2117.

LI, Hai - **Department of Biochemistry and Molecular Biology | Hai Li** [Em linha], atual. 2013. [Consult. 12 ago. 2015]. Disponível em WWW:<URL:https://med.uth.edu/bmb/postdoctoral-research-fellows/hai-li/>.

LI, Nan *et al.* - Optogenetic-guided cortical plasticity after nerve injury. **Proceedings of the National Academy of Sciences of the United States of America**. . ISSN 1091-6490. 108:21 (2011) 8838–43. doi: 10.1073/pnas.1100815108.

LI, Xiang *et al.* - Fast noninvasive activation and inhibition of neural and network activity by vertebrate rhodopsin and green algae channelrhodopsin. **Proceedings of the National Academy of Sciences of the United States of America**. . ISSN 0027-8424. 102:49 (2005) 17816–21. doi: 10.1073/pnas.0509030102.

LIN, Bin *et al.* - Restoration of visual function in retinal degeneration mice by ectopic expression of melanopsin. **Proceedings of the National Academy of Sciences of the United States of America**. . ISSN 1091-6490. 105:41 (2008) 16009–14. doi: 10.1073/pnas.0806114105.

LIN, John Y. *et al.* - Characterization of engineered channelrhodopsin variants with improved properties and kinetics. **Biophysical journal**. . ISSN 1542-0086. 96:5 (2009) 1803–14. doi: 10.1016/j.bpj.2008.11.034.

LIN, John Y. - A user's guide to channelrhodopsin variants: features, limitations and future developments. **Experimental physiology**. . ISSN 1469-445X. 96:1 (2011) 19–25. doi: 10.1113/expphysiol.2009.051961.

LIN, John Y. *et al.* - ReaChR: a red-shifted variant of channelrhodopsin enables deep transcranial optogenetic excitation. **Nature neuroscience**. . ISSN 1546-1726. 16:10 (2013) 1499–508. doi: 10.1038/nn.3502.

LIN, Sue-Hwa; GUIDOTTI, Guido - Purification of membrane proteins. **Methods in enzymology**. . ISSN 1557-7988. 463:2009) 619–29. doi: 10.1016/S0076-6879(09)63035-4.

LIN-CEREGHINO, Geoff P. *et al.* - The effect of α-mating factor secretion signal mutations on recombinant protein expression in Pichia pastoris. **Gene**. . ISSN 1879-0038. 519:2 (2013) 311–7. doi: 10.1016/j.gene.2013.01.062.

LLEWELLYN, Michael E. *et al.* - Orderly recruitment of motor units under optical control in vivo. **Nature medicine**. . ISSN 1546-170X. 16:10 (2010) 1161–5. doi: 10.1038/nm.2228.

LÓRENZ-FONFRÍA, Víctor A. *et al.* - Transient protonation changes in channelrhodopsin-2 and their relevance to channel gating. **Proceedings of the National Academy of Sciences of the United States of America**. . ISSN 1091-6490. 110:14 (2013) E1273–81. doi: 10.1073/pnas.1219502110.

MACAULEY-PATRICK, Sue *et al.* - Heterologous protein production using the Pichia pastoris expression system. **Yeast (Chichester, England)**. . ISSN 0749-503X. 22:4 (2005) 249–70. doi: 10.1002/yea.1208.

MACÉ, Emilie *et al.* - Targeting channelrhodopsin-2 to ON-bipolar cells with vitreally administered AAV Restores ON and OFF visual responses in blind mice. **Molecular therapy: the journal of the American Society of Gene Therapy**. . ISSN 1525-0024. 23:1 (2015) 7–16. doi: 10.1038/mt.2014.154.

MARK CIGAN, A.; DONAHUE, Thomas F. - Sequence and structural features associated with translational initiator regions in yeast — a review. **Gene**. . ISSN 03781119. 59:1 (1987) 1–18. doi: 10.1016/0378-1119(87)90261-7.

MARQUES, M. A. L.; GROSS, E. K. U. - Time-dependent density functional theory. **Annual review of physical chemistry**. . ISSN 0066-426X. 55:2004) 427–55. doi: 10.1146/annurev.physchem.55.091602.094449.

MARQUES, Miguel A. L. *et al.* - Time-Dependent Density-Functional Approach for Biological Chromophores: The Case of the Green Fluorescent Protein. **Physical Review Letters**. . ISSN 0031-9007. 90:25 (2003) 258101. doi: 10.1103/PhysRevLett.90.258101.

MATSUNO-YAGI, A.; MUKOHATA, Y. - Two possible roles of bacteriorhodopsin; a comparative study of strains of Halobacterium halobium differing in pigmentation. **Biochemical and biophysical research communications**. . ISSN 0006-291X. 78:1 (1977) 237–43.

MATTIS, Joanna *et al.* - Principles for applying optogenetic tools derived from direct comparative analysis of microbial opsins. **Nature methods**. . ISSN 1548-7105. 9:2 (2012) 159–72. doi: 10.1038/nmeth.1808.

Method of the Year 2010 - **Nature Methods**. . ISSN 1548-7091. 8:1 (2010) 1–1. doi: 10.1038/nmeth.f.321.

MICHEL, H.; OESTERHELT, D. - Light-induced changes of the pH gradient and the membrane potential in H. halobium. **FEBS letters**. . ISSN 0014-5793. 65:2 (1976) 175–8.

MIESENBÖCK, Gero - The optogenetic catechism. **Science (New York, N.Y.)**. . ISSN 1095-9203. 326:5951 (2009) 395–9. doi: 10.1126/science.1174520.

MIESENBÖCK, Gero - Optogenetic control of cells and circuits. **Annual review of cell and developmental biology**. . ISSN 1530-8995. 27:2011) 731–58. doi: 10.1146/annurev-cellbio-100109-104051.

MIESENBÖCK, Gero; KEVREKIDIS, Ioannis G. - Optical imaging and control of genetically designated neurons in functioning circuits. **Annual review of neuroscience**. . ISSN 0147-006X. 28:2005) 533–63. doi: 10.1146/annurev.neuro.28.051804.101610.

MUDERS, Vera *et al.* - Resonance Raman and FTIR spectroscopic characterization of the closed and open states of channelrhodopsin-1. **FEBS letters**. . ISSN 1873-3468. 588:14 (2014) 2301–6. doi: 10.1016/j.febslet.2014.05.019.

MÜLLER, Maria *et al.* - Projection structure of channelrhodopsin-2 at 6 Å resolution by electron crystallography. **Journal of molecular biology**. . ISSN 1089-8638. 414:1 (2011) 86–95. doi: 10.1016/j.jmb.2011.09.049.

MÜLLER, Maria *et al.* - Light-induced helix movements in channelrhodopsin-2. **Journal of molecular biology**. . ISSN 1089-8638. 427:2 (2015) 341–9. doi: 10.1016/j.jmb.2014.11.004.

NACK, Melanie *et al.* - The retinal structure of channelrhodopsin-2 assessed by resonance Raman spectroscopy. **FEBS letters**. . ISSN 1873-3468. 583:22 (2009) 3676–80. doi: 10.1016/j.febslet.2009.10.052.

NACK, Melanie *et al.* - The DC gate in Channelrhodopsin-2: crucial hydrogen bonding interaction between C128 and D156. **Photochemical & photobiological sciences : Official journal of the European Photochemistry Association and the European Society for Photobiology**. . ISSN 1474-9092. 9:2 (2010) 194–8. doi: 10.1039/b9pp00157c.

NACK, Melanie *et al.* - Kinetics of proton release and uptake by channelrhodopsin-2. **FEBS letters**. . ISSN 1873-3468. 586:9 (2012) 1344–8. doi: 10.1016/j.febslet.2012.03.047.

NAGEL, G. *et al.* - Functional expression of bacteriorhodopsin in oocytes allows direct measurement of voltage dependence of light induced H+ pumping. **FEBS letters**. . ISSN 0014-5793. 377:2 (1995) 263–6.

NAGEL, G. *et al.* - Channelrhodopsins: directly light-gated cation channels. **Biochemical Society transactions**. . ISSN 0300-5127. 33:Pt 4 (2005) 863–6. doi: 10.1042/BST0330863.

NAGEL, Georg *et al.* - Channelrhodopsin-1: a light-gated proton channel in green algae. **Science (New York, N.Y.)**. . ISSN 1095-9203. 296:5577 (2002) 2395–8. doi: 10.1126/science.1072068.

NAGEL, Georg *et al.* - Channelrhodopsin-2, a directly light-gated cation-selective membrane channel. **Proceedings of the National Academy of Sciences of the United States of America**. . ISSN 0027-8424. 100:24 (2003) 13940–5. doi: 10.1073/pnas.1936192100.

NAGEL, Georg *et al.* - Light activation of channelrhodopsin-2 in excitable cells of Caenorhabditis elegans triggers rapid behavioral responses. **Current biology : CB**. . ISSN 0960-9822. 15:24 (2005) 2279–84. doi: 10.1016/j.cub.2005.11.032.

NIKOLIC, Konstantin *et al.* - Photocycles of channelrhodopsin-2. **Photochemistry and Photobiology**. . ISSN 00318655. 85:1 (2009) 400–411. doi: 10.1111/j.1751-1097.2008.00460.x.

NISHIKAWA, Taichi; MURAKAMI, Midori; KOUYAMA, Tsutomu - Crystal structure of the 13-cis isomer of bacteriorhodopsin in the dark-adapted state. **Journal of molecular biology**. . ISSN 0022-2836. 352:2 (2005) 319–28. doi: 10.1016/j.jmb.2005.07.021.

NOGLY, Przemyslaw; STANDFUSS, Jörg - Light-driven Na(+) pumps as next-generation inhibitory optogenetic tools. **Nature structural & molecular biology**. . ISSN 1545-9985. 22:5 (2015) 351–3. doi: 10.1038/nsmb.3017.

NONNENGÄSSER, C. *et al.* - The nature of rhodopsin-triggered photocurrents in Chlamydomonas. II. Influence of monovalent ions. **Biophysical journal**. . ISSN 0006-3495. 70:2 (1996) 932–8. doi: 10.1016/S0006-3495(96)79636-4.

OESTERHELT, D.; STOECKENIUS, W. - Rhodopsin-like protein from the purple membrane of Halobacterium halobium. **Nature: New biology**. . ISSN 0090-0028. 233:39 (1971) 149–52.

OKADA, Tetsuji *et al.* - The retinal conformation and its environment in rhodopsin in light of a new 2.2 A crystal structure. **Journal of molecular biology**. . ISSN 0022-2836. 342:2 (2004) 571–83. doi: 10.1016/j.jmb.2004.07.044.

PALCZEWSKI, Krzysztof - G protein-coupled receptor rhodopsin. **Annual review of biochemistry**. . ISSN 0066-4154. 75:2006) 743–67. doi: 10.1146/annurev.biochem.75.103004.142743.

PAN, Zhuo-Hua *et al.* - ChR2 mutants at L132 and T159 with improved operational light sensitivity for vision restoration. **PloS one**. . ISSN 1932-6203. 9:6 (2014) e98924. doi: 10.1371/journal.pone.0098924.

PASHAIE, Ramin *et al.* - Optogenetic brain interfaces. **IEEE reviews in biomedical engineering**. . ISSN 1941-1189. 7:2014) 3–30. doi: 10.1109/RBME.2013.2294796.

PEÇA, João; FENG, Guoping - Neuroscience: When lights take the circuits out. **Nature**. . ISSN 1476-4687. 477:7363 (2011) 165–6. doi: 10.1038/477165a.

PLAZZO, Anna Pia *et al.* - Bioinformatic and mutational analysis of channelrhodopsin-2 protein cation-conducting pathway. **The Journal of biological chemistry**. . ISSN 1083-351X. 287:7 (2012) 4818–25. doi: 10.1074/jbc.M111.326207.

QIN, Xiulin *et al.* - GAP promoter library for fine-tuning of gene expression in Pichia pastoris. **Applied and environmental microbiology**. . ISSN 1098-5336. 77:11 (2011) 3600–8. doi: 10.1128/AEM.02843-10.

RADU, Ionela *et al.* - Conformational changes of channelrhodopsin-2. **Journal of the American Chemical Society**. . ISSN 1520-5126. 131:21 (2009) 7313–9. doi: 10.1021/ja8084274.

RAMÓN, Ana; MARÍN, Mónica - Advances in the production of membrane proteins in Pichia pastoris. **Biotechnology Journal**. . ISSN 18606768. 6:6 (2011) 700–706. doi: 10.1002/biot.201100146.

RITTER, Eglof *et al.* - Monitoring light-induced structural changes of Channelrhodopsin-2 by UV-visible and Fourier transform infrared spectroscopy. **The Journal of biological chemistry**. . ISSN 0021-9258. 283:50 (2008) 35033–41. doi: 10.1074/jbc.M806353200.

ROSKA, Botond *et al.* - [Retinitis pigmentosa: eye sight restoration by optogenetic therapy]. **Biologie aujourd'hui**. . ISSN 2105-0686. 207:2 (2013) 109–21. doi: 10.1051/jbio/2013011.

RUFFERT, Karelia *et al.* - Glutamate residue 90 in the predicted transmembrane domain 2 is crucial for cation flux through channelrhodopsin 2. **Biochemical and biophysical research communications**. . ISSN 1090-2104. 410:4 (2011) 737–43. doi: 10.1016/j.bbrc.2011.06.024.

RUIZ-GONZÁLEZ, Mario X.; MARÍN, Ignacio - New insights into the evolutionary history of type 1 rhodopsins. **Journal of molecular evolution**. . ISSN 0022-2844. 58:3 (2004) 348–58. doi: 10.1007/s00239-003-2557-8.

SASAKI, J. *et al.* - Conversion of bacteriorhodopsin into a chloride ion pump. **Science (New York, N.Y.)**. . ISSN 0036-8075. 269:5220 (1995) 73–5.

SCHALLER, K.; DAVID, R.; UHL, R. - How Chlamydomonas keeps track of the light once it has reached the right phototactic orientation. **Biophysical journal**. . ISSN 0006-3495. 73:3 (1997) 1562–72. doi: 10.1016/S0006-3495(97)78188-8.

SCHMIDT, J. A.; ECKERT, R. - Calcium couples flagellar reversal to photostimulation in Chlamydomonas reinhardtii. **Nature**. . ISSN 0028-0836. 262:5570 (1976) 713–5.

SCHOBERT, B.; LANYI, J. K. - Halorhodopsin is a light-driven chloride pump. **The Journal of biological chemistry**. . ISSN 0021-9258. 257:17 (1982) 10306–13.

SCHOLZ, Frank *et al.* - Tuning the primary reaction of channelrhodopsin-2 by imidazole, pH, and site-specific mutations. **Biophysical journal**. . ISSN 1542-0086. 102:11 (2012) 2649–57. doi: 10.1016/j.bpj.2012.04.034.

SCHROLL, Christian *et al.* - Light-induced activation of distinct modulatory neurons triggers appetitive or aversive learning in Drosophila larvae. **Current biology : CB**. . ISSN 0960-9822. 16:17 (2006) 1741–7. doi: 10.1016/j.cub.2006.07.023.

SHICHIDA, Yoshinori; YAMASHITA, Takahiro - Diversity of visual pigments from the viewpoint of G protein activation?comparison with other G protein-coupled receptors. **Photochemical & Photobiological Sciences**. . ISSN 1474-905X. 2:12 (2003) 1237. doi: 10.1039/b300434a.

SINESHCHEKOV, Oleg A. *et al.* - Intramolecular proton transfer in channelrhodopsins. **Biophysical journal**. . ISSN 1542-0086. 104:4 (2013) 807–17. doi: 10.1016/j.bpj.2013.01.002.

SINESHCHEKOV, Oleg A.; JUNG, Kwang-Hwan; SPUDICH, John L. - Two rhodopsins mediate phototaxis to low- and high-intensity light in Chlamydomonas reinhardtii. **Proceedings of the National Academy of Sciences of the United States of America**. . ISSN 0027-8424. 99:13 (2002) 8689–94. doi: 10.1073/pnas.122243399.

SPUDICH, J. L. *et al.* - Retinylidene proteins: structures and functions from archaea to humans. **Annual review of cell and developmental biology**. . ISSN 1081-0706. 16:2000) 365–92. doi: 10.1146/annurev.cellbio.16.1.365.

SPUDICH, John L. - The multitalented microbial sensory rhodopsins. **Trends in microbiology**. . ISSN 0966-842X. 14:11 (2006) 480–7. doi: 10.1016/j.tim.2006.09.005.

SPUDICH, John L.; LUECKE, Hartmut - Sensory rhodopsin II: functional insights from structure. **Current opinion in structural biology**. . ISSN 0959-440X. 12:4 (2002) 540–6.

STEHFEST, Katja *et al.* - The branched photocycle of the slow-cycling channelrhodopsin-2 mutant C128T. **Journal of molecular biology**. . ISSN 1089-8638. 398:5 (2010) 690–702. doi: 10.1016/j.jmb.2010.03.031.

STEHFEST, Katja; HEGEMANN, Peter - Evolution of the channelrhodopsin photocycle model. **Chemphyschem : a European journal of chemical physics and physical chemistry**. . ISSN 1439-7641. 11:6 (2010) 1120–6. doi: 10.1002/cphc.200900980.

STEINBECK, Julius A. *et al.* - Optogenetics enables functional analysis of human embryonic stem cell–derived grafts in a Parkinson's disease model. **Nature Biotechnology**. . ISSN 1087-0156. 33:2 (2015) 204–9. doi: 10.1038/nbt.3124.

SUZUKI, Takeshi *et al.* - Archaeal-type rhodopsins in Chlamydomonas: model structure and intracellular localization. **Biochemical and biophysical research communications**. . ISSN 0006-291X. 301:3 (2003) 711–7.

TERAKITA, Akihisa - The opsins. **Genome biology**. . ISSN 1465-6914. 6:3 (2005) 213. doi: 10.1186/gb-2005-6-3-213.

THE NEWS STAFF - Insights of the decade. Stepping away from the trees for a look at the forest. Introduction. **Science (New York, N.Y.)**. . ISSN 1095-9203. 330:6011 (2010) 1612–3. doi: 10.1126/science.330.6011.1612.

TØNNESEN, Jan *et al.* - Optogenetic control of epileptiform activity. **Proceedings of the National Academy of Sciences of the United States of America**. . ISSN 1091-6490. 106:29 (2009) 12162–7. doi: 10.1073/pnas.0901915106.

TSCHOPP, J. F. *et al.* - Expression of the lacZ gene from two methanol-regulated promoters in Pichia pastoris. **Nucleic acids research**. . ISSN 0305-1048. 15:9 (1987) 3859–76.

TSUNEMATSU, Tomomi *et al.* - Acute optogenetic silencing of orexin/hypocretin neurons induces slow-wave sleep in mice. **The Journal of neuroscience : the official journal of the Society for Neuroscience**. . ISSN 1529-2401. 31:29 (2011) 10529–39. doi: 10.1523/JNEUROSCI.0784-11.2011.

TSUNODA, Satoshi P.; HEGEMANN, Peter - Glu 87 of channelrhodopsin-1 causes pH-dependent color tuning and fast photocurrent inactivation. **Photochemistry and photobiology**. . ISSN 0031-8655. 85:2 (564–9. doi: 10.1111/j.1751-1097.2008.00519.x.

TYE, Kay M. *et al.* - Dopamine neurons modulate neural encoding and expression of depression-related behaviour. **Nature**. . ISSN 1476-4687. 493:7433 (2013) 537–41. doi: 10.1038/nature11740.

VÁRNAI, Anikó *et al.* - Expression of endoglucanases in Pichia pastoris under control of the GAP promoter. **Microbial cell factories**. . ISSN 1475-2859. 13:1 (2014) 57. doi: 10.1186/1475-2859-13-57.

VARSANO, Daniele *et al.* - A TDDFT study of the excited states of DNA bases and their assemblies. **The journal of physical chemistry. B**. . ISSN 1520-6106. 110:14 (2006) 7129–38. doi: 10.1021/jp056120g.

VAZEY, Elena M.; ASTON-JONES, Gary - New tricks for old dogmas: optogenetic and designer receptor insights for Parkinson's disease. **Brain research**. . ISSN 1872-6240. 1511:2013) 153–63. doi: 10.1016/j.brainres.2013.01.021.

VERHOEFEN, Mirka-Kristin *et al.* - The photocycle of channelrhodopsin-2: ultrafast reaction dynamics and subsequent reaction steps. **Chemphyschem : a European journal of chemical physics and physical chemistry**. . ISSN 1439-7641. 11:14 (2010) 3113–22. doi: 10.1002/cphc.201000181.

WANG, H. *et al.* - High-speed mapping of synaptic connectivity using photostimulation in Channelrhodopsin-2 transgenic mice. **Proceedings of the National Academy of Sciences of the United States of America**. . ISSN 0027-8424. 104:19 (2007) 8143–8. doi: 10.1073/pnas.0700384104.

WANG, Hongxia *et al.* - Molecular determinants differentiating photocurrent properties of two channelrhodopsins from chlamydomonas. **The Journal of biological chemistry**. . ISSN 0021-9258. 284:9 (2009) 5685–96. doi: 10.1074/jbc.M807632200.

WANG, Wenjing *et al.* - Tuning the electronic absorption of protein-embedded all-trans-retinal. **Science (New York, N.Y.)**. . ISSN 1095-9203. 338:6112 (2012) 1340–3. doi: 10.1126/science.1226135.

WASCHUK, Stephen A. *et al.* - Leptosphaeria rhodopsin: bacteriorhodopsin-like proton pump from a eukaryote. **Proceedings of the National Academy of Sciences of the United States of America**. . ISSN 0027-8424. 102:19 (2005) 6879–83. doi: 10.1073/pnas.0409659102.

WATANABE, Hiroshi C. *et al.* - Structural model of channelrhodopsin. **The Journal of biological chemistry**. . ISSN 1083-351X. 287:10 (2012) 7456–66. doi: 10.1074/jbc.M111.320309.

WATANABE, Hiroshi C. *et al.* - Towards an understanding of channelrhodopsin function: simulations lead to novel insights of the channel mechanism. **Journal of molecular biology**. . ISSN 1089-8638. 425:10 (2013) 1795–814. doi: 10.1016/j.jmb.2013.01.033.

WATERHAM, H. R. *et al.* - Isolation of the Pichia pastoris glyceraldehyde-3-phosphate dehydrogenase gene and regulation and use of its promoter. **Gene**. . ISSN 0378-1119. 186:1 (1997) 37–44.

WEISS, H. M. *et al.* - Expression of functional mouse 5-HT5A serotonin receptor in the methylotrophic yeast Pichia pastoris: pharmacological characterization and localization. **FEBS letters**. . ISSN 0014-5793. 377:3 (1995) 451–6.

WELKE, Kai *et al.* - Color tuning in binding pocket models of the chlamydomonas-type channelrhodopsins. **The journal of physical chemistry. B**. . ISSN 1520-5207. 115:50 (2011) 15119–28. doi: 10.1021/jp2085457.

WEN, Lei *et al.* - Opto-current-clamp actuation of cortical neurons using a strategically designed channelrhodopsin. **PloS one**. . ISSN 1932-6203. 5:9 (2010) e12893. doi: 10.1371/journal.pone.0012893.

WICKSTRAND, Cecilia *et al.* - Bacteriorhodopsin: Would the real structural intermediates please stand up? **Biochimica et biophysica acta**. . ISSN 0006-3002. 1850:3 (2015) 536–553. doi: 10.1016/j.bbagen.2014.05.021.

WIETEK, Jonas *et al.* - Conversion of channelrhodopsin into a light-gated chloride channel. **Science (New York, N.Y.)**. . ISSN 1095-9203. 344:6182 (2014) 409–12. doi: 10.1126/science.1249375.

WITMAN, G. B. - Chlamydomonas phototaxis. **Trends in cell biology**. . ISSN 0962-8924. 3:11 (1993) 403–8.

WITTEN, Ilana B. *et al.* - Recombinase-driver rat lines: tools, techniques, and optogenetic application to dopamine-mediated reinforcement. **Neuron**. . ISSN 1097-4199. 72:5 (2011) 721–33. doi: 10.1016/j.neuron.2011.10.028.

WOLFF, E. K. *et al.* - Color discrimination in halobacteria: spectroscopic characterization of a second sensory receptor covering the blue-green region of the spectrum. **Proceedings of the National Academy of Sciences of the United States of America**. . ISSN 0027-8424. 83:19 (1986) 7272–6.

WYK, Michiel VAN *et al.* - Restoring the ON Switch in Blind Retinas: Opto-mGluR6, a Next-Generation, Cell-Tailored Optogenetic Tool. **PLoS biology**. . ISSN 1545-7885. 13:5 (2015) e1002143. doi: 10.1371/journal.pbio.1002143.

WYKES, Robert C. *et al.* - Optogenetic and potassium channel gene therapy in a rodent model of focal neocortical epilepsy. **Science translational medicine**. . ISSN 1946-6242. 4:161 (2012) 161ra152. doi: 10.1126/scitranslmed.3004190.

YIZHAR, Ofer *et al.* - Microbial opsins: a family of single-component tools for optical control of neural activity. **Cold Spring Harbor protocols**. . ISSN 1559-6095. 2011:3 (2011) top102. doi: 10.1101/pdb.top102.

YIZHAR, Ofer *et al.* - Optogenetics in neural systems. **Neuron**. . ISSN 1097-4199. 71:1 (2011) 9–34. doi: 10.1016/j.neuron.2011.06.004.

YIZHAR, Ofer *et al.* - Neocortical excitation/inhibition balance in information processing and social dysfunction. **Nature**. . ISSN 1476-4687. 477:7363 (2011) 171–8. doi: 10.1038/nature10360.

ZEMELMAN, Boris V *et al.* - Selective photostimulation of genetically chARGed neurons. **Neuron**. . ISSN 0896-6273. 33:1 (2002) 15–22.

ZHANG, Ai-Lian *et al.* - Recent advances on the GAP promoter derived expression system of Pichia pastoris. **Molecular biology reports**. . ISSN 1573-4978. 36:6 (2009) 1611–9. doi: 10.1007/s11033-008-9359-4.

ZHANG, Feng *et al.* - Multimodal fast optical interrogation of neural circuitry. **Nature**. . ISSN 1476-4687. 446:7136 (2007) 633–9. doi: 10.1038/nature05744.

ZHANG, Feng *et al.* - Circuit-breakers: optical technologies for probing neural signals and systems. **Nature reviews. Neuroscience**. . ISSN 1471-003X. 8:8 (2007) 577–81. doi: 10.1038/nrn2192.

ZHANG, Feng *et al.* - Red-shifted optogenetic excitation: a tool for fast neural control derived from Volvox carteri. **Nature neuroscience**. . ISSN 1097-6256. 11:6 (2008) 631–3. doi: 10.1038/nn.2120.

ZHANG, Feng *et al.* - Optogenetic interrogation of neural circuits: technology for probing mammalian brain structures. **Nature protocols**. . ISSN 1750-2799. 5:3 (2010) 439–56. doi: 10.1038/nprot.2009.226.

ZHANG, Feng *et al.* - The microbial opsin family of optogenetic tools. **Cell**. . ISSN 1097-4172. 147:7 (2011) 1446–57. doi: 10.1016/j.cell.2011.12.004.

ZHAO, Shengli *et al.* - Improved expression of halorhodopsin for light-induced silencing of neuronal activity. **Brain cell biology**. . ISSN 1559-7113. 36:1-4 (2008) 141–54. doi: 10.1007/s11068-008-9034-7.